

Old Dominion University

## ODU Digital Commons

---

Mechanical & Aerospace Engineering Theses & Dissertations

Mechanical & Aerospace Engineering

---

Spring 1979

# Curing and Flow of Thermosetting Resins for Composite Materials Pultrusion

Howard L. Price Jr.  
*Old Dominion University*

Follow this and additional works at: [https://digitalcommons.odu.edu/mae\\_etds](https://digitalcommons.odu.edu/mae_etds)



Part of the [Materials Science and Engineering Commons](#), [Mechanical Engineering Commons](#), and the [Structures and Materials Commons](#)

---

### Recommended Citation

Price, Howard L.. "Curing and Flow of Thermosetting Resins for Composite Materials Pultrusion" (1979). Doctor of Philosophy (PhD), dissertation, Mechanical & Aerospace Engineering, Old Dominion University, DOI: 10.25777/p6ct-3a23  
[https://digitalcommons.odu.edu/mae\\_etds/298](https://digitalcommons.odu.edu/mae_etds/298)

This Dissertation is brought to you for free and open access by the Mechanical & Aerospace Engineering at ODU Digital Commons. It has been accepted for inclusion in Mechanical & Aerospace Engineering Theses & Dissertations by an authorized administrator of ODU Digital Commons. For more information, please contact [digitalcommons@odu.edu](mailto:digitalcommons@odu.edu).

CURING AND FLOW OF THERMOSETTING RESINS  
FOR COMPOSITE MATERIAL PULTRUSION

by

Howard L. Price, Jr.  
B.S., June 1957, Virginia Polytechnic Institute  
M. E., June 1970, Old Dominion University

A Dissertation Submitted to the Faculty of  
Old Dominion University in Partial Fulfillment of the  
Requirements for the Degree of

DOCTOR OF PHILOSOPHY  
ENGINEERING

OLD DOMINION UNIVERSITY  
May 1979

Approved by:

---

Stephen C. Gynsels

---

ABSTRACT

CURING AND FLOW OF THERMOSETTING RESINS  
FOR COMPOSITE MATERIAL PULTRUSION

by

Howard L. Price, Jr.  
B.S., June 1957, Virginia Polytechnic Institute  
M.E., June 1970, Old Dominion University

Stephen G. Cupschalk, Director

Fibrous composite materials for mechanical and structural applications often are expensive due to high labor costs. One economical way of making composites is pultrusion, a manufacturing process in which resin-impregnated fibers are pulled at a constant speed through a heated die which shapes the resin-fiber mass and cures the resin. Most of the work which has been done on the process has been of an empirical nature, with limited understanding of the process principles. Most of the experience with pultrusion has been gained with polyester resins and glass fibers. Very little experience has been gained with higher performance, more costly materials such as epoxy resins and graphite fiber. The higher cost of these latter materials makes the empirical approach to developing process parameters much too expensive.

Therefore, an investigation was made of the pultrusion process with the objective of developing a model of the process applicable to thermosetting resins. The intent was to express the model in both pultrusion material properties and pultrusion machine parameters. For this investigation, the pultruder die was regarded as a combination

reactor and rheometer; a chemical reactor in which low molecular weight, liquid resin undergoes a chemical reaction to become a higher molecular weight, crosslinked composite material matrix; a slit rheometer in which a volume of material entering the die undergoes changes which generate pressures and resisting forces. The approach to the investigation was:

- (i) Test and analyze several present and potential pultrusion materials.
- (ii) Analyze two pultrusion processes which have been used to manufacture pultruded stock.
- (iii) Develop a model from the tests and analyses and test it on a laboratory-scale pultruder constructed for that purpose as part of this investigation.

The model which was developed in the investigation expressed three, principal processing variables of temperature, time, and pressure as dimensionless numbers. These were the Arrhenius number (temperature), the Damköhler number (time), and the Coulomb number (pressure). All of these numbers were expressed in terms of machine parameters as well as material properties. The model was tested on a laboratory-scale pultruder using epoxy resin-graphite fiber prepreg tape. The Coulomb number served as a process limit in that the pulling force and generated pressures within the die had to remain in certain bounds. The other two numbers were used to define a temperature--time control variable plane. With such a plane, the effect of a temperature-time trade-off on the properties of pultruded stock was observed. Moreover, the control variable settings needed to give dense, well compacted pultruded stock were determined.

## ACKNOWLEDGEMENTS

Many people have assisted me in the research leading to and the preparation of this dissertation, and not all can be acknowledged here by name. Those named are: Stephen G. Cupschalk, the dissertation director, who encouraged me to work in a more applied area, and who has a talent for seeing the positive results from nearly any test or analysis; John M. Kuhlman, Old Dominion University, who was especially helpful in dimensionless number concepts and applications; Edward L. Hoffman, NASA-Langley Research Center, who directed me toward pultrusion process data which were available, and generously provided pultruded stock for testing; Claud M. Pittman, NASA-Langley Research Center, who modified an existing computer program which he had developed for heat transfer to include a heat generation term; Duane Davis, Morrison Molded Fiber Glass Company, and Robert J. Bradley, Boeing Commercial Airplane Company, who answered numerous questions, with patience and understanding, concerning the pultrusion process used by the two companies.

## TABLE OF CONTENTS

	Page
LIST OF TABLES . . . . .	iv
LIST OF FIGURES . . . . .	v
LIST OF SYMBOLS . . . . .	vii
Chapter	
1. INTRODUCTION . . . . .	1
2. REVIEW AND APPROACH . . . . .	7
3. MATERIALS, TESTS, AND NUMERICAL METHODS . . . . .	15
4. MASS BALANCE IN A PULTRUDER DIE . . . . .	24
5. ENERGY BALANCE IN A PULTRUDER DIE . . . . .	47
6. FORCE BALANCE IN A PULTRUDER DIE . . . . .	60
7. ISOMETRIC PROCESS ANALYSIS . . . . .	70
8. ISOBARIC PROCESS ANALYSIS . . . . .	85
9. PULTRUSION PROCESS MODEL . . . . .	106
10. CONCLUSIONS . . . . .	127
REFERENCES . . . . .	130
APPENDIX - INSTRUMENT CALIBRATION . . . . .	136

## LIST OF TABLES

	Page
1. Thermosetting Resins Investigated . . . . .	16
2. Prepreg Tapes Investigated . . . . .	17
3. Kinetic and Thermal Parameters for Polyester and Epoxy Resins . . . . .	32
4. Kinetic and Thermal Parameters for Epoxy Prepreg Tape . . . . .	42
5. Parameter Values Used in Finite Difference Program to Estimate Temperature Distribution in Resin-Fiber Mass . . . . .	49
6. Physical Properties of Pultruded Circular Rods of Polyester Resin and Glass Fiber . . . . .	75
7. Mechanical Properties of Pultruded Circular Rods of Polyester Resin and Glass Fiber . . . . .	79
8. Processing Parameters and Properties of Pultruded Flat Sections of Epoxy Resin and Graphite Fiber; Data From Reference 39 . . . . .	88
9. Processing Parameters and Properties of Pultruded Flat Sections of Epoxy Resin and Graphite Fiber . . . . .	89
10. Pultruder Settings and Pultruded Stock Properties for Hy-E 1079 Epoxy-Graphite Prepreg Tape . . . . .	120
11. Pultruder Settings and Pultruded Stock Properties for E 702 Epoxy-Graphite Prepreg Tape . . . . .	121

## LIST OF FIGURES

FIGURE	Page
1. Pultrusion Process Schematic . . . . .	3
2. Representative Pultruded Stock . . . . .	4
3. Rotary Rheometer . . . . .	20
4. Coordinate System . . . . .	22
5. Distance - Time - Temperature Relationship . . . . .	23
6. Idealized DSC Test Curve . . . . .	27
7. Reaction Rate Constant vs. Reciprocal Temperature . . . . .	29
8. DSC Curves for Polyester Resins . . . . .	30
9. DSC Curves for Epoxy Resins . . . . .	31
10. Reaction Heat vs. Initiator Concentration . . . . .	35
11. Reaction Fraction vs. Temperature . . . . .	36
12. Temperature - Time Curves for Various Reaction Fractions . . . . .	38
13. DSC Curves for Epoxy Prepreg Tape . . . . .	41
14. Normalized Concentration vs. Damköhler Number . . . . .	45
15. Temperature Distribution in Resin-Fiber Mass . . . . .	50
16. Adiabatic Temperature for Various Arrhenius Numbers . . . . .	55
17. Adiabatic Temperature for Various Adiabatic Temperature Rise . . . . .	56
18. Adiabatic Temperature Rise for Various Reaction Fraction . . . . .	57



FIGURE	Page
19. Pressure and Volume Changes in Landed and Un-Landed Dies . . . . .	66
20. Pultruded Tube Deformation . . . . .	73
21. Cross Section of 38 mm-Diameter Pultruded Rod . . . . .	77
22. Scanning Electron Micrographs of 38 mm-Diameter Pultruded Rod . . . . .	78
23. Die Temperature vs. Microwave Power . . . . .	90
24. Die Temperature vs. Processing Number . . . . .	94
25. Response Variable vs. Control Variable for Isobaric Process (Ref. 39) . . . . .	97
26. Die Pressure vs. Energy . . . . .	98
27. Variation in Short Beam Shear Strength of Pultruded Flat Sections . . . . .	100
28. Short Beam Shear Strength vs. Response Variables (Ref. 39) . . . . .	101
29. Response Variables vs. Control Variables . . . . .	103
30. Short Beam Shear Strength vs. Response Variables . . . . .	104
31. Laboratory-Scale Pultruder . . . . .	108
32. Pultruder Die. . . . .	109
33. Pulling Force vs. Relative Thickness for Epoxy Prepreg Tapes . . . . .	114
34. Pulling Force vs. Temperature for Epoxy Prepreg Tapes . . . . .	116
35. Viscosity and Pressure vs. Time for Epoxy Resins . . . . .	118
36. Density-Area Ratio for Hy-E Epoxy Prepreg Tape . . . . .	122
37. Density-Area Ratio for E 702 Epoxy Prepreg Tape . . . . .	123

## LIST OF SYMBOLS

The symbols and their dimensions, in Syst eme International (SI) units, are listed below. Any test values which were recorded or reported in customary units were reduced and analyzed in those units, and the results were converted to SI units to minimize conversion and round-off error.

A	area, $m^2$
c	specific heat, J/kg-K
C	concentration, $kg/m^3$
E	energy, J/kg or $J/m^3$
f	fraction of reaction completed, fiber volume fraction, dimensionless
F	force, N
h	half thickness, m
H	enthalpy, J; reaction heat, J/kg
k	reaction rate constant, $sec^{-1}$ ; thermal conductivity, $\frac{W}{m-K}$
K	compressibility modulus, Pa
l	die length, m
m	mass, kg
n	reaction order; number
N	dimensionless number; rotational speed, rev/sec
p	pressure, Pa
r	reaction rate, $sec^{-1}$ ; radius, m

R	gas constant, $8.314 \frac{\text{J}}{\text{kg-K}}$
s	pulling speed, m/sec
t	thickness, m
T	temperature, K
w	width, m
$\alpha$	thermal expansion coefficient, $\text{K}^{-1}$ ; thermal diffusivity coefficient, $\text{m}^2/\text{sec}$
$\Delta$	increment
$\eta$	viscosity, Pa-sec
$\theta$	time, sec
$\mu$	friction coefficient, dimensionless
$\rho$	density, $\text{kg}/\text{m}^3$ ; specific gravity, dimensionless
$\tau$	stress, Pa
$\phi$	microwave power, W

## Subscripts:

ad	adiabatic
A	Arrhenius
b	back flow
C	Coulomb
D	Damköhler
h	heat-up
k	kinetic
m	microwave
o	initial, limiting
p	processing; pressure
r	residence
s	sliding friction

t thermal

v viscous drag

## CHAPTER 1

### INTRODUCTION

Fibrous composite materials have had a long and useful history (ref. 1,2), from straw-reinforced sun-baked bricks of antiquity to the mechanical and structural spacecraft components of modern times. Such composites are used today because many of the material properties can be tailored to a particular application, and because some of the properties (e.g., specific strength and modulus) are higher than those of non-composite materials. Like concrete, another ancient composite, fibrous composite materials and the components which they form are generally made simultaneously. As with all good things, however, fibrous composite materials have some limitations. For example, these materials have a high degree of property anisotropy, an aspect which may trouble designers who have long worked with isotropic materials. Further, the properties in a given direction may vary from part to part, due, in large measure, to variations in processing. Such variation can result from inexact process monitoring and control. Finally, fibrous composite materials can be very expensive, in part because the constituents may be costly, but more often because such composites require a large amount of hand labor.

One relatively economical method of making fibrous composite materials, a method which is capital intensive rather than labor intensive, is pultrusion. Pultrusion is a process for manufacturing composite materials in which resin-impregnated fibers are pulled at a

constant speed through a heated die which shapes the resin-fiber mass to a predetermined cross section and cures the resin to some extent (ref. 3-5). A schematic of the process is shown in figure 1, and some representative pultruded stock is shown in figure 2 where the wide-flange beam section has a height of 150 mm. The name pultrusion may have arisen because, as in extrusion, the material being processed passes through a heated shaping die. Unlike extrusion, in which the material is pushed by a pressure gradient, in pultrusion the material is pulled through the die. Although the word pultrusion is not in widespread use, it apparently does convey some feel for shaping and pulling even to a non-technical person (ref. 6). The referenced article is a fictional recounting of yearly medical expenses for income tax purposes. Whatever the origin and implications of the word, the pultrusion process is a continuous one which takes place at equilibrium with very little attention required of the pultrusion machine operator. Like the process for making plywood, another composite material, the pultrusion process can provide material of a fixed cross section and of unlimited length. Handling and transportation considerations will, however, place a limit on the length. The pultrusion process has been used to make a wide variety of parts and components for structural, electrical, agricultural, and chemical processing applications. The use in these applications derives from the high unidirectional strength, high electrical resistivity, and high corrosion resistance of pultruded stock. Finally, the pultrusion process has a largely unrealized potential for in-process control and material inspection. Such control and inspection, if applied, would

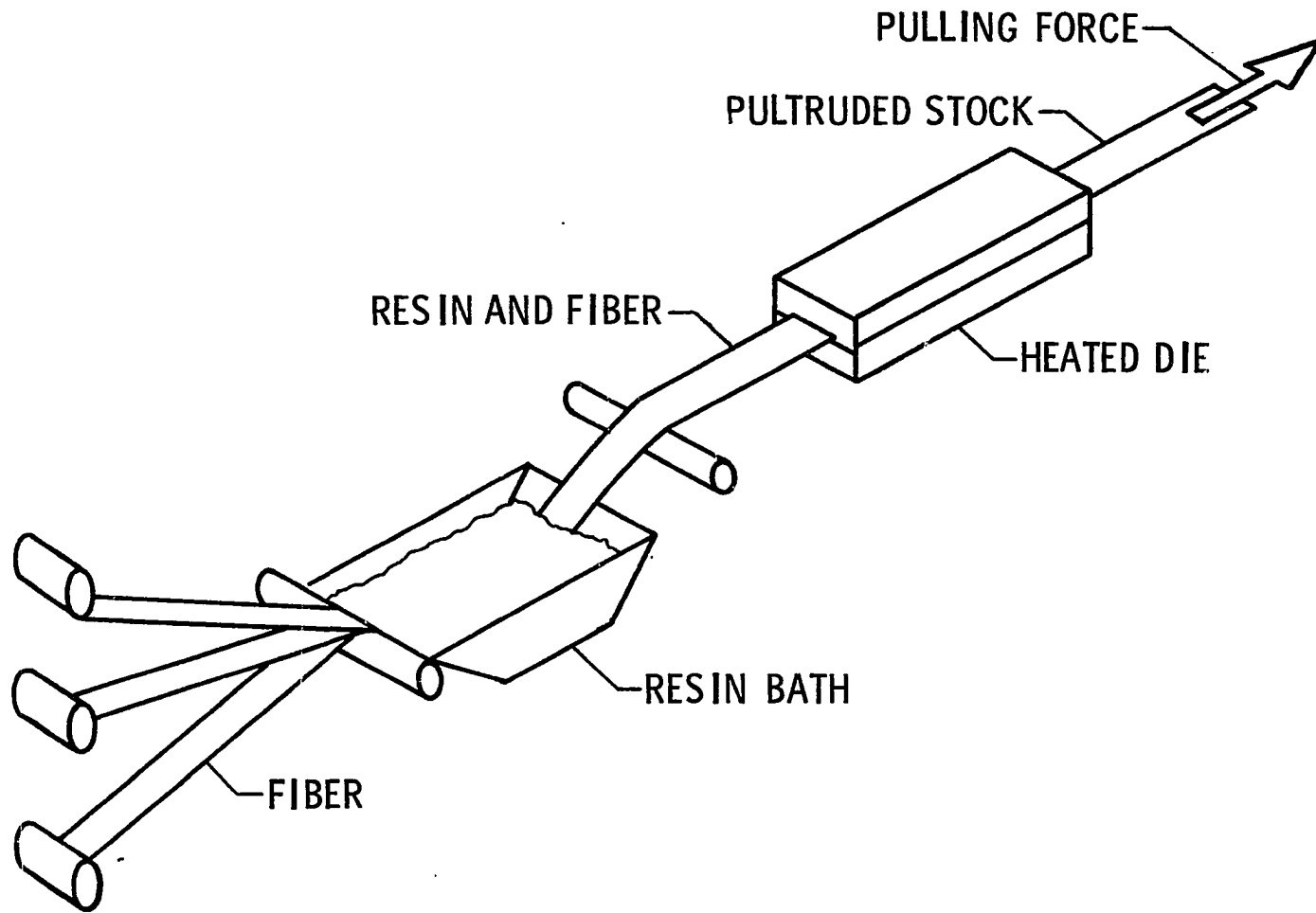


Figure 1.- Schematic of pultrusion process.



Figure 2.- Representative pultruded stock. Nominal height of the wide flange beam section is 150 mm.



lead to pultruded stock with a minimum variation in part-to-part properties.

As might be expected, the pultrusion process has some limitations. Much of the work which has been reported on the process (to be reviewed in a later section) has been of a cut-and-try nature. No doubt many pultrusion machine operators have a good working knowledge of the important process parameters and of the relationships among these parameters. But such knowledge does not seem to be widely disseminated, and much empiricism is still involved in the process. In addition, most of the experience in pultrusion has been obtained using polyester resins on glass fibers. These materials account for an estimated 90 percent of all pultruded stock made in this country (ref. 3). Obviously, much less experience is available using materials such as epoxy resins on graphite fibers. As the latter materials are far more costly than the former, the empirical approach to developing suitable process parameters becomes prohibitively expensive. Consequently, the potential cost savings of the pultrusion process are not being realized for more advanced and more expensive materials.

In response to this situation--a limited understanding of the process and limited application to newer materials--an investigation was made of the pultrusion process. The objective of the investigation was to develop a model of the process as that process applies to thermosetting resins. The intent was to express the model in both pultrusion material properties and in pultrusion machine parameters. The usefulness of such a model would be in the estimate of resin cure,

given the material properties and machine parameters, and in the estimate of how well new, untried materials could be pultruded. The approach used to develop the model is discussed in a later section. Briefly, tests and analyses were made of several present and potential pultrusion materials. An analysis was made of two pultrusion processes which had been used to make geometrically simple (circular rods and flat sheets) pultruded stock. The model developed from these tests and analyses was tested and modified on a laboratory-scale pultruder which was constructed for the purpose. The approach to this investigation then, was:

- (i) Test and analyze several present and potential pultrusion materials (Chapters 4, 5, 6).
- (ii) Analyze two pultrusion processes using known information on the process (Chapter 7, 8).
- (iii) Develop a model from the tests and analyses and test it on a laboratory-scale pultruder which was constructed for that purpose (Chapter 9).

The results of the investigation are reported in this paper.

## CHAPTER 2

### REVIEW AND APPROACH

#### Review of Previous Work

A review of the publications on pultrusion (ref. 3-5, 7-41) shows very clearly that, in this process at least, the art leads the science. The emphasis has been on operations, products and applications rather than on exploring and elucidating fundamentals. The large number of publications in recent years which have come from commercial and industrial interests attests to the economic importance of pultrusion. With a few exceptions to be noted below, most of these publications deal with the pultrusion process in a general way, being much more specific on the properties and applications of pultruded stock.

The properties of pultruded stock have received considerable attention (ref. 10, 12, 13, 15, 18, 23, 27, 28, 29, 32, 33, 36). Some of these investigations have been concerned with measuring the properties (ref. 15, 28, 32, 33). Others have compared pultruded properties to those of composites made by more conventional means (ref. 12, 15), while some have dealt with pultruded properties as they pertain to design and applications (ref. 10, 13, 18, 27, 28, 29, 36). As for applications of pultruded stock, most of the reports (ref. 21, 24, 28, 29, 31, 34, 37, 38, 41) tend to expound the advantages of using pultrusions in a particular application.

In contrast to the work on pultrusion properties, relatively few results have been reported on the characteristics of the resin and

fiber. One report on polyester resins (ref. 35) recommended that a four-zone temperature control be maintained along the die length. This control would give a profile which would be changed as the pulling speed was changed. This recommendation was based on experience rather than on test or analysis. Another investigation (ref. 23) was made of polyester resin and E-glass fiber. The die temperature and pulling speed (450 K, 5 mm/sec) was the same for all runs, and the procedure for impregnating the fibers with the resin was varied.

The concern of this investigation, however, was not applications or even properties, although some properties were measured. The main concern was with the pultrusion process itself.

The process which is now called pultrusion was developed as a way of making better fishing rods (ref. 7). The argument in favor of the process was that bamboo fly rods had variable flexibility, and that the process of tying together bamboo splits to obtain the right flexibility was costly. Such an argument reflects a valuable composite material concept (tailor properties as needed) and a pultrusion process advantage (reduce manufacturing costs). Another advantage of pultrusion was recognized early (ref. 8). This is the advantage of having the fibers under tension as the resin cures. Then, when the composite material is put under a mechanical load, the load is taken immediately by the high strength fibers, not by the low strength matrix. This concept is similar to that used in prestressed concrete in which the steel reinforcing strands are loaded in tension while the concrete member is still in the mold.

Although specialized machines and processes have been patented (ref. 5, 7, 8, 11, 40), the pultrusion process can take several forms (ref. 4,9) and many people have developed their own equipment (ref. 10, 12, 14, 16, 17, 18, 20, 23, 25, 26, 29, 30). This equipment has been used to make such pultruded products as structural and building components (ref. 10, 16, 18, 29), aerospace components (ref. 23, 25, 30, 39), and reinforced aluminum tubes (ref. 26). Some of the equipment originated in a laboratory investigation and developed to a semi-production machine (ref. 20, 26). Although most pultruders use a "wet" method of pulling the fibers through a resin bath and then into the heated die (fig. 1), at least one (ref. 25, 39) used a "dry" method in which previously prepared resin-impregnated collimated fibers (prepreg tape) was pulled through the die.

The pultrusion process itself has been described in general terms and investigated to some degree. Some reports (ref. 4, 16, 25) make some general statements about what should or should not be done. Other reports provide more specific information on the process and its parameters. For example, reference 5 identified two major considerations in pultrusion (resin reaction and cross reinforcement), cited a pulling speed of .3-1.0 m/min for a 1 m die, and mentioned possible fiber displacement due to high hydrostatic pressures generated by excess resin at the die entrance. In a similar vein, reference 12 pointed out that such die entrance resistance can be useful in maintaining fiber tension and reported a pressure there of 140-310 kPa (20-45 psi) for a .5 fiber fraction. Also (ref. 12), the resin exothermic temperature and gel time were measured for a combination of resin and fiber. This procedure

is in contrast to the more common practice of making such measurements on pure resin alone. The work with a laboratory-scale pultruder described in reference 12 was carried further and included the construction of a pilot-scale pultruder described in reference 20. This later pultruder had electrically-heated aluminum dies 150 mm long. The die mount had a strain gage so the total friction between the die and the resin-fiber mass could be measured. Shorter dies developed less friction, but, for a given die length, the friction was higher if the resin cured early. Friction was higher at the higher carbon fiber loadings, and a fiber fraction above .6 was not practical. By contrast, glass fiber fractions may approach .75 (ref. 29). As in the previous investigation, the exothermic temperature and gel time was measured with a resin-fiber combination. Accelerators were used in the epoxy resin to reduce gel time and to make lower curing temperatures practical.

Very few investigations have been reported in which the starting materials were characterized, the process parameters varied, and the pultruded stock properties measured. In one investigation (ref. 39) the parameters were varied and the properties were measured, although no analysis of the data was made. The results of that investigation will be analyzed in a later section of this report. Two investigations of the process (ref. 19, 22, 27) have dealt with a wide range of processing parameters and properties of the pultruded stock. One investigation (ref. 22, 27) reported on various factors which must be considered in pultruding epoxies by both the "wet" and "dry" methods. For example, amine curing agents were preferred over anhydride agents

because adhesion between resin and die was a problem with the latter agent. The room temperature viscosity remained low enough for good fiber impregnation even when the resin contained 14 percent metaphenylene-diamine. Attempts to pultrude epoxy-graphite prepreg tapes were not successful. The problem was that the semi-solid resin did not melt sufficiently to provide the needed flow and curing in the die.

A more fundamental investigation (ref. 19) examined the process parameters and the interaction between material characteristics and those parameters. The approach taken was that the pultrusion process is concerned with cure temperature-pressure-time relationships and with force-time relationships between the die and the resin-fiber mass. Experiments were made to follow the temperature rise in 25 mm (1 inch) diameter rods of polyester resin and E-glass fibers (roving, mat, and cloth). Similar experiments showed the advantage of using a radio frequency preheat of the resin-fiber mass. With the pre-heating, the cure was faster and the exothermic temperature was lower than was the cure without pre-heating. In order to measure forces, a production pultruder was fitted with strain gages on the die and central mandrel mount. A 25 mm (1 inch) diameter tube with a 1.6 mm (.06 inch) wall was pultruded at pulling speeds up to 30 mm/sec. (1.2 in/sec). The total force (on die and mandrel) increased with pulling speed up to about 25 mm/sec (1 in/sec). At this speed the force was about 1 kN (225 lbf), and the resulting average shear stress (between resin-fiber mass and the die and mandrel) was 26.3 kPa (3.8 psi). A special apparatus was constructed to measure the shear stress between a curing resin-fiber mass and a steel die. The stress generally was

low for most of the curing time, seldom exceeding 10 kPa (1.5 psi). However, the stress showed two peaks during curing, reaching stresses as high as 56 kPa (8.1 psi) for a few seconds. The investigation reported in reference 19 touched briefly on a number of important considerations in pultrusion, and provided some values of the temperatures, times, and forces which might be expected.

In general, then, previous work on pultrusion has been concerned largely with properties and applications of the pultruded stock. Relatively little work has been reported on the process itself, with virtually no attempts being made to put the process on a fundamental footing.

#### Approach to Present Investigation

All physical systems, including composite material processing, must satisfy the fundamental laws of the conservation of mass, energy, and momentum. As the laws apply to the pultrusion process, they are highly coupled, with the mass balance being influenced by the energy and momentum transfer, and so on. In order to make the analysis and description of the pultrusion process tractable, some uncoupling of the laws was necessary. However, in order to avoid an oversimplified and inaccurate model, some coupling had to be retained. With the requirements and complexities of the conservation laws in mind, the pultruder die was regarded as both a reactor and a rheometer, and the process analysis was made accordingly.

The pultruder die was regarded as a plug flow, packed bed, chemical reactor in which low molecular weight resin was converted through molecular weight increase and crosslinking into a glassy



composite material matrix. The plug flow description arises from the flat velocity profile over the cross section of the resin-fiber mass, with steep velocity gradients in a thin layer at the interface between the resin-fiber mass and the die wall. The packed bed description arises from the high concentration of fibers which exert a moderating effect on the chemical reaction, i.e., the curing of the resin from the liquid to the solid state. Chemical reactor analysis has been highly developed and widely applied (ref. 42-44) and concerns mainly the mass and energy balances and the interaction between them.

The pultruder was regarded as an isothermal, constant flow rate, slit rheometer. The die was taken to be isothermal although some temperature gradients would certainly exist in a real die. The constant flow rate description arose from the equality of the entering and emerging masses even though the molecular weight and physical form of those masses was different. The slit rheometer (ref. 45 and 46) is one which is sensitive to both the normal and shear forces at the interface between the resin-fiber mass and the die wall. Such forces act on a pultruder die and influence both the pultrusion process and the pultruded material. As a chemical reaction takes place along the long axis of the rheometer, the concerns are the mass and force (momentum) balances and the interaction between them.

With the reactor-rheometer concept as a basis, a model of the pultrusion process was developed by testing materials and analyzing processes. Kinetic, thermal, and rheological measurements and analyses

were made on present and potential resins to determine properties which would be useful in developing a process model. An analysis was made of an isometric (constant volume) process and of an isobaric (constant pressure) process to determine relationships among some material properties and processing variables. The model developed from these tests and analyses was tested and modified with the aid of a laboratory-scale pultruder using two types of epoxy-graphite prepreg tape.

## CHAPTER 3

## MATERIALS, TESTS, AND NUMERICAL METHODS

## Materials

The polyester and epoxy resins which were used in this investigation are listed in table 1. The polyesters represented the traditional pultrusion resins which are cured through the decomposition of peroxide initiators. The orthophthalic ester (SR 6325) contained styrene as a reactive diluent while the vinyl ester (V 7001) contained toluene. The diallylphthalate (Formulation A) was an experimental resin which did not have the vapor emission problem of the other two polyesters. However, the viscosity of the resin was so high that a heated resin bath would be necessary so the resin could impregnate a fiber bundle. This resin might be more useful as part of a prepreg tape.

The epoxies were of the 395 K (250°F) service type and thus represented a modest advance over the service range of the polyesters. A previous investigation (ref. 22, 27) has shown that amines are preferable to anhydrides as epoxy curing agents because the anhydrides cause adhesion between the resin-fiber mass and the steel die. Three of the epoxies in table 1 were used in the form of prepreg tape, and some tape properties are given in table 2. The tape fiber was 6000-filament Thornel 300 graphite fiber. The tapes were made in .3 m (12 in.) widths and then slit to a 20 mm (.8 in.) width for testing. Although no information was available on the resin composition, all three proprietary resins were assumed to be of the diglycidyl ether of

TABLE 1. - THERMOSETTING RESINS INVESTIGATED

Resin	Room Temperature State	Description/Source
Polyester		
SR 6325	Low Viscosity Liquid	Orthophthalic, benzoylperoxide (BPO) initiator; PPG Industries
V 7001	Low Viscosity Liquid	Vinyl, benzoyl peroxide (BPO) initiator; Koppers Corp.
Formulation A	Tacky Semi-solid	Diallylphthalate; tertiary butyl perbenzoate (TBPB) initiator; Celanese Research Co.
Epoxy		
Epon 828	Viscous Liquid	DGEBA, metaphenylene-diamine (MPDA) curing agent; Shell Chemicals Co.
F 979	Tacky Semi-solid	Proprietary 395 K (250°F) service epoxy on Thornel 300 (6K) graphite-fibers; Fiberite Corp.
E 702	Tacky Semi-solid	Proprietary 395 K (250°F) service epoxy on Thornel 300 (6K) graphite fibers; U. S. Polymeric
R 5209*	---	Proprietary 395 K (250°F) service epoxy on Thornel 300 (6K) graphite fibers; Narmco Materials, Inc.

\*Tested in prepreg form only but included here for completeness.

TABLE 2. - PREPREG TAPES INVESTIGATED

Tape	Nominal Ply Thickness mm (in)	Fiber Areal Weight, g/m <sup>2</sup>	Resin Content, weight percent	Volatiles, percent
Rigidite 5209-T300	.157 (.0062)	146	38	--
Hy-E 1079 C	.170 (.0067)	178	32	<1
E702/T300 (6K)	.139 (.0055)	146	32	<1

bis-phenol A (DGEBA) type. However, no attempt was made to analyze the proprietary resins. Of the four epoxy resins, one (Epon 828) was used in resin form only, two (F 979 and E 702) were used in both resin and prepreg tape form, and the remaining one (R 5209) was used in tape form only.

#### Tests

Thermal and mechanical tests were performed on resin, prepreg tape, and on pultruded stock. The tests of resin and prepreg tape were made to observe curing-induced changes in the resin. The pultruded stock tests were made to determine the effect of the pultrusion process on the stock properties.

A differential scanning calorimeter (Perkin-Elmer DSC-1) was used to measure the kinetic parameters of both resins and prepreg tape. The temperature rates were 10, 20, 40, and 80 K/min, and the sample mass was 5-10 mg for the resins, and 15-25 mg for the tapes. The DSC has been used extensively (ref. 47-49) for kinetic studies but very little in composite materials processing. The enthalpy rate-temperature curves generated in the test were manually read at 1 K (1.8°F) intervals. These data were reduced with the aid of a programmable calculator (Wang 2200S) to obtain the heat of reaction, as well as the reaction rate constant and fractional conversion with temperature. The reaction rate constants were then used to obtain reaction order, activation energy, and pre-exponential constant for the Arrhenius reaction rate expression.

The change of resin viscosity during curing was measured as a function of time on a rotary rheometer (Instron 3250) using the cone

and plate mode. The rheometer, described in detail in reference 50, is shown in figure 3. A 20 mm-radius, .018 radian cone was used and the strain rate was  $1 \text{ sec}^{-1}$ . During the test, simultaneous measurements were made of the torque and normal force. The semi-solid resins were frozen on solid carbon dioxide to facilitate handling. Once on the pre-heated plate, however, they melted quickly.

A mechanical testing machine was used to make room temperature diametral tests (ref. 32, 51) and notched shear tests (ref. 33, 52) of pultruded circular rods. The crosshead speed was set so that the strain rate was 1.3 percent per minute for both types of tests irrespective of the test specimen size. Short beam shear tests were made at room temperature on pultruded flat sheet. A 13 mm (.5 inch) span was used, the nominal span-to-depth ratio was four, and the nominal width-to-thickness ratio was two.

#### Numerical Methods

Numerical methods were used with a programmable calculator to reduce data as noted for the DSC tests. The calculator was also used to evaluate an integral relating dimensionless time, temperature, and temperature rise for an adiabatic reaction. All calculator programs were written in BASIC language.

An existing finite difference program (ref. 53), written in FORTRAN language for a Control Data 6000 series digital computer, was used to estimate the spatial and temporal distribution of temperature in a given cross-section of a resin-fiber mass. The program, as written, applied only to heat transferred through and heat stored in the material. The first author of reference 53 modified the program to

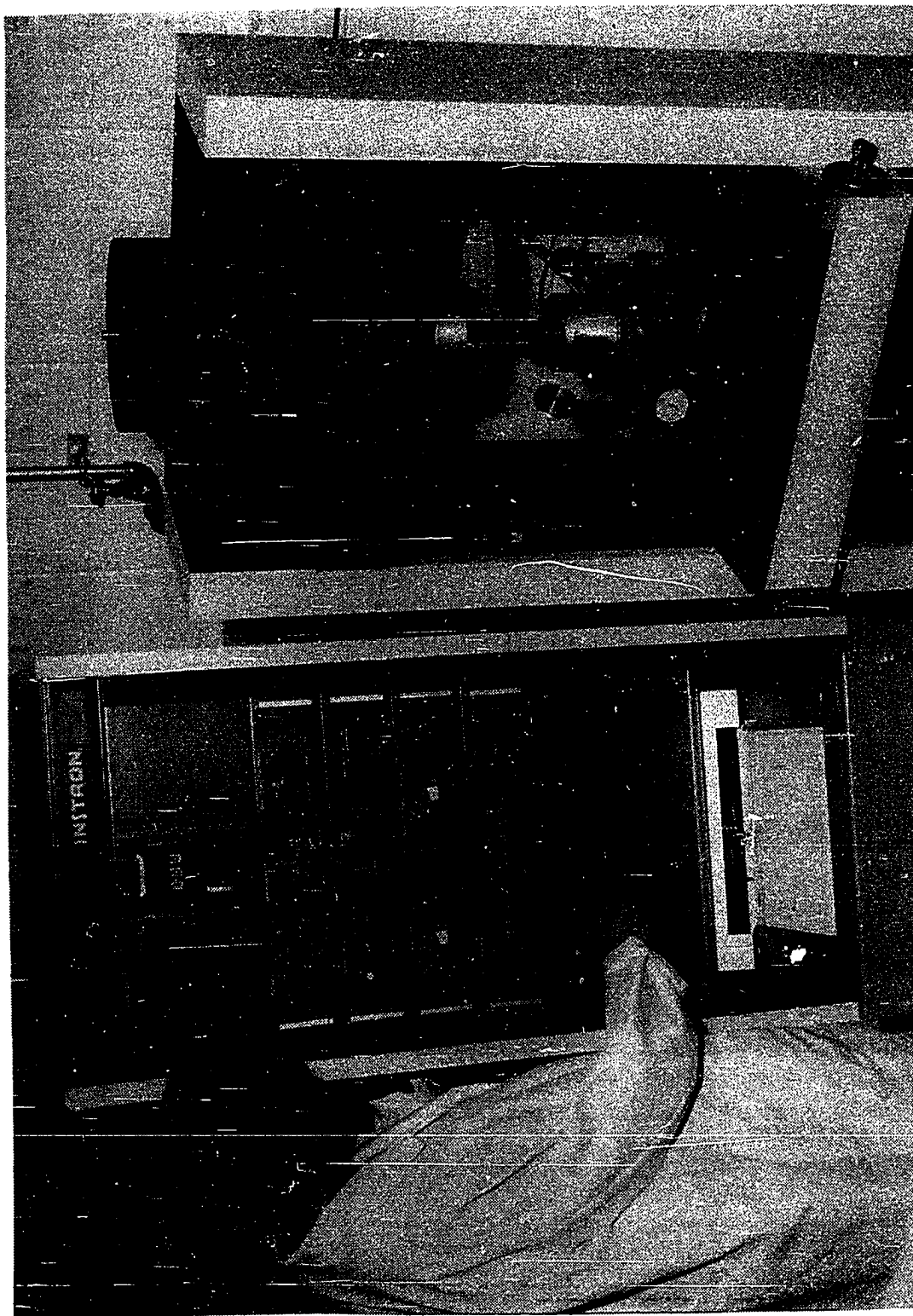


Figure 3.- Rotary rheometer showing control console and test frame.



include a heat generation term as well, thereby making the program applicable to thermosetting resins.

The coordinate systems used to show the estimated temperature distribution are shown in figure 4. The choice of the systems was based on the observations that the speed of the resin-fiber mass is uniform along the die length, and that pultruded stock often has a high width-to-thickness ratio. The aspect ratio for the stock shown in figure 2 ranged from about 11 to nearly 50. The x-axis was aligned with the motion of the resin-fiber mass. By virtue of the uniform speed through the die, the x-axis can also be thought of as a time axis. Heat transfer takes place from the die to the resin-fiber mass in the thickness direction and the y-axis was so aligned. The z-axis was then aligned with the width. The origin of the system was set at the front edge of the die equidistant from the die surfaces.

Hence, the temperature along any y-axis, as it moves through time  $\theta$ , can be represented by a time-temperature-distance solid as shown in figure 5. This figure shows three stations in the y direction at which the temperature is to be estimated. All the temperatures have been estimated at time  $\theta$ . For an increment of time  $\Delta\theta$ , the temperature of  $y_n$  is estimated from the  $y_{n+1}$ ,  $y_n$ , and  $y_{n-1}$  temperature at time  $\theta$ , plus the  $y_{n+1}$  and  $y_{n-1}$  temperatures at time  $\theta + \Delta\theta$ . As these latter two temperatures have not yet been estimated, the program must solve a set of simultaneous equations, one equation for each station in the y (thickness) direction. The resulting tri-diagonal matrix is solved by Gaussian elimination.

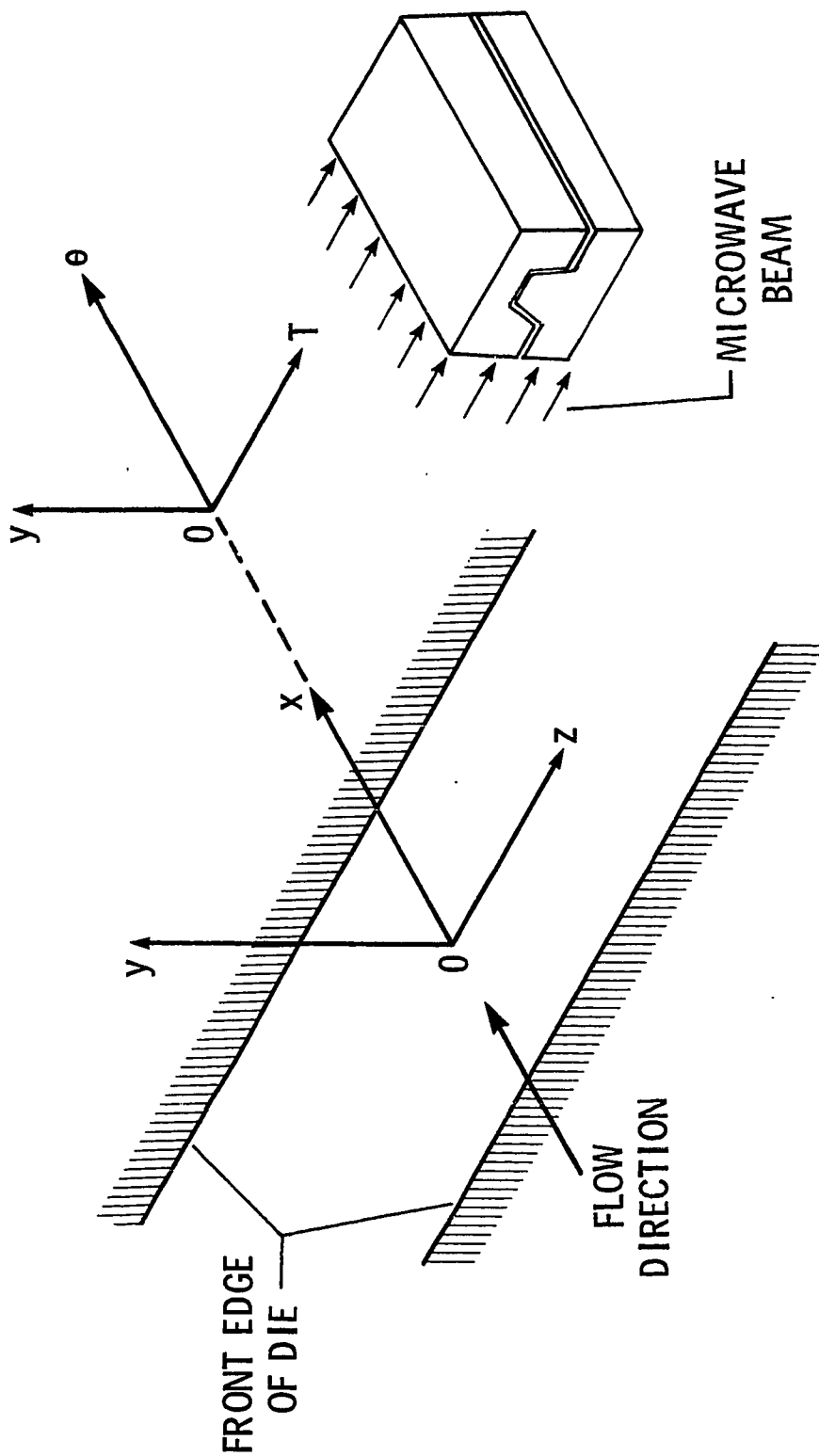


Figure 4.- Coordinate systems used in this investigation.

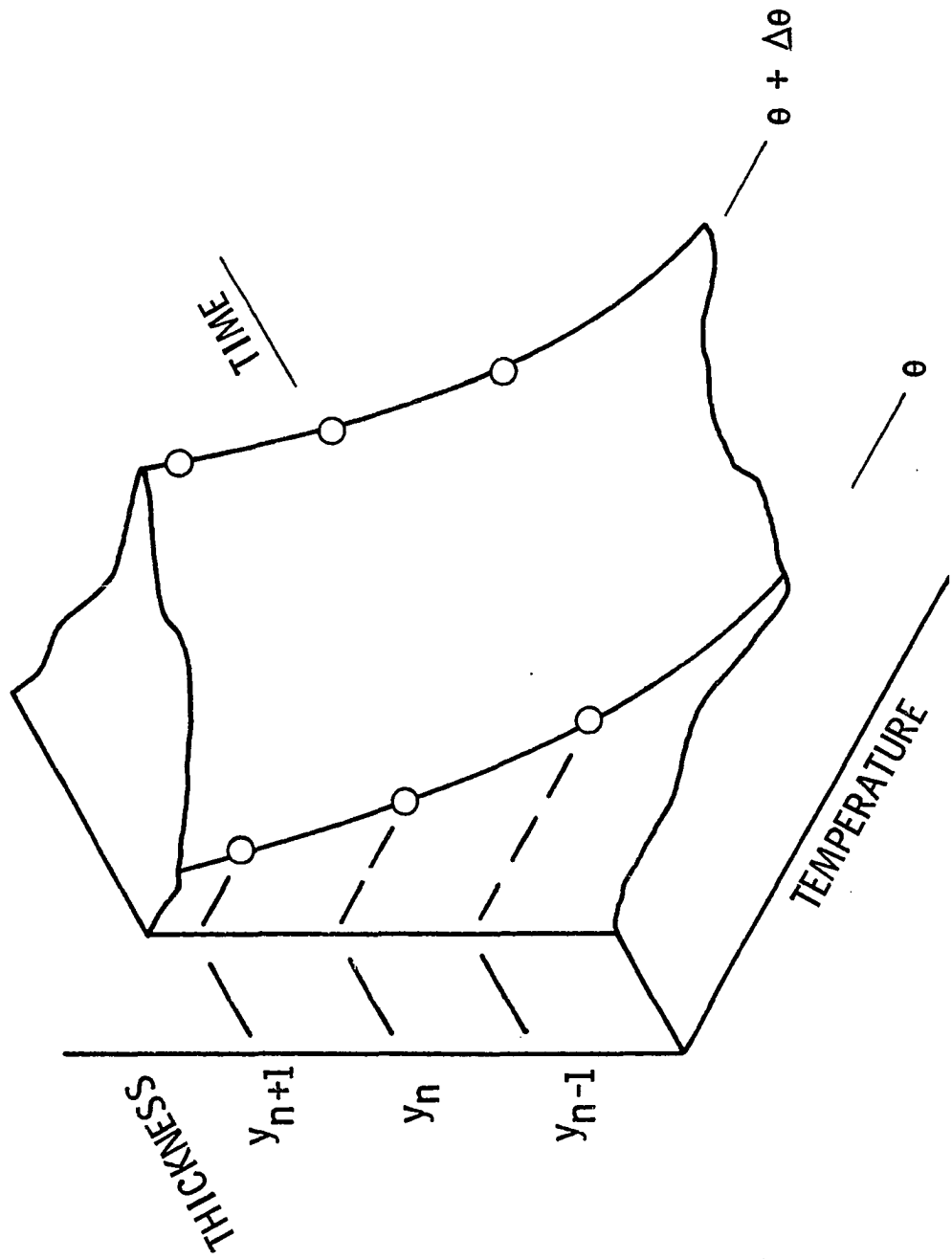


Figure 5.- Distance-time-temperature relationship for making finite difference estimate of temperature in resin fiber mass.

## CHAPTER 4

## MASS BALANCE IN A PULTRUDER DIE

Upon first consideration, a mass balance for a pultruder die might be regarded as a very simple, straightforward exercise. The cavity cross section is uniform along the die length, pulling speed is constant, no materials are introduced or extracted along the die length, so the mass exiting the die must equal the mass entering. However, while the total mass within the die is constant, the components and properties of that total mass undergo considerable change. Specifically, the low molecular weight, liquid resin reacts in the die (reactor) and changes into a higher molecular weight, crosslinked, solid matrix of a composite material. The usefulness of the material will depend to a large degree on the rate and extent of that reaction. Although the mass change and energy change are strongly coupled in a chemical reactor, they are treated separately in this report both for clarity and for emphasis.

## Cure Analysis by Differential Scanning Calorimetry

A basic assumption which was made in this investigation was that the cure reaction could be described by n-th order kinetics. If mass diffusion is small relative to the reaction, then the reaction rate,  $r$ , can be expressed

$$r = \frac{dC}{d\theta} = -kC^n \quad (1)$$

where  $C$  is the concentration of reactants. The reaction rate constant  $k$  is invariant with concentration and with time at a given temperature; however, the value of  $k$  is temperature dependent. This temperature dependence is often described by the Arrhenius expression

$$k = k_0 \exp - \frac{E_k}{RT} \quad (2)$$

The three kinetic parameters,  $n$ ,  $k_0$ ,  $E_k$ , appearing in equations 1 and 2 provide a way of describing how a cure reaction will proceed. The reaction order  $n$  is usually a small integer (0,1,2,3) or the ratio of small integers (1/2, 3/2). The reaction order, which must be determined by experiment, indicates the influence of concentration on reaction rate. The pre-exponential factor  $k_0$  can be thought of as the value of the reaction rate constant for an infinitely large temperature. The activation energy  $E_k$  is a reflection of how rapidly the reaction takes place over a temperature range. A high value of  $E_k$  indicates a sharp, rapid reaction taking place over a relatively narrow temperature range.

A widely used instrument for determining the three kinetic parameters of a cure reaction (ref. 54-56) is the differential scanning calorimeter (DSC). In the DSC, a test sample and reference sample are heated in such a way as to raise their temperature at a constant rate. The differential in the heat required for each sample depends only on their respective densities and specific heats as long as no reaction or

phase change takes place. When the test sample undergoes a reaction, the amount of heat required to maintain the temperature rise rate changes. If the reaction is endothermic, more heat is required; if exothermic, less. An idealized DSC test curve is shown in figure 6. The reaction typical of thermosetting resins results in an exothermic "bulge" in what would otherwise be an essentially straight baseline. The fundamental assumption in DSC analysis is that the area under the curve, bounded by the baseline, is proportional to the heat of reaction to the material. That is, when the curve returns to the baseline from its exothermic excursion, the moles which have reacted equal the moles available for reacting. Moreover, at an intermediate temperature  $T_i$ , the moles reacted are proportional to the heat evolved. Referring to figure 6, the moles reacted and the heat evolved at  $T_i$  are proportional to the ratio  $A_i/A$ , where  $A_i$  is the area to the left of the  $T_i$  ordinate and  $A$  is the total area under the curve.

Three different methods, all using the fundamental assumption described above, have been developed for extracting kinetic parameters from DSC tests. One method (ref. 57) uses an isothermal test and a four-parameter model. A second method (ref. 58) takes into account the dynamic effect of the temperature rate on the results. The third method (ref. 59) is probably the most widely used of the three and was used in this investigation. The reaction rate constant  $k_i$  at temperature  $T_i$  (see figure 6) is

$$k_i = \frac{(A/C_o)^{n-1} \partial H_i / \partial \theta}{(A-A_i)^n} \quad (3)$$

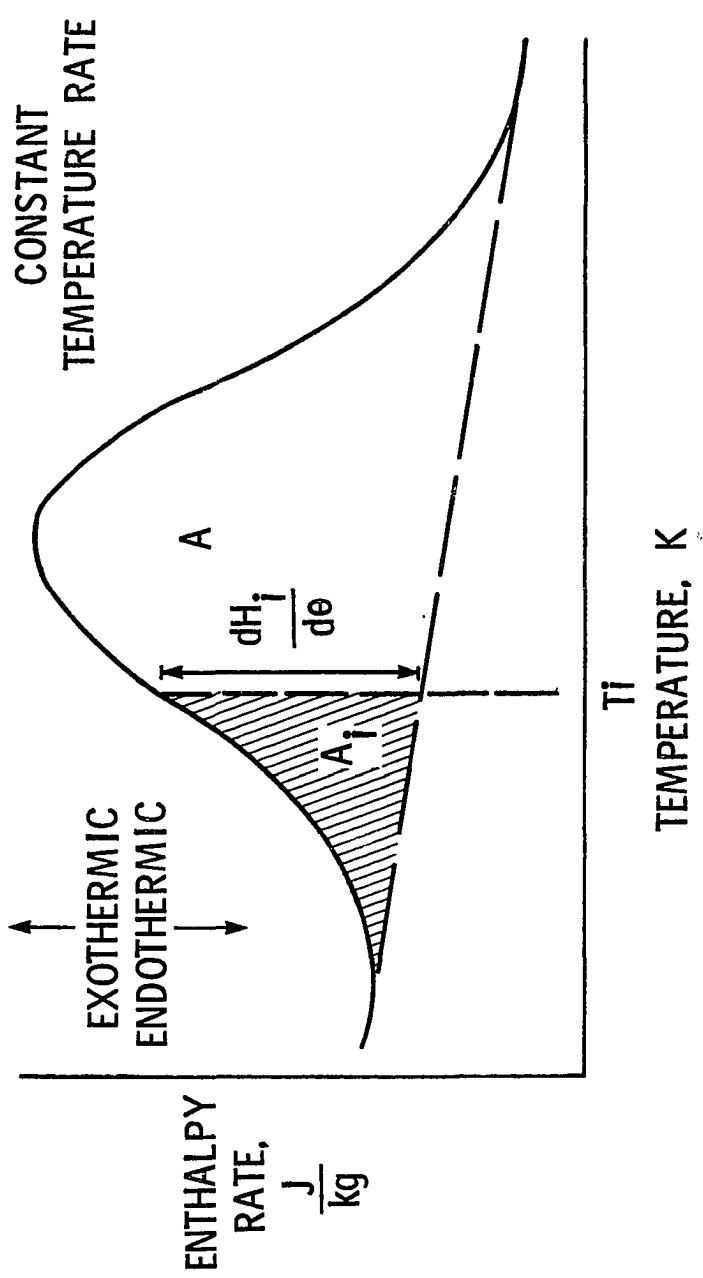


Figure 6.- Idealized DSC curve.

The curve height  $\partial H/\partial \theta$  for each one degree temperature increment was used to calculate  $k$  for four assumed reaction order,  $n=1/2, 1, 1-1/2, 2$ . For each assumed order for each of four tests at different temperature rates, three apparent reaction rate constants were used to obtain the kinetic parameters as shown in figure 7. The three points were the apparent rate at a fractional conversion of 0.5, and at temperatures 5 K and 10 K above the 0.5 conversion temperature. This procedure provided twelve points for fitting a straight line by linear regression. The  $F$  value for significant regression was used to select the best reaction order. Both mathematically and graphically (fig. 7) a reaction order of unity is better than the other assumed orders. The regression analysis also provided the slope of the line ( $E_k/R$ ), and the intersection of the line with the ordinate ( $\log k_0$ ).

#### Cure of Resin

Representative DSC curves for the polyester and epoxy resins, obtained at a temperature rise rate of 80 K/min, are shown in figures 8 and 9. The kinetic parameters are listed in table 3. The temperature range for figure 8 is 350 to 550 K, while that for figure 9 is 400 to 600 K. The SR 6325 and V 7001 resins with BPO, representative of currently used pultrusion resins, had a reaction peak which was centered in the 400-425 K range (fig. 8). Typical pultrusion temperatures range upward from  $\sim 390$  K. A higher concentration of initiator moved the peak to a lower temperature. A lower temperature rate would also move the peaks down scale. The peak for the Formulation A with tBPB resin fell some 50 K higher than that of the other polyesters,



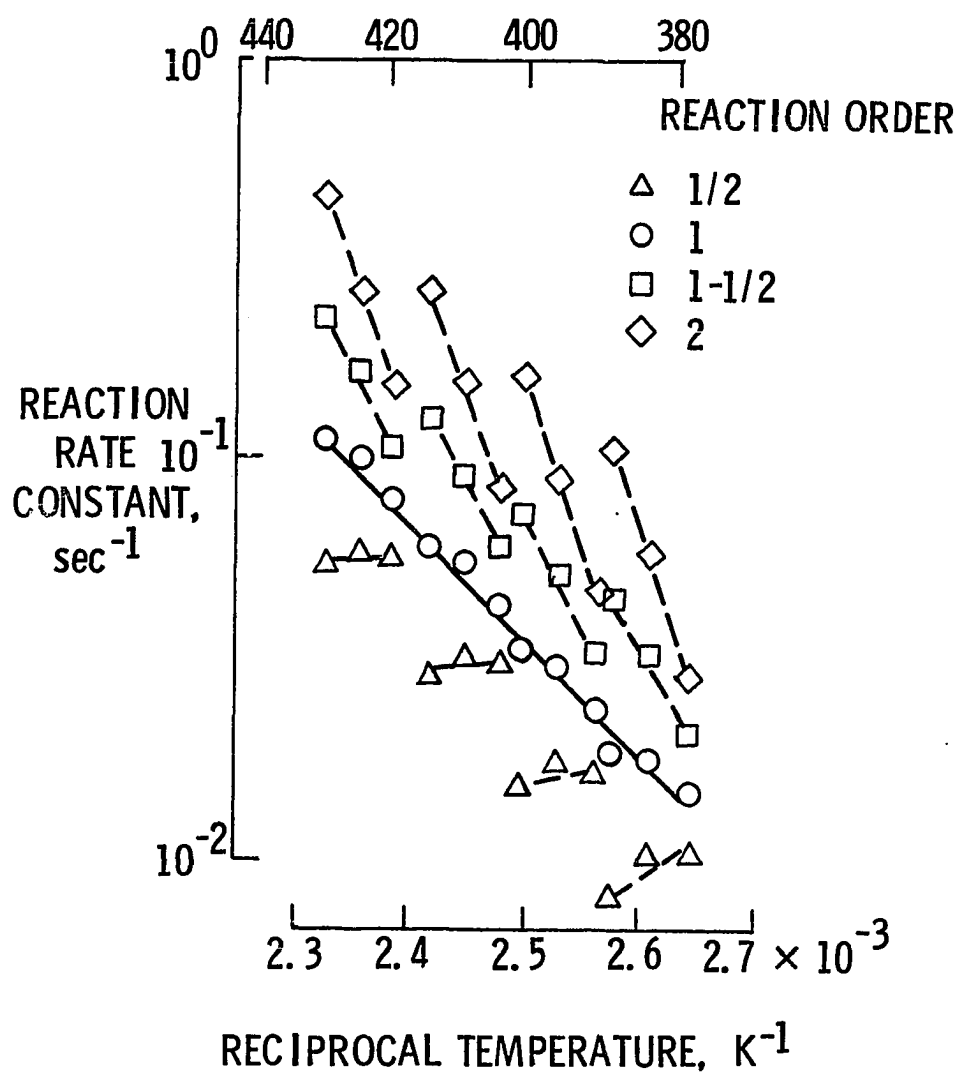


Figure 7.- Reaction rate constant as a function of reciprocal temperature for four assumed reaction orders for SR 6325 polyester resin.

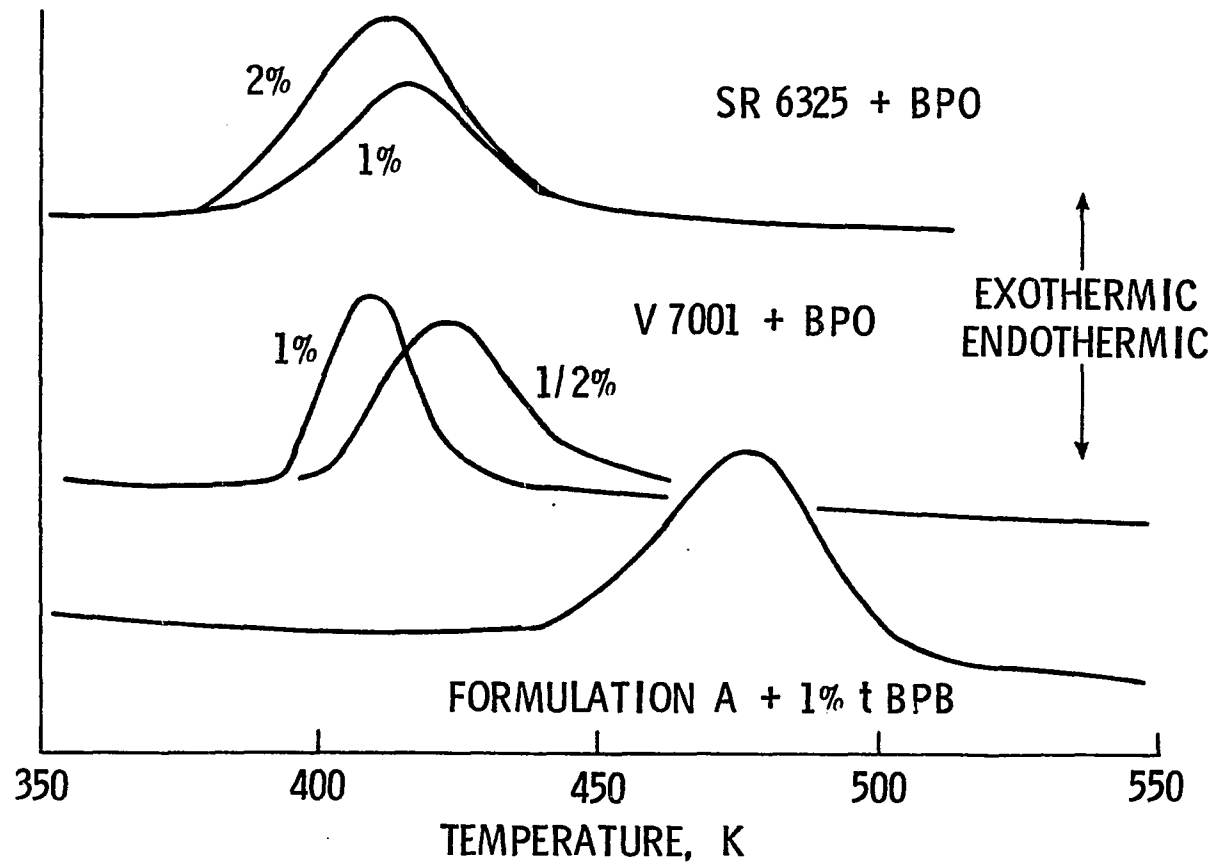


Figure 8.- DSC curves for polyester resins. Temperature rise rate was 80 K/min.

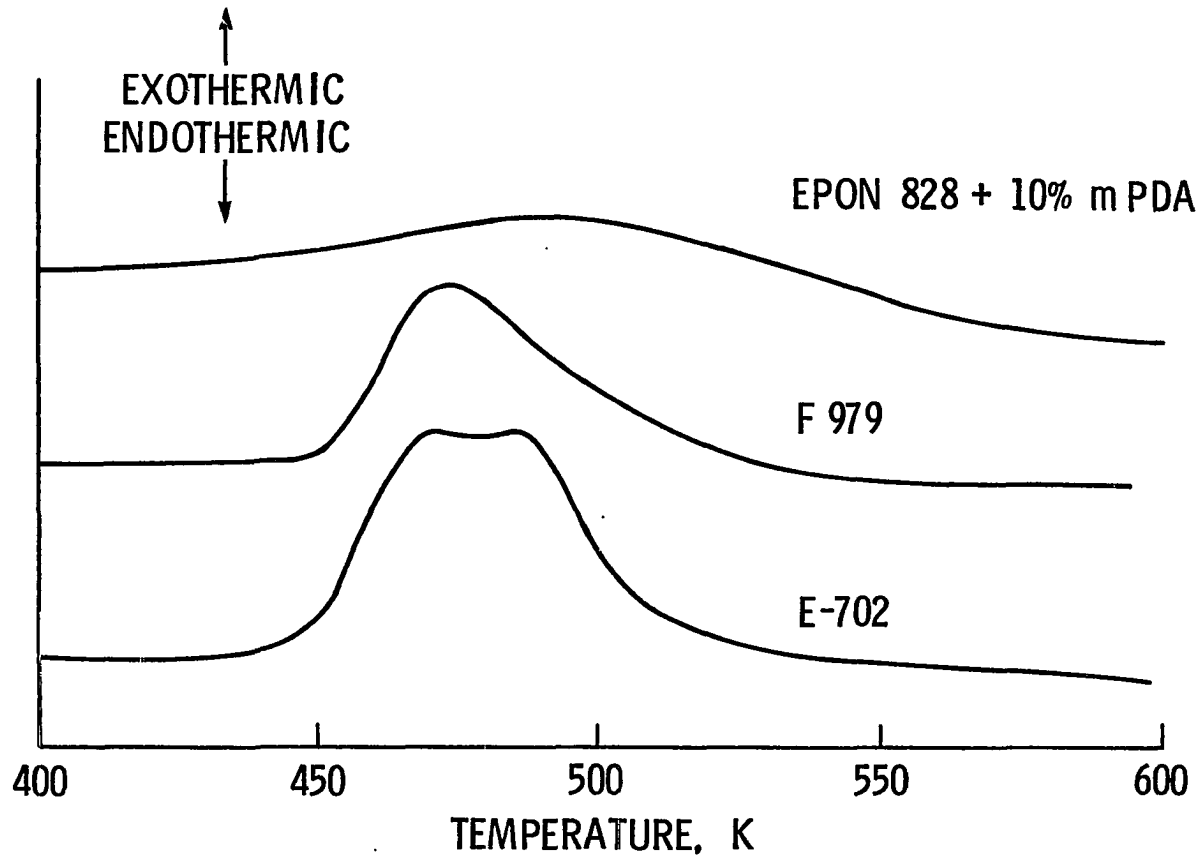


Figure 9.- DSC curves for epoxy resins. Temperature rise rate was 80 K/min.

TABLE 3. - KINETIC AND THERMAL PARAMETERS FOR  
POLYESTER AND EPOXY RESINS

Resin and Curing Agent	Reaction Order	Activation Energy kJ/mol.	Pre-exponential Constant sec <sup>-1</sup>	Reaction Heat, kJ/kg
Polyester				
SR 6325-1% BPO	1	56.3	8.22 x 10 <sup>5</sup>	302.2
-2% BPO	1 1/2	67.6	5.19 x 10 <sup>7</sup>	333.5
V 7001 - 1/2% BPO	1	47.2	4.71 x 10 <sup>4</sup>	274.9
- 1% BPO	1	58.6	2.10 x 10 <sup>6</sup>	298.4
Formulation A-1% tBPB	1	97.5	4.51 x 10 <sup>9</sup>	202.4
Epoxy				
Epon 828-10% mPDA	1	36.5	2.41 x 10 <sup>2</sup>	488.5
F 979	1	56.0	7.93 x 10 <sup>4</sup>	266.8
E 702	1/2	53.0	2.37 x 10 <sup>4</sup>	622.4

reflecting higher temperature stability of tBFPB compared to BPO. All the polyesters tested had clean, distinct reaction peaks with the DSC curve returning to the baseline at the end of the reaction.

The DSC curves for the epoxy resins are shown in figure 9. The Epon 828 with mPDA had a diffuse reaction which extended from about 450 to 550 K. A reaction such as this would require high temperatures or long residence times in the pultruder die, suggesting that this resin might be difficult to pultrude when the mPDA curing agent is used. The other two epoxy resins, F 979 and E 702, had well-defined reactions which were centered near 475 K, about the same temperature as the Formulation A polyester. The E 702 resin had a relatively uniform heat generation rate over an approximately 15 K range as shown by the flattened peak. Such uniformity may result from blending curing agents so that, as the reaction due to one agent begins to decrease, a higher temperature agent causes an increase. No attempt was made, however, to determine if the E 702 resin had more than one curing agent.

The kinetic parameters for the resins are listed in table 3. The reaction orders were unity with two exceptions, SR 6325-2% BPO and E 702. The activation energies were about in the same range except for the Epon 828 (low) and the Formulation A (high). These two resins also represented the extremes with regard to the preexponential constant. For Epon 828 the constant was only  $\sim 10^2$ , while for Formulation A it was  $\sim 10^9$ . Table 3 also shows that an increase in the amount of initiator brings about an increase in the activation energy and pre-exponential constant.

The heat of reaction is also listed in table 3. The value listed for a given resin is the average obtained from tests at all temperature rates (10, 20, 40, and 80 K/min) inasmuch as no trend of heat with rate was evident. The values ranged from a low of  $\sim 200$  kJ/kg for Formulation A to a high of  $\sim 600$  kJ/kg for the E 702. The effect of BPO concentration on the reaction heat of two of the polyesters was determined. The results are shown in figure 10 where the data points are the average of all tests at a given concentration, and the range of values is indicated by the bars on the points. Despite the fact that the data are for two resins with three concentrations of BPO and tested at four temperature rates, the heat of reaction is nearly constant. The straight line, fitted by linear regression analysis, extrapolated to a value of  $\sim 260$  kJ/kg at zero concentration. The analysis indicated, however, that the line could, with 95 percent confidence, have a zero as well as a non-zero slope. Reference 55 shows that, while a higher initiator concentration will give both higher reaction rates and reaction heat, the effect is more pronounced with some initiators than it is with others. Apparently BPO is one of the more concentration-insensitive initiators.

The DSC curves (fig. 8 and 9) can be analyzed to determine what fraction of the reaction has taken place at a given temperature. The values of reaction fraction as a function of temperature for SR 6325-2% BPO are shown in figure 11 as an example. As noted previously, a lower temperature rate shifted the reaction to a lower temperature. This temperature-rate-dependent shift, however, also reflects longer times at lower temperatures. For example, at a rate of 10 K/min, nine

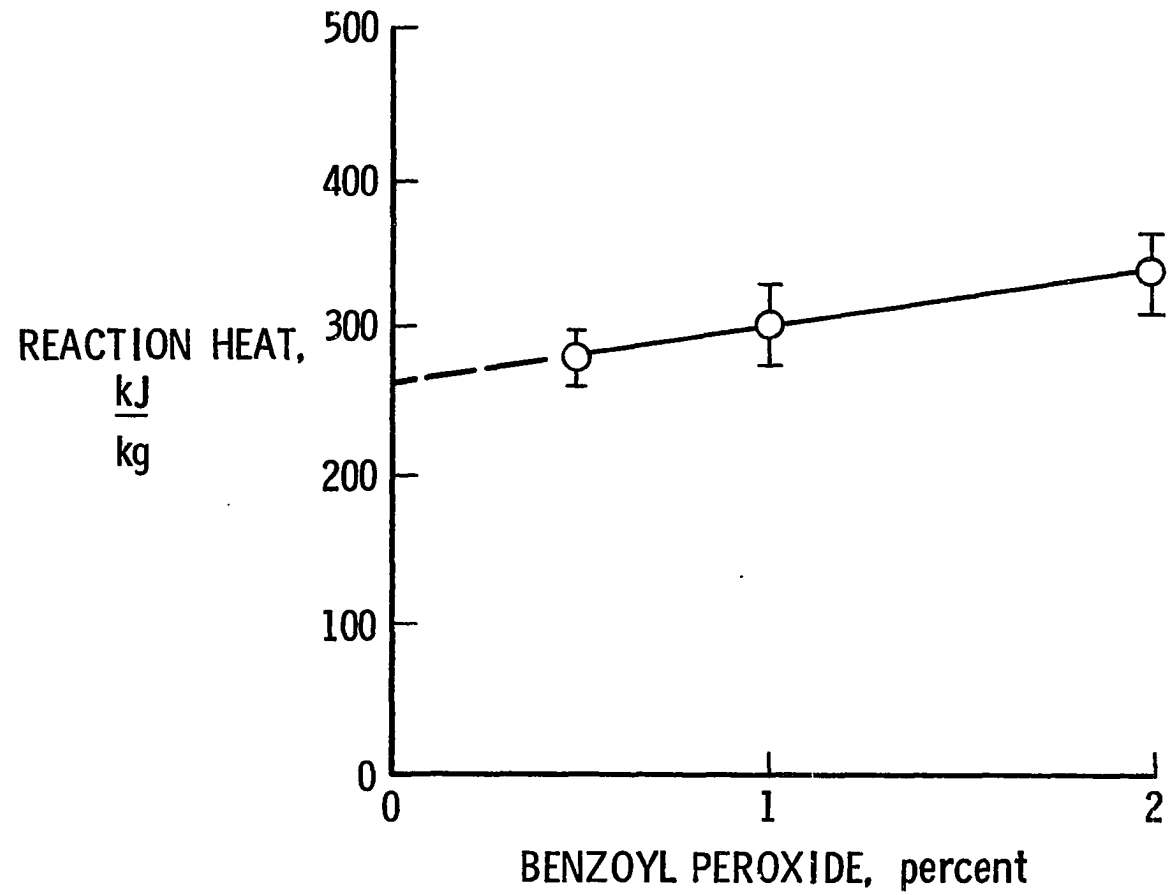


Figure 10.- Reaction heat as a function of initiator (benzoyl peroxide) concentration in SR 6325 and V 7001 polyester resins.

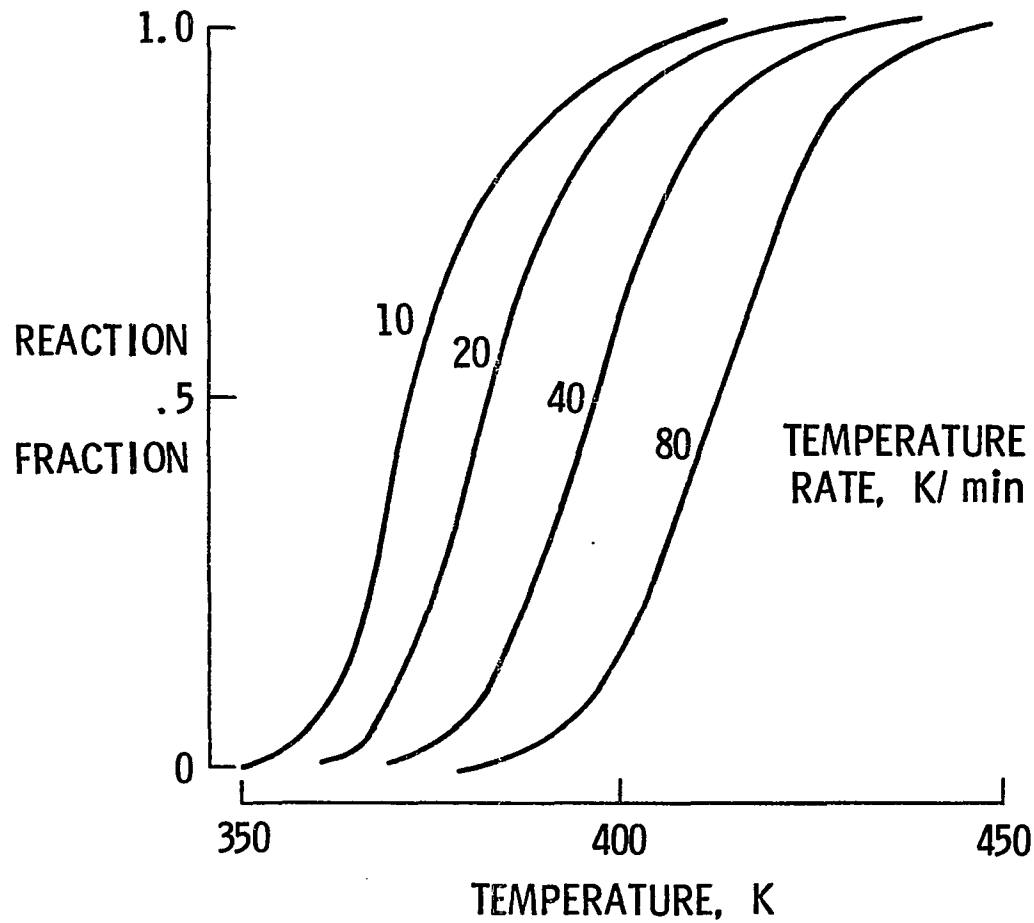


Figure 11.- Reaction fraction as a function of temperature at four temperature rise rates for SR 6325 polyester resin.



minutes were needed to pass from 300 K (room temperature) to 390 K (a typical pultrusion temperature for polyesters). By contrast, at a rate of 80 K/min, only 1.25 minutes was needed to reach the same 390 K. However, the resin heated at the lower rate had reached a fraction of 0.9, while that at the higher rate had not reached a fraction of 0.1 (see figure 11). Both temperature and time, then, must be considered in determining how far a resin has reacted. Such a consideration is important in pultrusion where two important variables are die temperature and die residence time.

The curves in figure 11 can be cross-plotted to illustrate the time-temperature-fraction relation as shown in figure 12 where the time is shown in seconds. At a temperature of 390 K, an induction time (taken as the time to reach a fraction of 0.1) of 100 seconds is required, and the reaction will be nearing completion ( $f=0.9$ ) after an estimated 640 seconds. If the die temperature should increase to 400 K, however, the induction time would be shortened to 63 seconds, and the reaction would be nearly complete in 408 seconds. The die temperature might rise because of inadequate temperature control or because of a continuing reaction heat release. Whatever the cause, the result is that the reaction begins and approaches completion earlier in the die. An early cure (ref. 20) can cause excessive friction forces.

#### Cure of Prepreg Tape

The curing kinetics of the resins are important as a means of establishing reference points and making comparisons. However, both resin and fiber are pulled through the die, and other investigators (ref. 12, 19, 20, 55) have recognized the need to make kinetic and

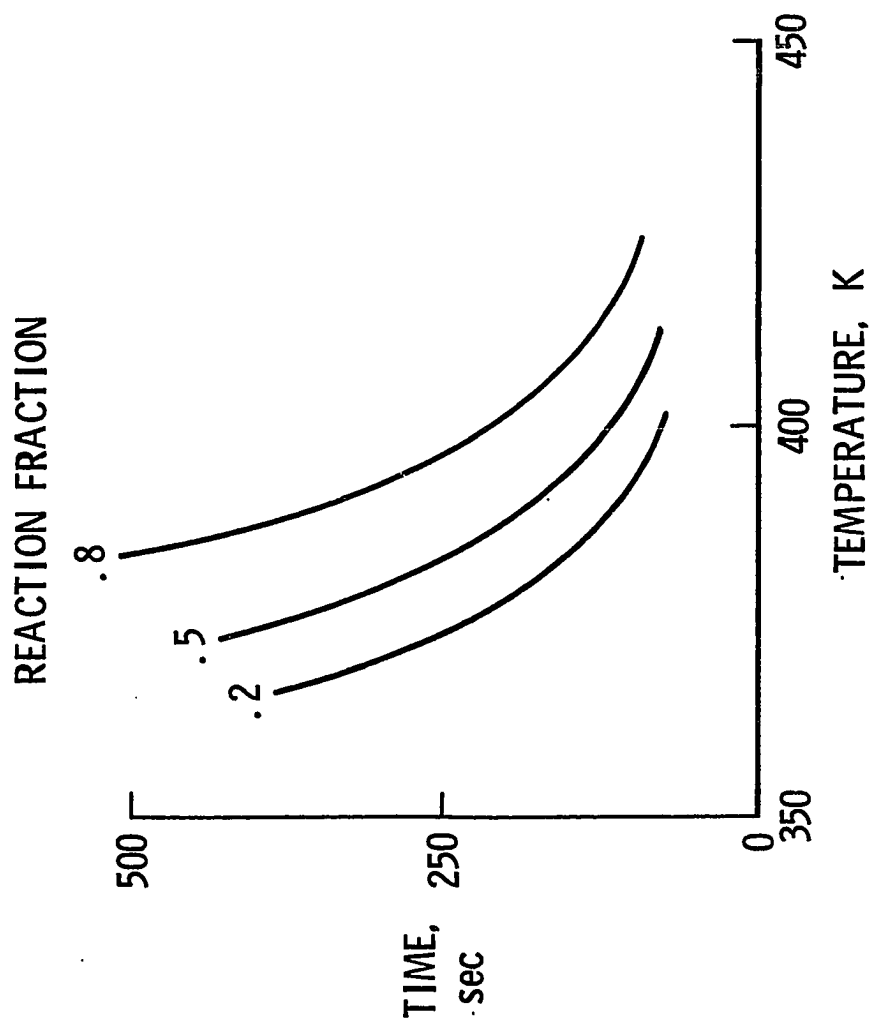


Figure 12.- Temperature-time curves at three reaction fractions for SR 6325 polyester resin.

thermal measurements on resin-fiber combinations. Indeed, one of the common ideas in composite material processing is that the fiber or filler has a moderating influence on the cure reaction and reduces the maximum exothermic temperature.

The moderating effect on the reaction may be due to both the mass and the surface of the fiber. The mass of the fiber acts as a thermal diluent by displacing some of the reactive, heat-producing resin. In addition, since the density-specific heat product of the fiber is generally larger than that of the resin, the fiber absorbs more heat than the resin it displaced. For example, consider a hypothetical polyester resin with an exothermic temperature rise of 100 K. A composite made of equal volumes of the resin and glass fiber would have only one half the reaction heat per unit volume compared to the resin alone. But with additional heat being absorbed by the fiber, and using typical values for density and specific heat, the estimated temperature rise would be 35-40 K, greatly reduced from 100 K for resin only.

The fiber surface can also have an effect on the reaction. Although any interaction between resin and fiber surface might be slight, the surface area is large and the overall effect can be significant. A cubic metre of a resin-glass fiber composite contains  $2 \times 10^5 \text{ m}^2$  of glass surface (assuming equal volumes of resin and fiber and 10  $\mu\text{m}$ -diameter fibers). Moreover, a uniform coating of resin on the fiber would be only 2.5  $\mu\text{m}$  thick so that most of the resin would be within a short distance of the fiber surface. A reacting species at the surface would, assuming a mass diffusion coefficient of  $10^{-12} \text{ m}^2/\text{sec}$ , diffuse through the uniform coating in about three seconds. Such a time is small

relative to most processing times. An investigation of the effect of surface treatments of mineral fillers (ref. 60) has shown that the curing reaction of a polyester resin can be either accelerated or retarded by appropriate surface treatments. In another investigation (ref. 55), the reaction heat of a diallyl phthalate-kaolinite clay combination was reduced to one percent that of the resin alone. A useful composite could not be made from such a combination. This extreme effect was attributed to the decomposition of the peroxide initiator by the acidic surface of the clay.

Representative DSC curves for the prepreg tape, obtained at a temperature rise rate of 80 K/min, are shown in figure 13. Comparing these curves with those for the resins (fig. 9) shows that the general curve shape is the same. However, the curves for the tape tend to be smaller and spread over a wider temperature range. All three curves had a high temperature tail, indicating that some reactions were still taking place even at the very high temperatures. The temperature for a reaction fraction of 0.5 moved from 479 K for the resins to 484 K for the tapes.

The kinetic and thermal parameters for the tapes are listed in table 4. The resin used for the Rigidite 5209 tape was not available so no comparison between the two can be made. For the Hy-E and E 702, a comparison can be made with the F 979 and E 702 resins in table 3. Compared to the resins, the tapes had the same reaction order but a lower activation energy and pre-exponential constant. In other words, the tapes reacted slower and over a wide temperature range than did the resins. For example, at 475 K (a possible pultrusion temperature for epoxies) the reaction rate constant would be  $5.51 \times 10^{-2} \text{ sec}^{-1}$  for the

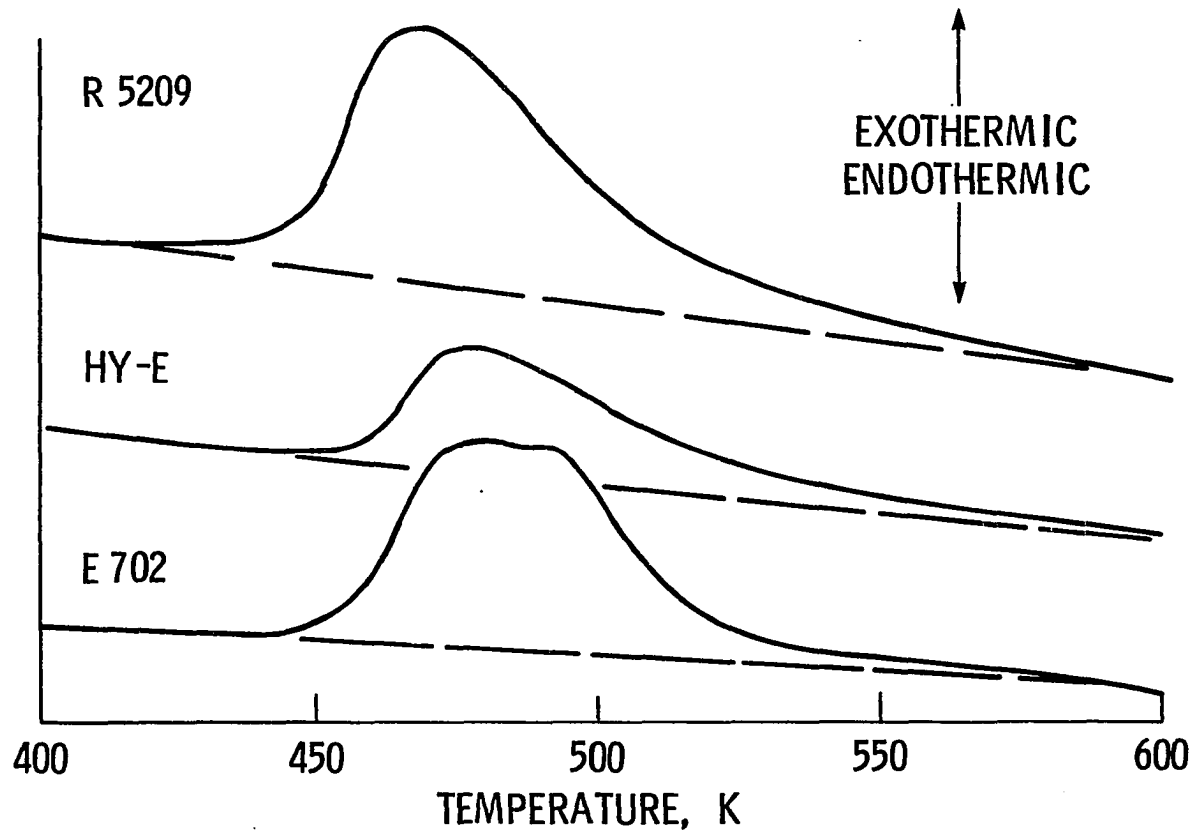


Figure 13.- DSC curves for epoxy resin-graphite fiber prepreg tapes. Temperature rise rate was 80 K/min.

TABLE 4. - KINETIC AND THERMAL PARAMETERS FOR EPOXY PREPREG TAPE

Tape	Reaction Order	Activation Energy kJ/mol	Pre-exponential Constant, sec <sup>-1</sup>	Reaction Heat, kJ/kg
Rigidite 5209-T300	1	30.7	$1.31 \times 10^2$	164.6
Hy-E 1079 C	1	54.7	$4.16 \times 10^4$	60.3
E 702/T300 (6K)	1/2	49.2	$7.64 \times 10^3$	174.5

F 979 resin, and  $3.52 \times 10^{-2} \text{ sec}^{-1}$  for the E 702 resin. For the tapes, the corresponding rates would be  $4.02 \times 10^{-2} \text{ sec}^{-1}$ , and  $2.97 \times 10^{-2} \text{ sec}^{-1}$ . The rate for the tapes was about 75-85 percent that for the resins. Hence, using the DSC to measure reaction rates for the resin will provide an upper bound for the rates, and so a lower bound for the residence time in the die for the prepreg tape. The heat of reaction for the prepreg tapes is also listed in table 4. A lower reaction heat for the tapes, compared to the resin, would be expected and this was the case. If the reaction heat of the resin is known (table 3), and the proportion of resin is given (table 2), then the reaction heat for the prepreg tapes can be estimated. The estimated values for the Hy-E and E 702 tapes was 66.7 and 199.2 kJ/kg, reasonably close to the measured values of 60.3 and 174.5 kJ/kg. Apparently, the graphite fiber exerts a mass effect but very little surface effect on the epoxy reaction.

Both the rate of reaction and the heat of reaction are important in the reaction which takes place in a pultruder die. The heat of reaction will be used in the energy balance section. The concern here is the rate of reaction, and how much time is required to achieve a given fraction of the total reaction. A useful technique for following the reaction (ref. 43, p. 92) is to observe that the variables in equation 1 can be separated to give

$$\frac{dC}{C^n} = - kd\theta \quad (1')$$

Equation 1' can be integrated to give an expression for concentration, C, which is

$$C = C_o [1 + (n-1) C_o^{n-1} k\theta]^{-\frac{1}{(n-1)}} \quad (4)$$

Dividing by  $C_o$  gives

$$\frac{C}{C_o} = [1 + (n-1) C_o^{n-1} k\theta]^{-\frac{1}{(n-1)}} \quad (4')$$

The group of variables on the right hand side of equation 4' is a dimensionless group referred to (ref. 42, p. 527) as the Damköhler number,  $N_D$ . This number is

$$N_D = C_o^{n-1} k\theta \quad (5)$$

The change of dimensionless concentration,  $\frac{C}{C_o}$ , with dimensionless time,  $N_D$ , is shown in figure 14. The curves in figure 14 apply to an isothermal case. If the reaction fraction  $f$  is considered to be inversely related to dimensionless concentration,  $\frac{C}{C_o}$ , then figure 14 provides a way of estimating reaction times for a given resin at a given temperature. Of considerable importance in the pultrusion process, however, is the Damköhler number (equation 5) which relates the important process variables of (residence) time,  $\theta$ , and die temperature (through the reaction rate constant  $k$ ). As the die temperature is increased, the residence time can be decreased; how much depends in large measure on the kinetic parameters of the resin.



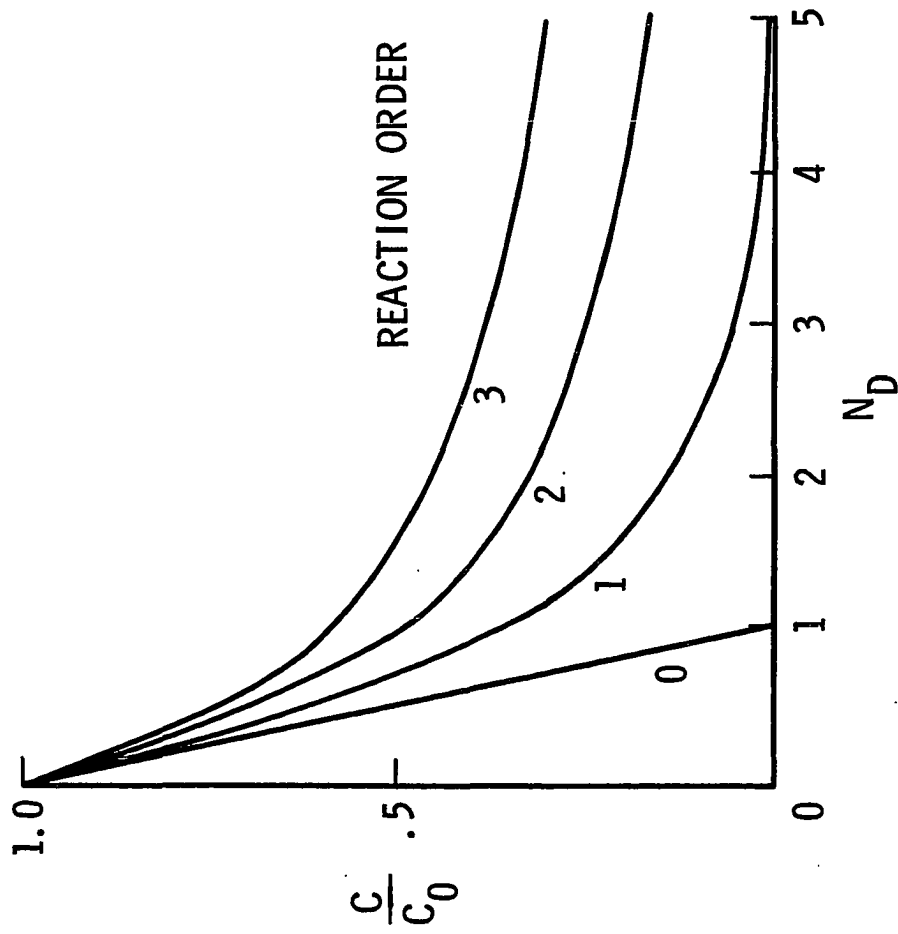


Figure 14.- Normalized reactant concentration as a function of Damköhler number for four reaction orders.

### Mass Balance

The pultruder die can be regarded as a chemical reactor in which a mass change takes place. Specifically, the low molecular weight, liquid resin reacts to form a higher molecular weight, crosslinked matrix for a composite material. The resin is the reactive component, and the reinforcing fibers have a moderating effect on the reaction. Useful kinetic and thermal parameters can be obtained from DSC tests. While tests of the resin-fiber combination are preferable, tests of the resin itself can provide reasonable estimates of the results to be expected from such a combination. Once the kinetic parameters are determined, the Damköhler number,  $N_D$ , provides a useful means of estimating reaction times, or die residence times, and the effect that die temperature would have on those times.

## CHAPTER 5

## ENERGY BALANCE IN A PULTRUDER DIE

In a pultruder die (reactor), energy causes a mass change which, in turn, releases energy. This balance can be expressed simply as the energy stored in the resin-fiber mass within the die is equal to the energy transferred into the mass plus the energy generated by the cure reaction. The mathematical form of this simple statement, for heat transfer in the y-direction, is

$$\rho c_p \frac{\partial T}{\partial \theta} = \frac{\partial}{\partial y} \left( k \frac{\partial T}{\partial y} \right) + rH \quad (6)$$

This partial differential equation expresses the spatial and temporal variation of temperature in the resin-fiber mass if certain material properties are known. The equation has dimensions of  $W/m^3$  so it could be thought of as an expression for power density, analogous to the expression for mass density. In equation 6, the heat of reaction, H, can be treated as a constant as it is essentially independent of the concentration of the curing agent. However, the reaction rate, r, is strongly dependent on concentration (equation 1) and on temperature (equation 2). Although a general analytical solution to equation 6 is not available, the equation can be evaluated by numerical methods. Such an evaluation was made, using the finite difference program described in reference 53. The program was modified to include the energy

generation term. Two limiting cases were examined, the isothermal case in which the die was at a constant temperature along its length (x-axis), and the adiabatic case in which heat in the resin-fiber mass was being generated and stored but not transferred.

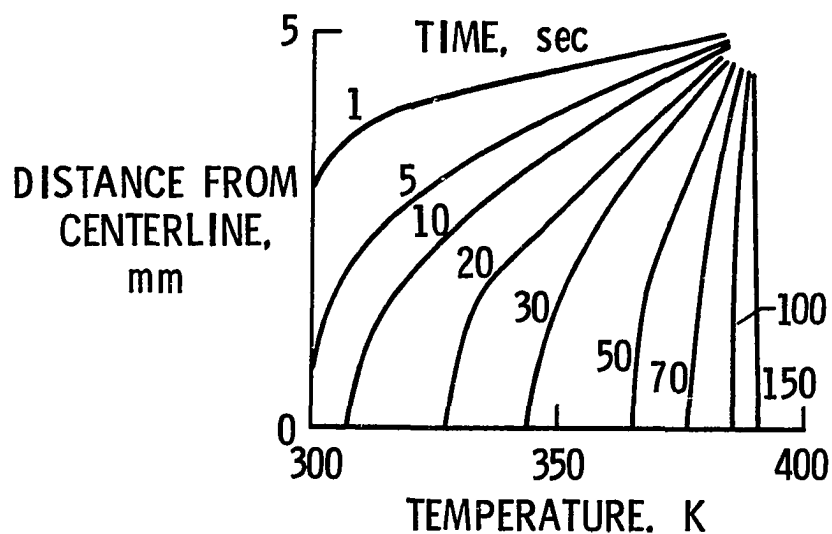
#### Isothermal Case

Estimates were made of the spatial and temporal variation of temperature for four combinations of resin and fiber, two of polyester and glass, and two of epoxy and graphite. The assumed thicknesses and die temperatures, and the material parameters, are listed in table 5. The kinetic parameters and heat of reaction as measured in this investigation were used in the calculations. Thermal conductivity and specific heat were taken from reference 19 for the polyester and glass, and from reference 64 for the epoxy and graphite.

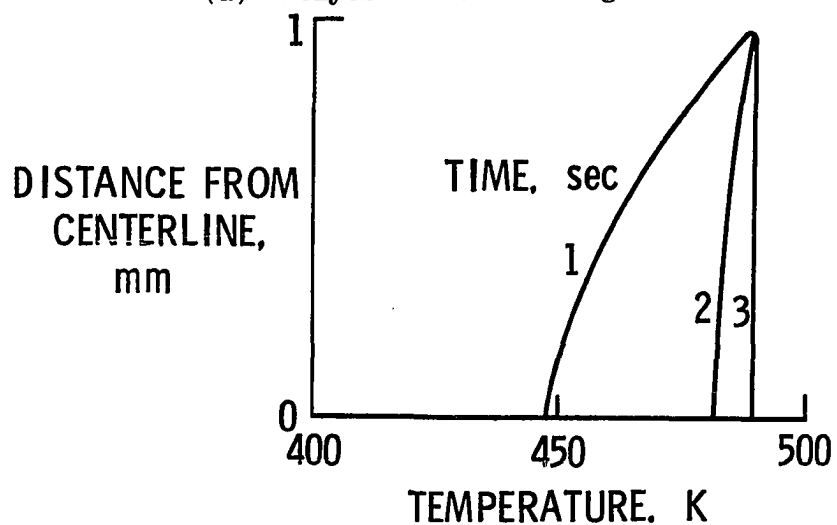
The estimated temperature distribution, over one-half of the cross-section, for the polyester-glass combinations is shown in figure 15. One set of curves is shown for both combinations because the estimates were nearly identical. As expected, the temperature rise proceeded from the surface inward, with steep gradients at the shorter times. At about six seconds, the centerline temperature began to increase. The gradients and the center lag were fairly large until about 40-50 seconds, and the temperature profile did not flatten out until 70-80 seconds. The centerline was virtually at the die temperature of 390 K after 120-130 seconds. (If no reaction were taking place, the time would have been 10-15 seconds longer.) Beyond that time, the temperature profile was flat, with the centerline temperature rising less than 1 K

TABLE 5. - PARAMETER VALUES USED IN FINITE DIFFERENCE PROGRAM  
TO ESTIMATE TEMPERATURE DISTRIBUTION IN RESIN-FIBER  
MASS

Parameter	SR325 and glass fiber	V 7001 and glass fiber	Hy-E prepreg tape	E 702 prepreg tape
Total thickness, mm	10		2	
Stations per half thickness	17		9	
Initial temperature, K	300		300	
Die temperature, K	390		490	
Thermal conductivity, $\frac{W}{m-K}$	$.6 + \frac{(T-300)}{1200}$		$.9 + \frac{(T-300)}{800}$	
Density, $\frac{kg}{m^3}$	2000		1500	
Specific heat $\frac{J}{kg-K}$	1046		$800 + 2(T-300)$	
Reaction heat, $\frac{J}{kg}$	$1.50 \times 10^5$	$1.5 \times 10^5$	$2.66 \times 10^5$	$6.23 \times 10^5$
Reaction Order	1	1	1	1/2
Concentration, $\frac{kg}{m^3}$	11.65	11.65	120	120
Pre-exponential constant, $sec^{-1}$	$8.22 \times 10^5$	$2.10 \times 10^6$	$7.93 \times 10^4$	$2.37 \times 10^4$
Activation energy, $\frac{J}{kmol}$	$56.3 \times 10^3$	$58.3 \times 10^3$	$56.0 \times 10^3$	$52.7 \times 10^3$



(a) Polyester resin and glass fiber.



(b) Epoxy resin and graphite fiber.

Figure 15.- Temperature distribution in resin-fiber mass as estimated by finite difference program.

above the die temperature. No exothermic temperature peak developed in the cross section for times up to 480 seconds. Apparently the combined effects of kinetic and thermal parameters, coupled with a thickness of only 10 mm, would moderate the polyester reaction and keep the temperature rise to a small, manageable value.

The estimated temperature distribution for the epoxy-graphite combinations is shown in figure 15 where, again, one set of curves is used. The thickness for this combination was 2 mm, the same as the height of the die cavity of the laboratory-scale pultruder to be discussed later. The obvious results for the epoxy and graphite (fig. 15) is an extremely rapid temperature rise. The centerline temperature reached 490 K (die temperature) in three seconds, increased to slightly over 491 K at four seconds, and remained virtually unchanged for times up to 480 seconds. The high thermal conductivity together with the small distance (1 mm from surface to centerline) served to shorten the heat-up time.

The results shown in figure 15 are somewhat surprising in light of the usual temperature rise associated with an exothermic reaction. However, the heats of reaction were not extremely high, and the assumed sizes were not large. From these temperature distribution estimates, the indications are that the materials would not have a large exothermic temperature rise. Hence, the method of heating the die would be immaterial as long as the die were isothermal.

#### Adiabatic Case

Polymeric resins typically have relatively low thermal conductivities. Consequently, with thick sections or highly reactive resins, the heat of reaction may be generated faster than it can be transferred.

Without heat transfer, the temperature in the affected volume can become quite high. The temperature in an adiabatic situation such as this can be described by equation 6 with the heat conduction term set to zero. This equation can be made dimensionless by the transformations

$$\begin{aligned}
 y' &= \frac{y}{h} \\
 \theta' &= \frac{\theta}{h^2/\alpha} \\
 C' &= \frac{C}{C_o} \\
 T^* &= \frac{T - T_o}{T_{ad} - T_o} \\
 \Delta T'_{ad} &= \frac{T_{ad'} - T_o}{T_o} = \frac{HC_o}{\rho c_p T_o}
 \end{aligned}
 \tag{7}$$

Then, following the procedure given in reference 61, equation 1 is divided into equation 6 to give a relationship between concentration and adiabatic temperature which is

$$C' = 1 - T^* \tag{8}$$

Note that equations 21-23 of reference 61 contain an error ( $-T^*$  rather than  $1 - T^*$ ) which was corrected in reference 62. With equation 8 substituted into the dimensionless form of equation 6 (and the heat conduction term dropped), the dimensionless equation 6 can be integrated to give



$$\theta^* = \int_0^{T^*} \frac{dT^*}{(1 - T^*)^n \exp \left[ N_{A0} \left( \frac{\Delta T'_{ad} T^*}{\Delta T'_{ad} T^* + 1} \right) \right]} \quad (9)$$

This dimensionless time can also be expressed

$$\theta^* = N_D = k' \theta' = C_0^{n-1} k \theta \quad (10)$$

which is a form of the Damköhler number (ref. 42, p. 527). The dimensionless reaction rate,  $k'$ , in equation 10 is the ratio of the actual reaction rate to the heat transfer rate

$$k' = \frac{C_0^{n-1} k}{\alpha/h^2} \quad (11)$$

Equation 9, which gives a relationship between temperature and time for the adiabatic case, contains two parameters which can be set through material properties or machine parameters. The dimensionless Arrhenius number,  $N_A$ , is often referred to as a dimensionless activation energy. For this investigation, the concept of a dimensionless temperature is more useful. The number is

$$N_A = \frac{E_k}{RT} \quad (12)$$

where  $T$  is the temperature of the resin-fiber mass.

The Arrhenius number  $N_{AO}$  in equation 9 refers to the temperature of the resin-fiber mass entering the die. Thus, for a given resin which would fix  $E_k$ , the Arrhenius number can be changed. The other parameter in equation 9 is the adiabatic temperature rise as given in equation 5. In that expression, the product  $\rho c_p$  is set by the resin and fiber and the proportions of each. The choice of a curing agent essentially fixes  $H$ . The feed temperature,  $T_o$ , can be set or at least measured. Then the value of  $C_o$  will be established depending on what value of  $\Delta T'_{ad}$  will be allowed.

Some effects of varying these two parameters on the temperature was determined using equation 9. The integral was replaced by a summation and the expression was evaluated numerically on a programmable calculator. The results are shown in figures 16-18. Figure 16 shows the variation of  $T^*$  with  $N_D$  ( $\theta^*$  in equations 9 and 10) for  $\Delta T'_{ad} = 0.15$  and a range of dimensionless temperatures  $N_A$ . A value of  $N_A$  near 20 was typical of the materials used in this investigation. As  $N_A$  increased (fig. 16), the temperature rise became more rapid, with the curvature as  $T^*$  approached unity becoming increasingly sharp. For the unrealistically high value  $N_A = 100$ , the temperature rise was essentially instantaneous. A rapid temperature rise is to be avoided, however, because it causes high thermal stresses and excessive shrinkage, and often leads to internal cracking and voids. As noted above, the value of  $N_A$  can be changed slightly by processing conditions. For example, if  $E_k = 50$  kJ/mol and  $T_o = 300$  K, then  $N \approx 20$ . If the feed temperature is increased to 350 K, then  $N_A \approx 17$  and the temperature rise under adiabatic conditions would not be so severe. Possibly this is reflected

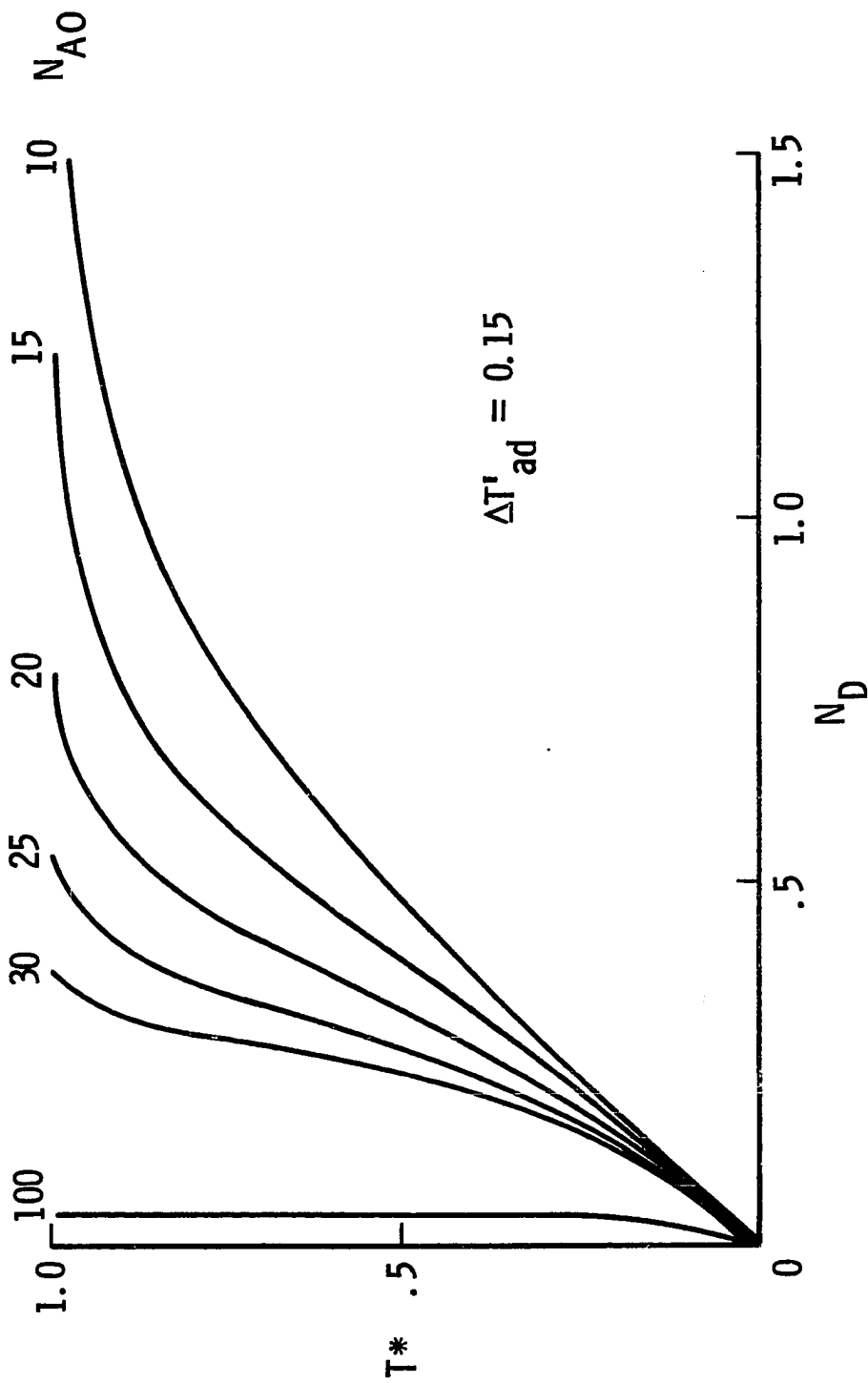


Figure 16.- Normalized temperature as a function of Damköhler number for various initial Arrhenius numbers and a constant adiabatic temperature rise.

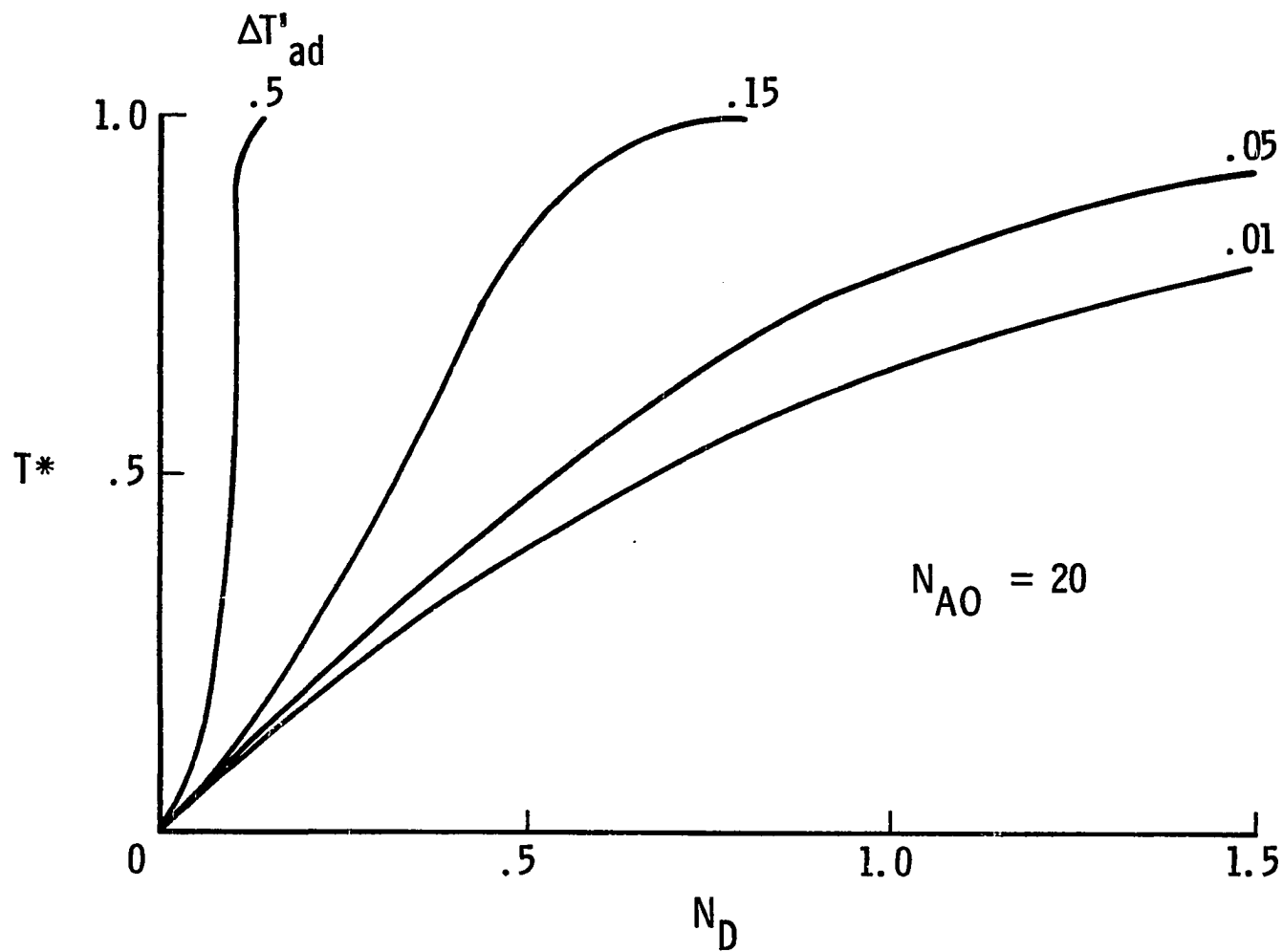


Figure 17.- Normalized temperature as a function of Damköhler number for four adiabatic temperature rises and a constant initial Arrhenius number.

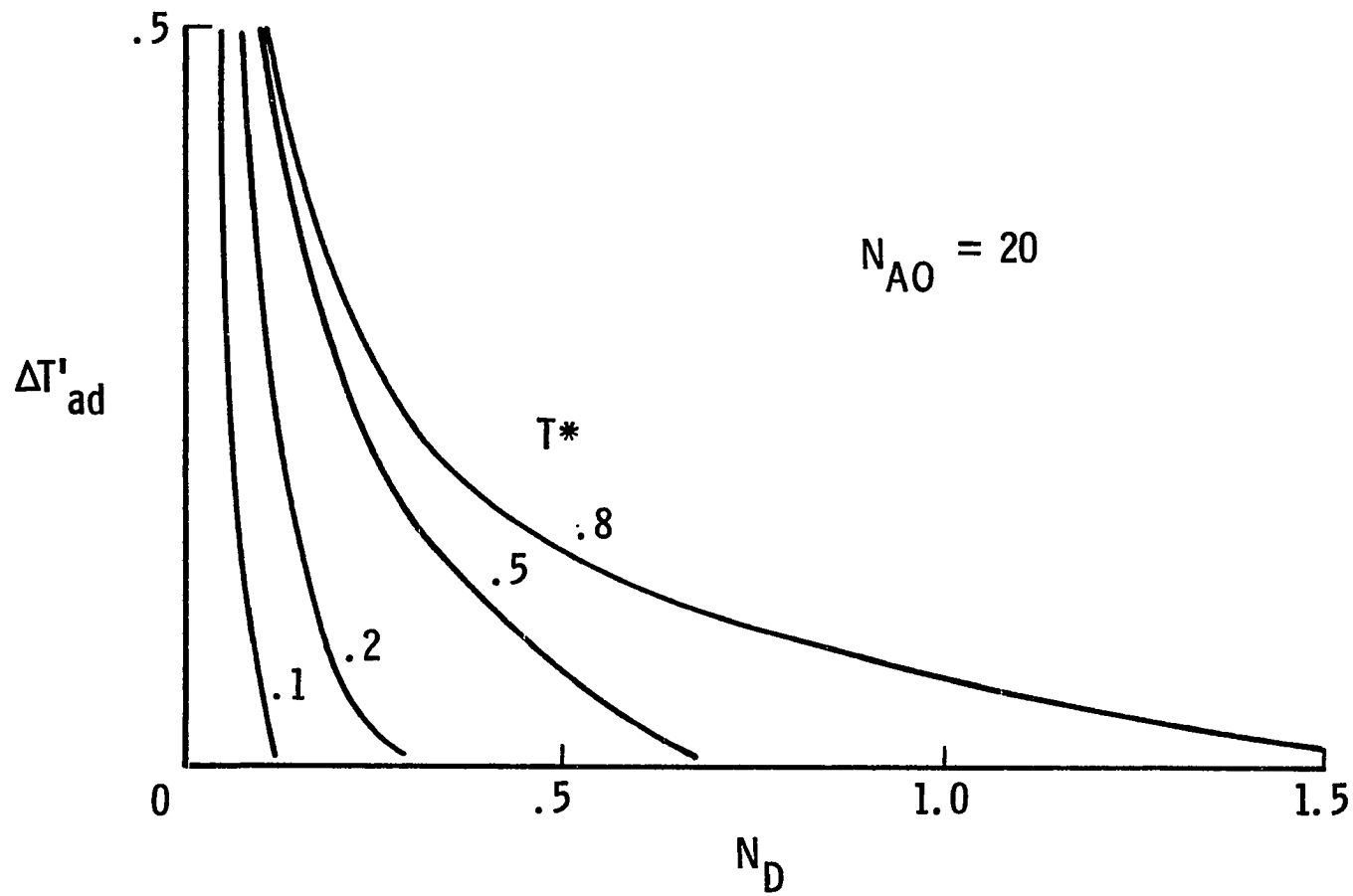


Figure 18.- Adiabatic temperature rise as a function of Damköhler number for four reaction fractions and a constant initial Arrhenius number.

in the observation (ref. 4, 9, 11, 14, 19) that a dielectric pre-heating of the resin-fiber mass before it enters the die gives higher production rates or higher quality in thick parts.

The effect of the other parameter, the adiabatic temperature rise, is shown in figure 17 for a fixed value of  $N_A = 20$ . In this investigation, a typical range of  $\Delta T'_{ad}$  was 0.01 to 0.05. As  $\Delta T'_{ad}$  increased, the temperature rise rate increased also. Inasmuch as temperature and concentration are related (equation 8), the time needed to complete the reaction under adiabatic conditions can be established by setting the value of  $\Delta T'_{ad}$ . To obtain high production rates, a short die residence time and reaction time are needed. But, as noted above, too short a time can cause trouble. Even if cracking or resin degradation does not occur, too rapid a reaction in the die may preclude making corrective adjustments to the pulling speed or die temperature.

To better illustrate the effect that  $\Delta T'_{ad}$  can have on the time needed for certain fractions of the reaction to take place, the curves from figure 17 were cross plotted for selected temperatures. The results are shown in figure 18 where  $T^*$  and the reaction fraction  $f$  are considered to be the same. For high values of  $\Delta T'_{ad}$ , the reaction would be completed in a very short time. As  $\Delta T'_{ad}$  is set to lower and lower values, however, the curves for different values of  $T^*$  (and hence, of  $f$ ) begin to spread apart. At  $\Delta T'_{ad} = 0.1$ , the time to reach  $T^* = 0.8$  would be seven times that at  $\Delta T'_{ad} = 0.5$ . In addition, while the time between  $T^* = 0.2$  and  $T^* = 0.5$  curves increases as  $\Delta T'_{ad}$  decreases, the time between the 0.5 and 0.8 curves increases even more. One wide-spread practice with composite materials is the addition of low cost, inert fillers to the resin. Since the  $\rho c_p$  product of the

fillers generally will be greater than that of the resin, the heat of reaction will be a low value. Hence, in a filled system, the temperature rise during a reaction, or "peak exotherm" in the commonly used terms, is small relative to that of the unfilled system. Considering the results shown in figure 18, however, a highly filled composite may be partially cured in a reasonable time. A complete cure ( $T^*$  and  $f$  approaching unity) may not be practical.

#### Energy Balance

As the resin-fiber mass enters an isothermal die, heating begins at the surface and proceeds inward. For a modest 10 mm thickness, the centerline temperature in a polyester-glass combination would require 120-130 seconds to reach die temperature. By contrast, the heat-up time for an epoxy and graphite combination is virtually zero. Neither combination had large exothermic temperature rises. Under adiabatic conditions, the exothermic reaction can be controlled through two parameters, the Arrhenius number,  $N_A$ , and the adiabatic temperature rise  $\Delta T'_{ad}$ . Both parameters are functions of the resin and fiber and can be adjusted to some extent. The Arrhenius number can be thought of as a dimensionless temperature which is a function of the actual temperature and activation energy of the material. As such, it may be of more value than the temperature alone.

## CHAPTER 6

## FORCE BALANCE IN A PULTRUDER DIE

Like most composite materials processing, pultrusion involves the application of a force and the generation of resisting forces. Unlike most other processes, however, pultrusion generates significant shear forces at the interface between the die wall and the resin-fiber mass. In this investigation, the concept of the pultruder die as a slit rheometer was employed. Another concept was that of a coefficient of friction, defined broadly as a dimensionless ratio between shearing forces and normal forces. Traditionally, the coefficient of friction for a given material couple at a fixed temperature and speed has been thought of as a constant. In the case of pultrusion, the die-resin interface undergoes considerable change due to changes in the resin. For example, the resin enters the die as a low viscosity liquid or perhaps semi-solid, becomes less viscous as its temperature increases, then becomes more viscous and changes to a semi-solid (gel) as polymerization takes place, and finally leaves the die as a hot solid. Under such conditions the likelihood of a constant coefficient of friction is small indeed. However, the concept of a dimensionless ratio of forces is still valid.

## Coefficient of Friction

The resisting forces arising in a pultrusion die, separate from the collimation forces outside of the die, are due in large measure to three causes: (1) resin back flow at the die entrance; (2) viscous drag



of the resin; and (3) sliding friction of the curing stock.

Considering first the sliding friction, a generally familiar concept, the coefficient is (ref. 65, p. 18)

$$\mu_s = \frac{F_x}{F_y} \quad (13)$$

Normalizing relative to the area over which the forces act gives

$$\mu_s = \frac{\tau_x}{p_s} \quad (14)$$

The pressure  $p_s$  is often thought of as the independent variable, with a change of pressure causing a corresponding change in the shearing stress  $\tau_x$ . A reduction in stock thickness as curing takes place would reduce the pressure and hence the friction.

In the upstream portion of the die the resisting force is caused by viscous drag. From lubrication theory (ref. 65, pp. 15, 16) the coefficient of friction is

$$\mu_v = \frac{\eta N}{p_v} \quad (15)$$

The rotational speed  $N$  is the reciprocal of a characteristic time, the time for a bearing shaft to make  $N$  revolutions. For the pultrusion process, a characteristic time is the residence time  $\theta$  of a given cross section in the die. Noting that  $\theta = \ell/s$  and substituting the reciprocal into equation 15 gives

$$\mu_v = \frac{\eta}{p_v \theta} = \frac{\eta s}{p_v \ell} \quad (16)$$

This equation might give the idea that a long die ( $\ell$  large) would reduce the friction, an idea which is contrary to both intuition and experience (ref. 20). Instead, the die length  $\ell$  and pulling speeds should be considered coupled through the residence time  $\theta$ . If viscosity and pressure are considered constant, the change of friction with residence time is

$$\frac{d\mu}{d\theta} = - \frac{\eta}{p_v} \frac{1}{\theta^2} \quad (17)$$

Then one way of reducing the friction is to reduce the residence time (short die, high pulling speed). Or, as has been observed (ref. 20), a short die permits high pulling speeds. Of course, it is unlikely that the viscosity would be constant in view of the reaction which takes place in the die. If viscosity and pressure were coupled in some way, then the ratio of the two might be a constant or at least behave in some predictable manner. This idea will be discussed later.

The third cause of resisting forces is resin back flow at the die entrance. A measurement of this force showed that it could be significant, in the range of 140-310 kPa (20-45 psi). This back flow arises from the temperature rise of the resin entering the die. As the temperature rises, the resin attempts to expand, expansion is limited

by the die, so the resin pressure increases. Some of the pressure can be relieved by flow away from the high pressure region, back toward the die entrance. This pressure can be estimated as follows. The one-dimensional thermal expansion coefficient in the y-direction is, by definition

$$\alpha = \frac{1}{y} \frac{\Delta y}{\Delta T} \quad (18)$$

Similarly, the bulk modulus (inverse of compressibility) is

$$K = \frac{y}{\Delta y} \Delta p_b \quad (19)$$

Solving equation 18 for  $\Delta y$ , substituting that value into equation 19 and rearranging gives

$$\Delta p_b = K\alpha\Delta T \quad (20)$$

The pressure gradient is directly proportional to the temperature gradient between the surface and the center of the resin-fiber mass in the y-direction. Taking the ratio of the pressure gradient to the pressure (probably atmospheric) of the resin-fiber mass provides another coefficient of friction, this one for back flow.

$$\mu_b = \frac{\Delta p}{p_b} = \frac{K\alpha\Delta T}{p_b} \quad (21)$$

Note that the pressure can be expressed as the product of the bulk modulus  $K$  and a volume change  $\Delta V$ . As many pultruded stocks have a high aspect ratio, a change of thickness,  $\Delta t$ , is a good measure of volume change. Hence, equation 21 can also be written

$$\mu_b = \frac{\alpha \Delta T}{\Delta t} \quad (21')$$

The thickness change is the difference between the thickness of the resin-fiber mass in the die (i.e. the cavity thickness), and the limiting thickness of the same mass under a very high pressure (expected to be less than the thickness in the die). In other words, as more and more material is introduced into the die, the difference between the limiting thickness and the die cavity height becomes smaller. Hence, the pressure and the resisting force at the die entrance increase.

The overall coefficient of friction for a pultruder die is the sum of the three coefficients discussed above. Setting this overall coefficient as the ratio of the resisting forces to the breaking forces of the resin-fiber mass gives

$$N_c = \frac{F}{F_{\text{fracture}}} = \frac{K\alpha\Delta T}{P_b} + \frac{\eta s}{P_v \ell} + \frac{\tau x}{P_s} \quad (22)$$

The dimensionless ratio of forces is given the name here of Coulomb number which is consistent with the practice of identifying a Damköhler and Arrhenius number. The Coulomb number is influenced by the mass and energy balances, and it serves essentially as a process limit. To

insure that the pulling force does not fracture the resin-fiber mass, the Coulomb number always should be small compared to unity.

#### Pressure and Volume Effects

The expression for the Coulomb number,  $N_C$ , (equation 22) contains a pressure term, the normal component, in the denominator. At a constant temperature, pressure and volume are inversely related for an unchanging system. In the case of pultrusion, two limiting types of dies can be identified. The first type is the isometric or constant volume die in which the pressure will vary along the die length (x-axis). The second type is the isobaric or constant pressure die in which the volume will vary along the length.

Both types of dies were used in an investigation of compression molding of several thermosetting resins combined with chopped fiber (ref. 66, 67). The change of pressure with time in a landed (isometric) die, and the change of volume in an unlanded (isobaric) die, were measured. A landed die has mating surfaces (lands) between the die sections which set the volume of the die cavity and carry some of the press load. An unlanded (isobaric) die has sections which can slide freely past one another (as a piston and cylinder, for example) so the full press load is carried by the resin-fiber mass.

Representative results for a diallylphthalate resin with cellulose fiber, molded at 420 K, are shown in figure 19 where the time axis refers to time in the die after it has been closed or after the pressure has been applied. The volume was normalized relative to the final volume of the part, and the pressure was normalized relative to that applied by the press. In the isobaric die (top curve), the relative volume decreased from a high initial value of  $\sim 1.71$  to  $\sim 1.13$  at

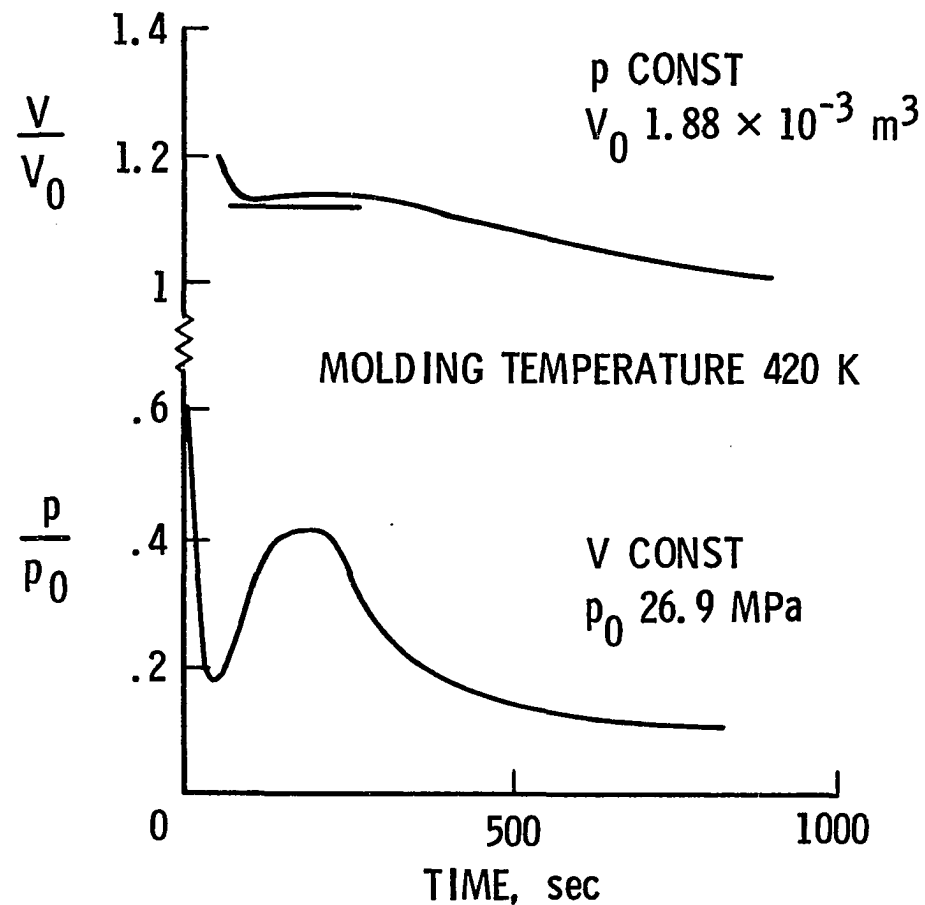


Figure 19.- Pressure and volume changes in landed (V const) and unlanded (p const) dies for compression molding of diallyl phthalate - chopped fiber molding compound.

90 seconds as the resin-fiber mass was heated and compacted. Then a slight expansion ( $\sim 0.1$ ) took place due to thermal expansion and initial polymerization until about 300 seconds. Following that, the part shrank as curing took place. In the isometric die (bottom curve), the relative pressure began at  $\sim 0.65$  and dropped rapidly to  $\sim 0.17$  at 50 seconds as the resin-fiber mass was heated and compacted together. Then a combination of thermal expansion and polymerization caused a pressure increase to  $\sim 0.41$  at 200 seconds which was followed by a cure-induced drop to  $\sim 0.10$  at the end of the cure.

If the time axis in figure 19 is regarded as residence time in a pultruded die, and if it is recalled that pulling speed is constant, then the time axis can also be regarded as distance along the x-axis of the die. Indeed, the similarity between a plug flow reactor (such as a pultruder die) and a batch reactor (such as a compression molding die) has been noted elsewhere (ref. 43, p. 239). For the isobaric die, the pressure presumably would be constant and the volume qualitatively would change along the die length as shown by the top curve (fig. 19). However, the relatively compliant resin-fiber mass will probably conform to the relatively rigid die, with small pressure variations at those points where mass would be expected to depart from linearity. For the isometric die, the volume presumably would be constant and the pressure qualitatively would change along the die length as shown by the bottom curve (fig. 19). Still, the die would be expected to deflect slightly at the high pressure point, relieving the pressure somewhat and causing a small variation in volume. In the isobaric die, the pressure is caused by some pneumatic or hydraulic device which presses the die

sections together. In the isometric die, the pressure is caused by the confining of the resin -fiber mass within the essentially constant volume. The larger the amount of resin and fiber, the higher the pressure will be. A high pressure would increase the back flow and the sliding friction, whereas it would seem to reduce the viscous drag (equation 16) if the viscosity and residence time are constant.

The pressure change in the dies was caused by a volume increase of the resin as the cure reaction (polymerization) took place. Such volume changes have been measured with sensitive dilatometers (ref. 68, 69) and have been related to curing kinetics (ref. 69). In the later stages of cure, shrinkage and a pressure reduction take place (fig. 19). This change in volume also reflects curing kinetics (ref. 44, pp. 57-59). In fact, the importance of dimensional and volume changes as an indication of extent and completeness of cure seems to have been overlooked (ref. 70). Making volume or thickness measurements of pultruded stock may be one way of tracking the course of the curing reaction.

#### Force Balance

The force balance in a pultrusion die can be thought in terms of a coefficient of friction, a ratio of shearing forces to normal forces. The components of friction arise from resin back flow at the die entrance, viscous drag as the resin begins to cure, and sliding friction of the curing stock. If these three resisting forces do not exceed the fracture force of the resin-fiber mass, then the Coulomb number,  $N_C$ , will be less than unity, and the pultrusion processes will not be limited by an unfavorable force balance. The pressure (normal force) affects the magnitude of the resisting forces. The pressure, in turn, can be affected by volume changes. A large volume of resin and fiber confined



in a die will generate high pressures and large resisting forces. The volume changes accompanying the cure reaction not only change the pressure but also provide a means of following that reaction.

## CHAPTER 7

### ISOMETRIC PROCESS ANALYSIS

Pultrusion, taken in its entirety, is a process. The mass, energy, and force balances discussed in the previous sections represented needed connections with more fundamental physiochemical aspects. Such connections had not been made heretofore. An examination of a pultrusion process and the pultruded stock produced by that process was considered to be of value also. An examination of an actual process is difficult in many cases because the process often must meet certain "boundary conditions", such as the need to meet shipping schedules, satisfy customers' demands, and deal with varying sources of supply. In many respects an examination of a working process will not be as clean as might be desired. On the other hand, a working process does represent the real world, however inefficient it may be. Accordingly, two working processes were analyzed, one which used isobaric dies (to be discussed in the next section) and one which used isometric dies.

#### Description of the Process

The isometric die process is used almost exclusively for pultrusion. This process was used to make all the pultruded stock shown in figure 2 except the black plate and hat section which will be discussed later. Detailed information on the process and properties has been given elsewhere (ref. 16, 18, 29, 36). Briefly, the process was the "wet" type which consisted of pulling glass roving through a

room temperature bath of isophthalic polyester resin. The resin contained an initiator (benzoyl peroxide), an inhibitor (parabenzquinone or hydroquinone), and an internal release agent to reduce adhesion between resin and die surface. If required, the resin might also contain a filler (e.g. aluminum silicate or calcium carbonate), a fire retardant (antimony oxide), and inorganic pigments for coloring. After the glass fiber left the resin bath, the resin-fiber mass passed through bushings which forced out air bubbles and excess resin. Then the mass entered chrome-plated steel dies, of length 0.75 or 1.5 m (30 or 60 inches), which were heated by a circulating hot oil jacket to 390 K (240°F) or higher. Circulation of hot oil tends to maintain an isothermal profile along the die length, and helps control the temperature rise associated with the exothermic reaction (ref. 4). On emerging from the die, the hot, cured, pultruded stock was cooled by a water spray or compressed air so the catapillar-type pulling mechanism could engage it without causing surface marks or distortions. Once beyond the pulling mechanism, the stock was cut to standard lengths of 3 or 6 m (10 or 20 ft).

#### Properties of the Pultruded Stock

Pultruded stock made by the process described above was obtained from a vendor, not the manufacturer, and so presumably represented stock which would be available to any purchaser. The stock length was 3 m (10 ft). Of the polyester and glass stock shown in figure 2, four were selected for evaluation, the square tube and the three circular rods.

The square tube had nominal dimensions of 50 mm (2 in.) with a 3.2 mm (1/8 in.) wall thickness, giving an aspect ratio of 16. Oven burn-out

of the resin revealed the tube construction consisted of five layers, two of unidirectional roving among three layers of quasi-isotropic mat. The roving carried most of the pulling force, and the mat provided a degree of cross reinforcement. Indeed, cross reinforcement has been identified as one of the major problems in pultrusion (ref. 5), and others have noted (ref. 14) the persistent idea that pultruded stock contains only unidirectional fibers. The resin burn-out showed that, based on the mass of the residue of fiber and filler, one side (assumed to be the bottom side) had a higher resin fraction (0.435) than did the others. The opposite side had a lower resin fraction (0.417). A square tube, like other closed, hollow sections, requires the use of a carefully aligned central mandrel. If the mandrel is off center, then the narrower side will have a slightly higher pressure. The resin will tend to flow away from the high pressure toward the low pressure area. Such pressure differentials might also lead to residual stresses. To test for the presence of such stresses, a length of the tube was slit lengthwise for 300 mm. The slits were made at the third points of each face. The resulting deformation at the free end is shown in figure 20. The four corners did not deflect as they were stabilized by their geometry. The sections in the center of the faces did deflect, however. The sides, with a parting line showing on the nearer side, deflected outward, as did the assumed top section. The assumed bottom section deflected inward. The deflections were not excessive however, on the order of three or four wall thicknesses for a span of  $\sqrt{100}$  thicknesses. However, they do illustrate some of the difficulties encountered in pultruding closed, hollow stock.

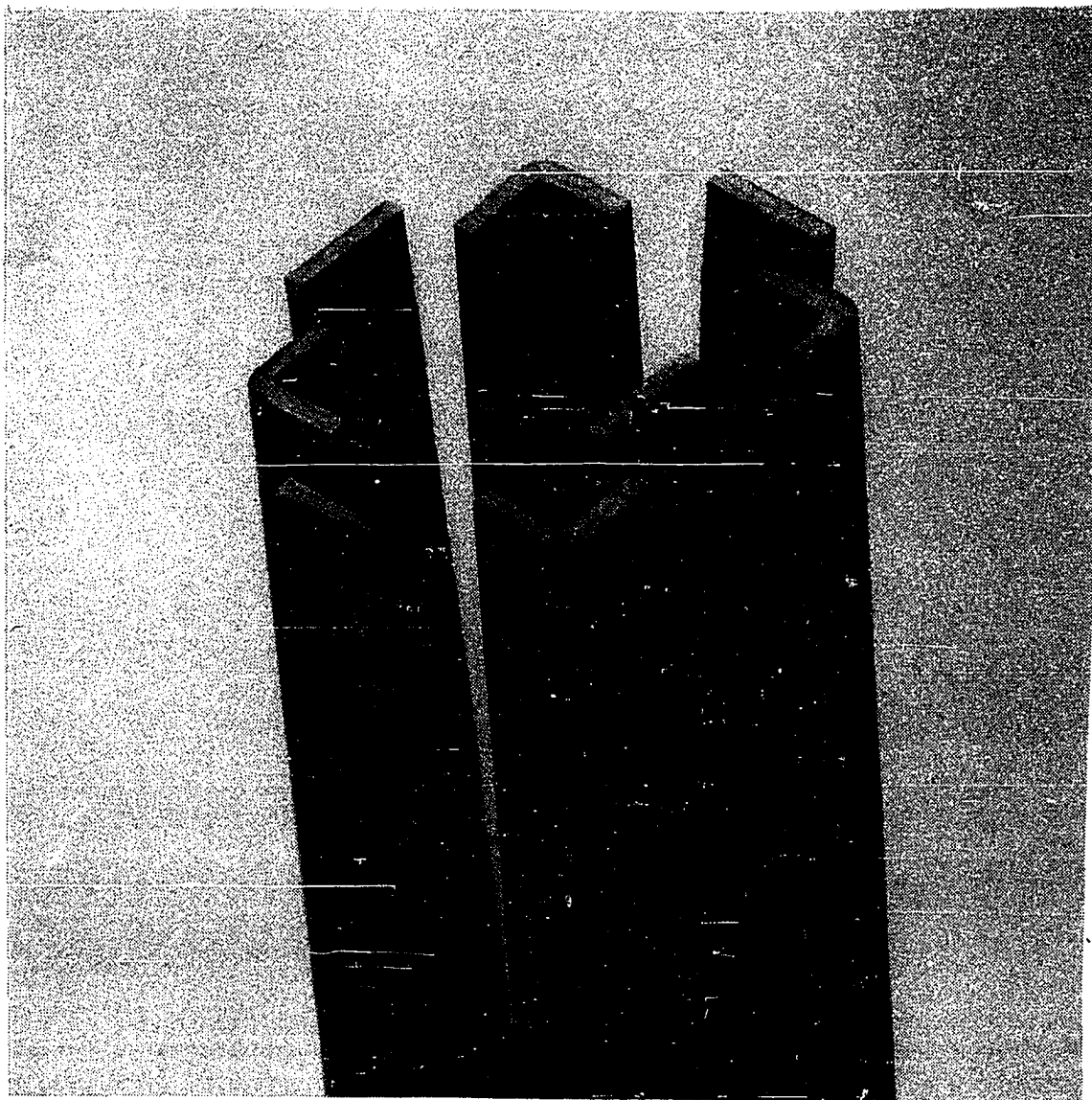


Figure 20.- Deformation of pultruded square tube after lengthwise splitting.

The other polyester and glass stock evaluated was the three circular rods shown in figure 2. The rods had nominal diameters of 9.5, 19, and 38 mm ( $3/8$ ,  $3/4$ , and  $1\ 1/2$  in.), and hence relative diameters of 1, 2, and 4. These rods were all unidirectional fiber in roving form, and the resin did not contain a filler. Some properties of the rods are given in table 6. The central core refers to specimens of the largest rod which were machined to half the original diameter, thereby leaving the center fourth of the original rod. The specific gravity was high for all the rods, with little variation from one rod to another. Of more interest, however, was the low specific gravity of the central core as compared to that of the entire cross section. This difference was corroborated in the glass volume fraction. Although there was a rod-to-rod difference, it was smaller than the difference between the central core and the entire cross section of the largest rod. As the cross section value is an average for the entire rod, the low values of the central core imply considerably higher values for the rest of the rod surrounding the core.

This pattern of resin concentration in the center and fiber concentration around the periphery may indicate that large collimation forces were generated as the resin-fiber mass entered the die. In fact, early in the resin burn-out tests of the largest rods, the specimens would be surrounded by a fine dust of short lengths of broken fibers which had fallen from the outer surface. The interior fibers showed little sign of breakage. If the outer-surface was subjected to high collimation forces, then the resin would flow away from the surface to the center where back flow would relieve some of the pressure.

TABLE 6. - PHYSICAL PROPERTIES OF PULTRUDED CIRCULAR RODS

Relative Diameter	1	2	4
Nominal Diameter, mm (in.)	9.5(3/8)	19(3/4)	38 (1 1/2)
Relative Cross Sectional Area and Mass per Unit Length	1	4	16
Specific Gravity			
Cross Section	2.04	1.99	2.04
Central Core	--	--	1.94
Glass Volume Fraction			
Cross Section	.652	.596	.634
Central Core	--	--	.559

A pattern of resin-rich areas and fine cracks was observed in the inner portion of the largest rod. This pattern is shown in figure 21 where the large crack across the rod was due to a diametral test described below. The other cracks were present before the test. The pattern was nearly circular and extended over roughly two-thirds of the diameter. Electron micrographs of this pattern (fig. 22) showed a general view (14x), figure 22a, a resin-rich area (140x), figure 22b, and a crack (140x), figure 22c. This pattern was observed only in the largest diameter 4 rod (38 mm) which presents considerable problems as far as uniform curing is concerned. The intermediate diameter 2 rods (19 mm) showed slight evidence of cracking over the central third of the diameter. The smallest diameter 1 rods (9.5 mm) which were the easiest to cure were sound and uniform.

The diametral strength and notched shear strength was measured for the rods and the results are listed in table 7. Although the diametral test is useful for solid polymer moldings (ref. 71) and has been used for pultruded rods (ref. 32, 51), it was of limited value in this investigation. The specimen fracture often was not along the loaded diameter, a requirement for a valid diametral test. Moreover, the coefficient of variation was sometimes high. (A coefficient of variation of 0.008 was reported in reference 51). Even so, the test results may be of value for comparing the apparent resin tensile strength (as indicated by the diametral strength) in the various rods. The overall mean of all the diametral tests of the as-received rods was 12.4 MPa (1800 psi). Only the diameter 2 rods differed significantly (at the 95 percent confidence level) as indicated by the  $t$  test. A



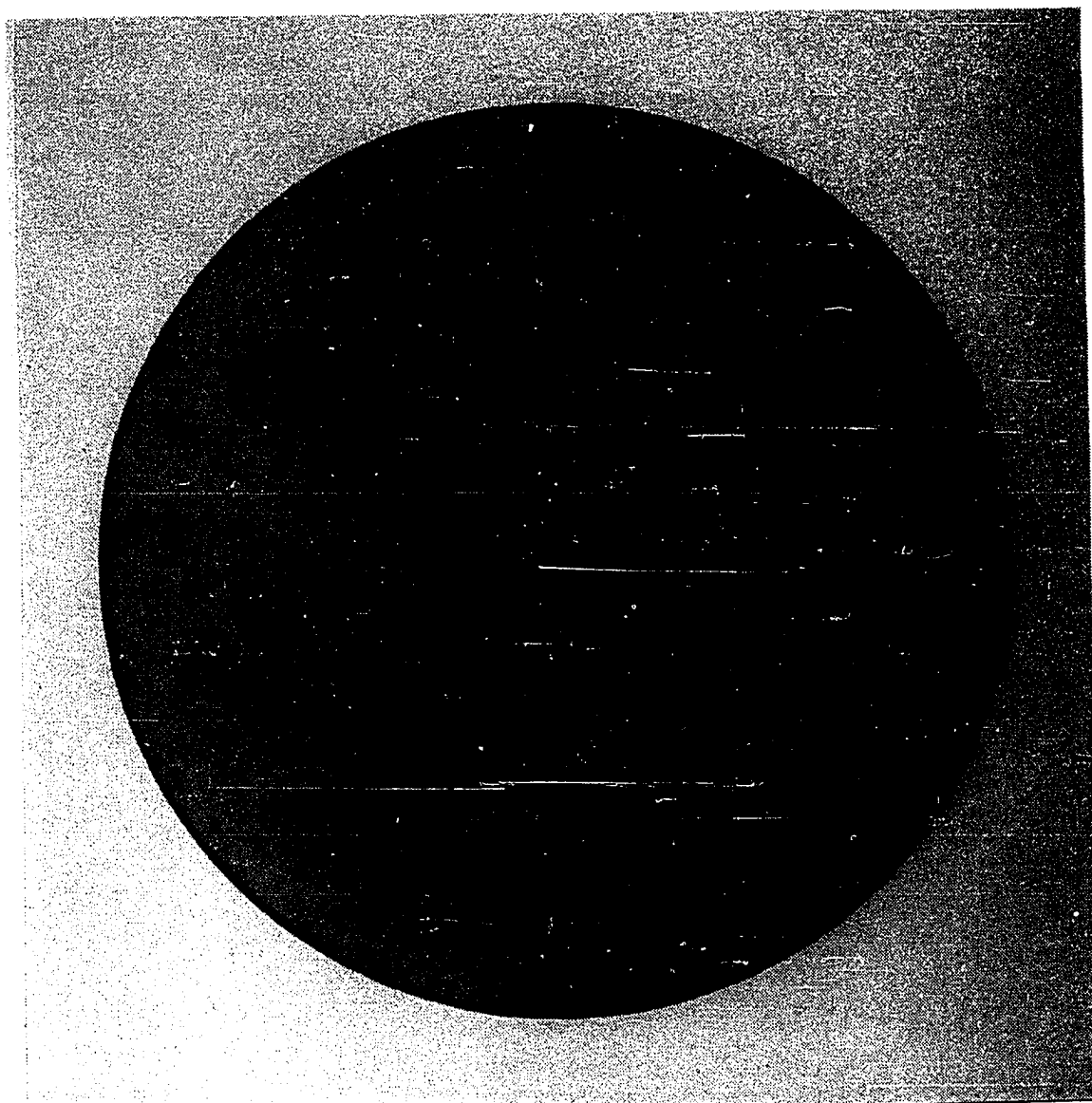
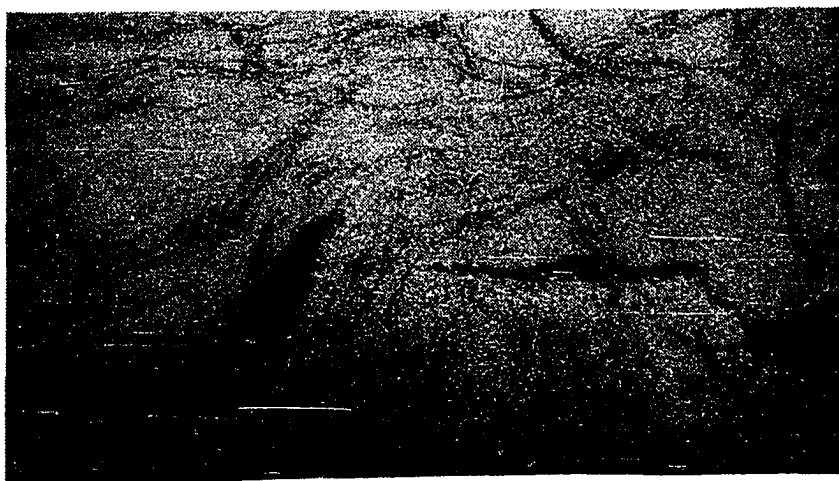
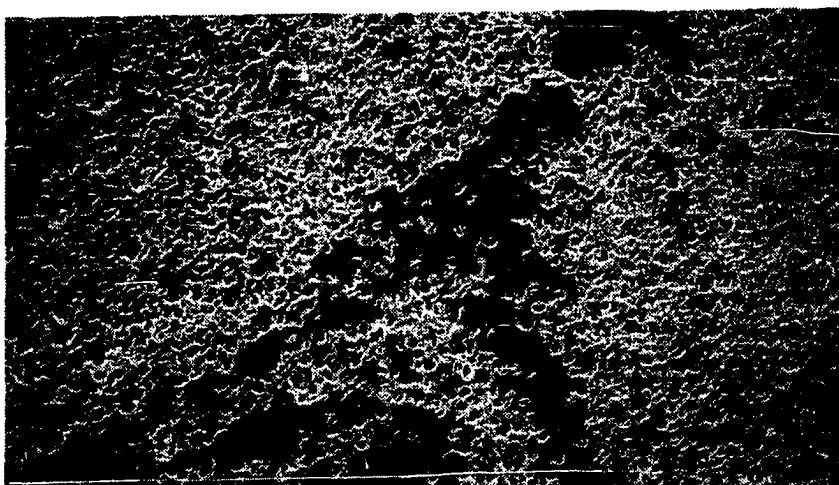


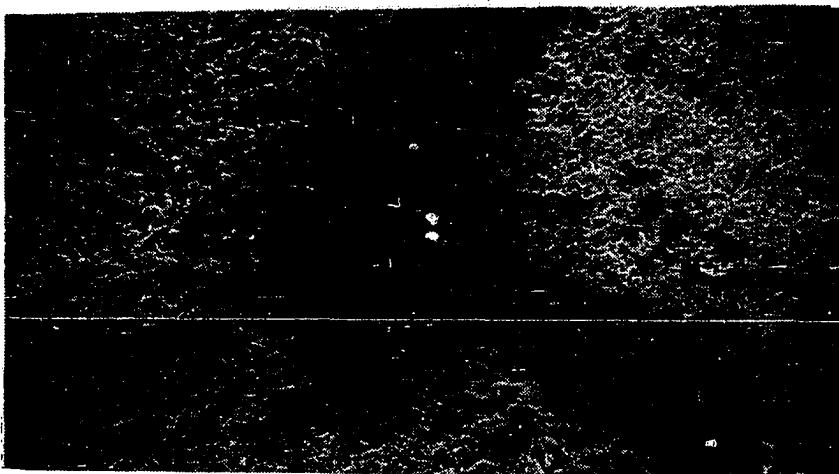
Figure 21.- Cross section of 38-mm-diameter pultruded circular rod.



(a) General view (14X).



(b) Resin-rich area (140X).



(c) Crack (140X).

Figure 22.- Scanning electron micrographs of 38-mm-diameter pultruded circular rod.

TABLE 7. - MECHANICAL PROPERTIES OF PULTRUDED CIRCULAR RODS

Property	Value*	Relative Diameter		
		1	2	4
Diametral Strength, MPa				
As Received	N	6	11	5
	M	14.9	11.5	11.3
	V	.227	.089	.240
Post Cured	N	6	--	4
	M	15.5	--	13.2
	V	.225	--	.056
Central Core	N	--	--	11
	M	--	--	14.8
	V	--	--	.057
Notched Shear Strength MPa				
As Received	N	6	12	6
	M	45.7	39.1	36.7
	V	.065	.131	.051
Post Cured	N	6	--	6
	M	50.3	--	36.2
	V	.044	--	.083
Central Core	N	--	--	12
	M	--	--	38.5
	V	--	--	.124

\*Value refers to number of tests (N); mean value(M), and coefficient of variation (V).

post cure (1.5 hours at 390 K (240°F)) was given to the rods which would be easiest (diameter 1) and hardest (diameter 4) to cure uniformly in the die. The post cure increased the diametral strength (table 7) but not significantly above the mean of the as-received rods. Surprisingly, the diametral strength of the central core of the diameter 4 rod was significantly higher than the mean of the as-received rods the coefficient of variation was very low. Apparently the cracks and resin-rich areas of the core did not have a detrimental effect on the diametral strength.

The notched shear test has also been recommended for pultruded rods (ref. 32, 33, 52). The test results are listed in table 7 where the overall mean for the as-received rods was 40.7 MPa (5900 psi). The shear strength for the diameter 1 rods was significantly above, while that for the diameter 4 rods was significantly below, that average. When the rods were post cured, the strength of the diameter 1 rod increased as if it had not been sufficiently cured. Such a result could be due to a low die residence time or a low concentration of initiator. The diameter 4 rods, with a shear strength already below the mean, dropped in strength on post curing. This result is difficult to explain in light of the fact that the diametral strength of this rod increased on post curing. But consistent with the diametral tests, the shear strength of the central core was higher than that of the full size diameter 4 rod, and, in fact, was not significantly different from the overall mean of the as-received rods. Once again, the cracks and resin-rich areas did not degrade the strength.

### Analysis of the Process

Consider three rods of relative diameter 1, 2, and 4, which contain the same proportion of unreacted polyester resin and glass fiber, and the resin has the same initiator concentration for all three rods. The objective is to pass the rods through a 390 K die so that each rod reaches a given reaction fraction (say 0.8) at the centerline. The fraction should be reached at the die exit. If it is reached sooner, the residence time is too long; if later, the time is not long enough.

As the rods are being heated from the outside, the time required for the centerline to reach the die temperature can be found from the Fourier number.

$$N_F = \frac{\theta_h}{r^2/\alpha} \quad (23)$$

Time  $\theta_h$  is the heat-up time. Setting  $N_F$  to unity,

$$\theta_h = \frac{r^2}{\alpha} \quad (24)$$

Hence, assuming the same thermal diffusivity,  $\alpha$ , for all three rods and a linear temperature rise rate, the relative heat-up times will be 1, 4, and 16 for the centerline.

The centerline reaction is to proceed adiabatically in order to keep the residence time to a minimum. The adiabatic temperature rise,  $\Delta T'_{ad}$ , is to be held to 0.01 in order to keep the reaction under control.

Then, from figure 18, for  $\Delta T'_{ad} = 0.01$  and  $T^* = f = 0.8$ , the Damköhler number  $N_D = 1.5$ . But

$$N_D = c_o^{n-1} k\theta \quad (10, \text{repeated})$$

and the reaction order,  $n$ , is unity for polyester resins so the concentration term can be dropped. The residence time for the reaction is

$$\theta_r = \frac{1.5}{K} \quad (25)$$

The total residence time is the sum of the heat-up and reaction times, or

$$\theta = \frac{r^2}{\alpha} + \frac{1.5}{k} \quad (26)$$

The residence time given by equation 26 is really an upper bound, as the reaction time,  $\theta_r$ , was estimated as if no reaction took place until the centerline temperature reached 390 K. As to whether this approximation should be refined depends in part on the relative magnitudes of  $\theta_h$  and  $\theta_r$ . For example, using values from table 3 for activation energy and pre-exponential constant of polyester resin with one percent BPO, the reaction rate constant at 390 K is  $\sim 2.4 \times 10^{-2} \text{ sec}^{-1}$ . The reaction time,  $\theta_r$ , is  $\sim 60$  seconds. By contrast, the heat-up time,

$\theta_h$ , for a 9.5 mm - diameter rod, assuming a thermal diffusivity of  $3 \times 10^{-7} \frac{\text{m}^2}{\text{sec}}$  is  $\sim 75$  seconds. In that heat-up time, the accumulated  $N_D$  is  $\sim 0.4$ . Hence the required reaction time is

$$\theta_r = \frac{1.5 - 0.4}{k} \approx 46 \text{ sec} \quad (27)$$

and the total residence time is  $75 + 46 = 121$  seconds.

By contrast, the largest rod would have a heat-up time of  $\sim 1200$  seconds. But the accumulated  $N_D$ , when the centerline reached 390 K, would be  $\sim 6.5$ . The centerline would have been reacted to the 0.8 fraction after a residence time of  $\sim 833$  seconds, when the centerline temperature had risen to 363K. In other words, by the time the centerline temperature reached the die temperature, the center of the rod would be reacted to a fraction greater than 0.99.

An inquiry to the manufacturer of the rods used in this investigation revealed the following: the BPO concentration was in the 1.0 - 1.6 percent range (1.0 percent was used in the above calculations); the die temperature was 240°F (390 K) in general, but may range up to  $\sim 310^\circ\text{F}$ ; the pulling speed for the 9.5 mm rod was  $\sim 30$  in/min through a 30-inch die ( $\sim 60$  second residence time); the pulling speed for the 38 mm rod was 2-5 in/min through a 60-inch die (720-1800 second residence time). The estimated residence time for the 38 mm rod (833 to 1200 seconds) fell in the low end (and the high production rate end) of the reported range. The estimated residence time for the 9.5 mm rod (121 seconds) was twice the reported time. However, the strength of these rods was increased significantly by a 390 K post cure. The implication

is that the residence time of ~60 seconds is not sufficient to cure the 9.5 mm rods.

#### Isometric Process

The isometric process has been used to pultrude a wide variety of open and closed, hollow and solid, cross sections using polyester resin and glass fiber: a hollow square tube was found to have an uneven resin distribution over the cross section, and a low level of residual stress. Solid circular rods of three different diameters were used as a means of estimating die residence times for a 390 K die temperature. The estimated time for the largest rod fell within the range reported by the manufacturer. The estimated time for the smallest rod was twice the reported time. However, the strength of this rod was increased by post curing at 390 K, suggesting that the residence time should have been longer than it was.



## CHAPTER 8

## ISOBARIC PROCESS ANALYSIS

The isobaric process, as the name implies, is one in which the die applies a constant pressure to the resin-fiber mass. This process is not in wide use for pultrusion, but it has been developed for making aircraft structural shapes (ref. 25, 39). This process was used to pultrude the black hat-shaped section and flat panel shown in figure 2. Some processing details and properties of the pultruded stock were reported in reference 39. However, the data were not analyzed for the purpose of defining important process variables or relating properties to those variables. Such an analysis was made as part of this investigation. As only average property values were reported, the author of reference 39 provided individual test values so a more detailed analysis could be made.

## Description of the Process

The isobaric process described in references 25 and 39 is a "dry" process which uses prepreg tape. An epoxy-graphite tape (E 702/T300) was used in the investigation reported in reference 39. The pultruder die was made of alumina and mounted in a rubber tube in which the air pressure could be regulated and measured. Energy for curing the resin was supplied by both hot air and by a microwave beam which impinged on the die from the -z to +z direction (see axes in figure 4). The beam had a 915 MHz frequency and a  $TM_{01}$  wave form. As the alumina die had a very low dielectric loss, it essentially was not heated by the microwave energy. How-

ever, the resin-fiber mass (e.g. epoxy resin and graphite fiber) was very "lossy" and converted part of the microwave energy into heat. This heat, in addition to that of the circulating hot air, initiated the exothermic curing reaction in the epoxy. The air temperature was set to lower values as the microwave power setting was increased, but neither form of energy was used by itself for curing. As the thickness of the resin-fiber mass changed during its passage through the die, the die sections moved relative to one another to accommodate those changes. Pulling of the mass through the die was accomplished by a clamp, cable, and winch arrangement so that pultruded lengths up to 12 m (40 ft.) could be produced in one pulling cycle.

#### Hat-Shaped Section

The hat sections not only were a useful structural shape, but also were a means of illustrating some problems which might be encountered in pultruding such shapes. The hat had a nominal 115 mm width which included a 32 mm cap and 25 mm flanges. The nominal height was 30 mm. The nominal thickness of the cap was 2.8 mm, of the webs and flanges, 1.4 mm.

Test specimens were taken from the cap, web, and flange locations. Specific gravity and fiber fraction determinations showed that the web values (1.57 and 0.632) were significantly above those of the cap (1.52 and 0.592) and the flanges (1.51 and 0.581). Considering the distribution of these values and the shape of the cross section, it would seem that much of the die pressure was being taken in the webs. Then the webs would be a high pressure area from which the resin might flow into the lower pressure cap and flanges.

Short beam shear tests of web and flange specimens showed a significant -z to +z difference. For example, for lower die pressures, the +z web had  $\sim 28$  percent higher strength than the -z web. For higher die pressures, the -z web had a higher strength. A similar pattern was observed with the flanges, the +z flange generally having a higher strength than the -z flange. Such an effect might be due to distortion of the microwave beam. Although the beam would be fairly uniform in an empty cavity, the presence of the die and resin-fiber mass would distort the beam, causing regions of higher- or lower-than-average energy density. As a result, some parts of the hat would be cured more, and some less, than other parts. For simple shapes, such as a flat plate or a circular rod, microwave beam distortion probably would not be as much of a problem.

#### Analysis of the Process

The flat plates (fig. 2) provided a simple shape which could be used for process analysis. Plates were also made by a conventional autoclave process (a pressure of 585 kPa at 395 K for 2 hours) to provide a standard against which the pultruded plates could be compared. The plates had a nominal width of 150 mm and thickness of  $\sim 3$  mm, thus giving a very high ( $\sim 50$ ) aspect ratio.

The processing variables and resulting properties are listed in tables 8 and 9. The four processing variables were the die pressure, pulling speed, and the inversely related microwave power and die temperature. That inverse relationship can be seen in figure 23 where the die temperature is plotted against the microwave power. The slope of the lines is about  $-22.1$  K/kW, indicating that the die temperature was reduced about 22 K ( $40^\circ\text{F}$ ) for each 1 kW increase in microwave power.

TABLE 8. - PROCESSING PARAMETERS AND PROPERTIES OF PULTRUDED FLAT SECTIONS OF EPOXY RESIN AND GRAPHITE FIBER;  
DATA FROM REFERENCE 39

Test Number	Processing Parameters				Physical Properties			Short Beam Shear Strength, MPa	Flexural Strength, GPa
	Die Pressure, kPa	Microwave Power kW	Pulling Speed mm/sec	Die Temperature K	Thickness, mm	Specific Gravity	Fiber Volume Fraction		
1	185	2.0	1.25	445	3.25	1.50	.575	66.1	1.09
2	185	2.5	2.55	445	3.25	1.49	.579	61.8	1.08
3	185	3.0	1.70	429	3.28	1.48	.575	63.5	1.07
4	200	3.0	1.25	453	3.35	1.47	.558	57.4	1.11
5	205	1.5	1.70	465	3.18	1.54	.608	71.6	1.08
6	205	1.5	2.55	471	3.12	1.55	.621	72.2	1.09
7	205	1.5	2.55	472	3.18	1.52	.608	66.6	1.12
8	205	2.0	1.70	452	3.10	1.55	.626	78.6	1.09
9	205	2.0	2.55	459	3.15	1.53	.619	68.1	1.01
10	205	3.0	1.70	446	3.10	1.56	.630	73.4	1.10
11	235	1.5	2.55	484	3.15	1.52	.593	66.5	1.08
12	235	1.8	2.55	476	3.12	1.55	.628	71.9	1.10
13	235	2.5	2.55	461	3.07	1.56	.642	73.0	1.08
14	235	2.5	1.70	450	3.02	1.51	.597	72.7	1.04
15	235	3.0	2.55	450	3.07	1.56	.629	70.9	1.11
Pultrusion Average					3.15	1.53	.606	69.0	1.08
Autoclave Average of 2 Panels					3.02	1.57	.623	87.0	1.08

TABLE 9. - PROCESSING PARAMETERS AND PROPERTIES OF PULTRUDED FLAT SECTIONS OF EPOXY RESIN AND GRAPHITE FIBER

Test Number	Processing Parameters				Physical Properties			Short Beam Shear Strength, MPa
	Die Pressure, kPa	Microwave Power, kW	Pulling Speed mm/sec	Die Temperature, K	Thickness, mm	Specific Gravity	Fiber Volume Fraction	
16	185	2.0	1.05	442	3.28	1.47	.555	53.2
17	205	1.5	1.70	467	3.17	1.47	.560	59.5
18	205	1.5	1.70	469	3.18	1.48	.584	58.5
19	205	1.5	2.55	479	3.16	1.47	.558	59.4
20	235	1.5	2.55	479	3.13	1.50	.572	63.5
21	235	2.0	2.55	469	3.09	1.50	.582	64.7
22	235	2.5	1.70	450	3.05	1.46	.535	56.6
23	235	2.5	2.55	456	3.07	1.52	.592	63.7
Average					3.14	1.48	.567	59.9

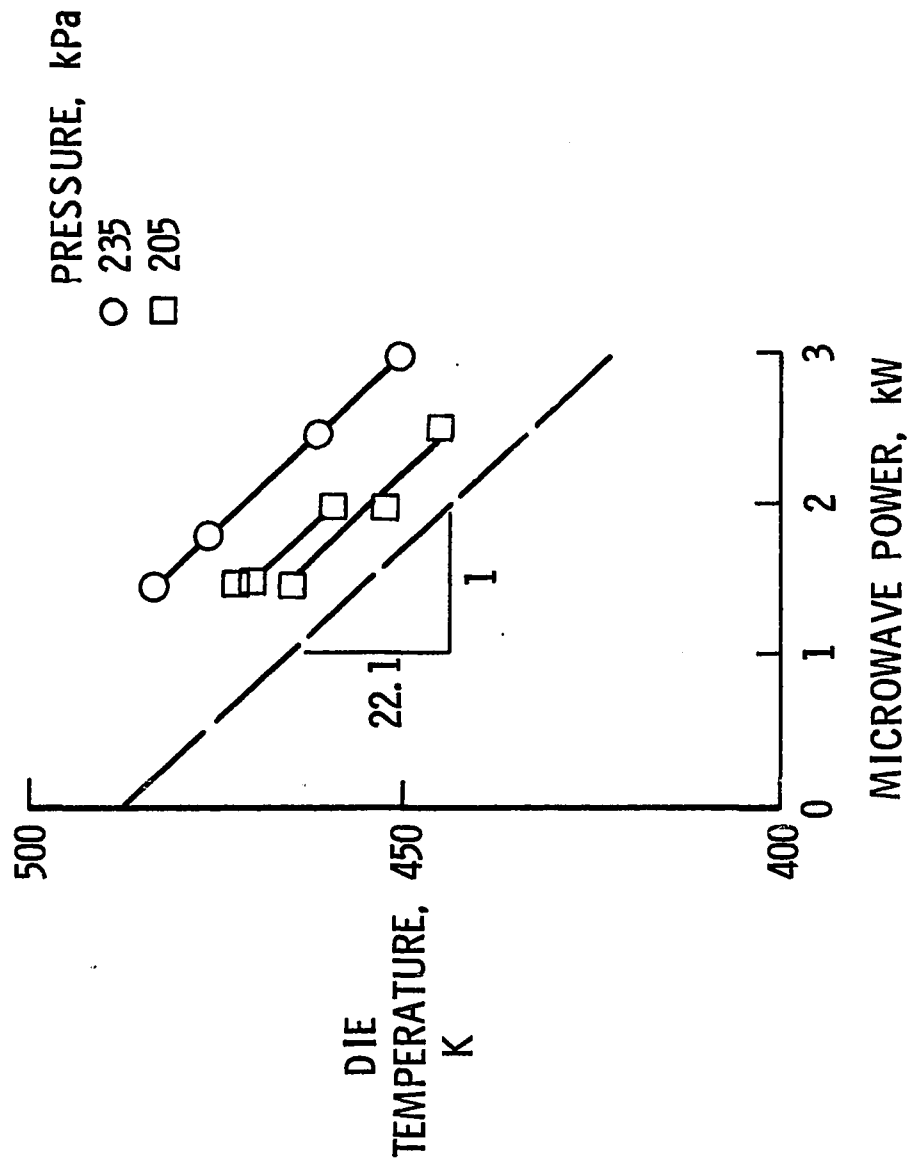


Figure 23.- Die temperature as a function of microwave power for isobaric process.

Figure 23 also shows that the die temperature was higher for the higher pulling speed. The higher pressure presumably increased the heat transfer from the resin-fiber mass to the die. The higher speed might be expected to reduce the die temperature because each unit volume of the mass spends less time in the die and hence provides less heat to the die. However, the higher speeds led to higher shear strain rates at the resin die interface, and such higher rates can increase the heat transfer coefficient (ref. 72). The die temperature, then, was directly proportional to pressure and speed, and inversely proportional to microwave power, or

$$T \sim \frac{P \cdot s}{\phi} = \frac{P}{\phi/s} \quad (28)$$

The form of equation 28 suggested a dimensionless number which might be useful, because pressure is also specific force ( $N/m^2$ ). If the denominator could be cast into specific energy ( $N \cdot m/m^3$ ) then the number would be dimensionless. The energy to which the resin-fiber mass was exposed included both thermal and microwave energy. The thermal energy per unit volume was

$$E_t = \frac{c_p m dT}{w t l} \quad (29)$$

For a fiber volume fraction  $f=0.6$ , specific heat and density of 1045 J/kg-K and 1200 kg/m<sup>3</sup> for epoxy, and 690 J/kg-K and 1800 kg/m<sup>3</sup> for graphite,

$$E_t = 1.25 dT \text{ MJ/m}^3 \quad (30)$$

For a temperature change of 22.1K such as that associated with a 1 kW microwave power change,

$$E_t = 27.6 \text{ MJ/m}^3 \quad (31)$$

By contrast, the microwave energy impinging on the resin-fiber mass was a product of the microwave power and residence time divided by the volume within the die, or

$$E_m = \frac{\theta d\phi}{wtl} = \frac{d\phi}{wtl} \frac{l}{s} = \frac{d\phi}{wts} \quad (32)$$

For a speed of 2.55 mm/sec, a thickness of 3 mm, and a power change of 1 kW,

$$E_m = 858 \text{ MJ/m}^3 \quad (33)$$

Hence,  $E_m \approx 30 E_t$ , and at least numerically, the microwave energy was more significant than the thermal energy. (From the standpoint of curing kinetics, however, both energy forms may be important.) If the microwave energy only is used, then a dimensionless number might be

$$\frac{p}{\phi/wts} = \frac{wtsp}{\phi} \quad (34)$$

As the thickness of the resin-fiber mass can vary in an isobaric process, it can be used as an indicator of the extent of the curing reaction (ref. 70). However, only a portion of the total thickness (the resin portion) undergoes the reaction. In addition, the thickness, fiber



fraction, and specific gravity are coupled. The product of the three, for any test in table 8, was very close to 2.95 mm. Hence a somewhat more accurate form of the dimensionless number, call it a processing number, is

$$N_p = \frac{t(1-f)}{\rho} \frac{(wps)}{\phi} \quad (35)$$

The processing number was calculated for each of the tests listed in table 7, and the die temperature was plotted as a function of that number (figure 24). Although some scatter in the data is apparent, the die temperature appeared to be a monotonically increasing function of the processing number. A least squares regression analysis of the data indicated that the die temperature could be expressed

$$T = 429 + 3.28 \times 10^{11} N_p \quad (36)$$

Although no value of the base die temperature was given in reference 39, that temperature may have been near 429 K (312°F) as suggested by equation 22 when  $N_p = 0$ . Presumably the base temperature would be no higher than 429 K (the lowest temperature listed in table 8) and no lower than the 395 K used for the autoclave cure.

Using equations 35 and 36 and rearranging, a form which relates the control and response variables can be obtained. That form is

$$\frac{\rho}{t(1-f)} = \left( \frac{3.28 \times 10^{11}}{T-429} \right) \frac{wps}{\phi} \quad (37)$$

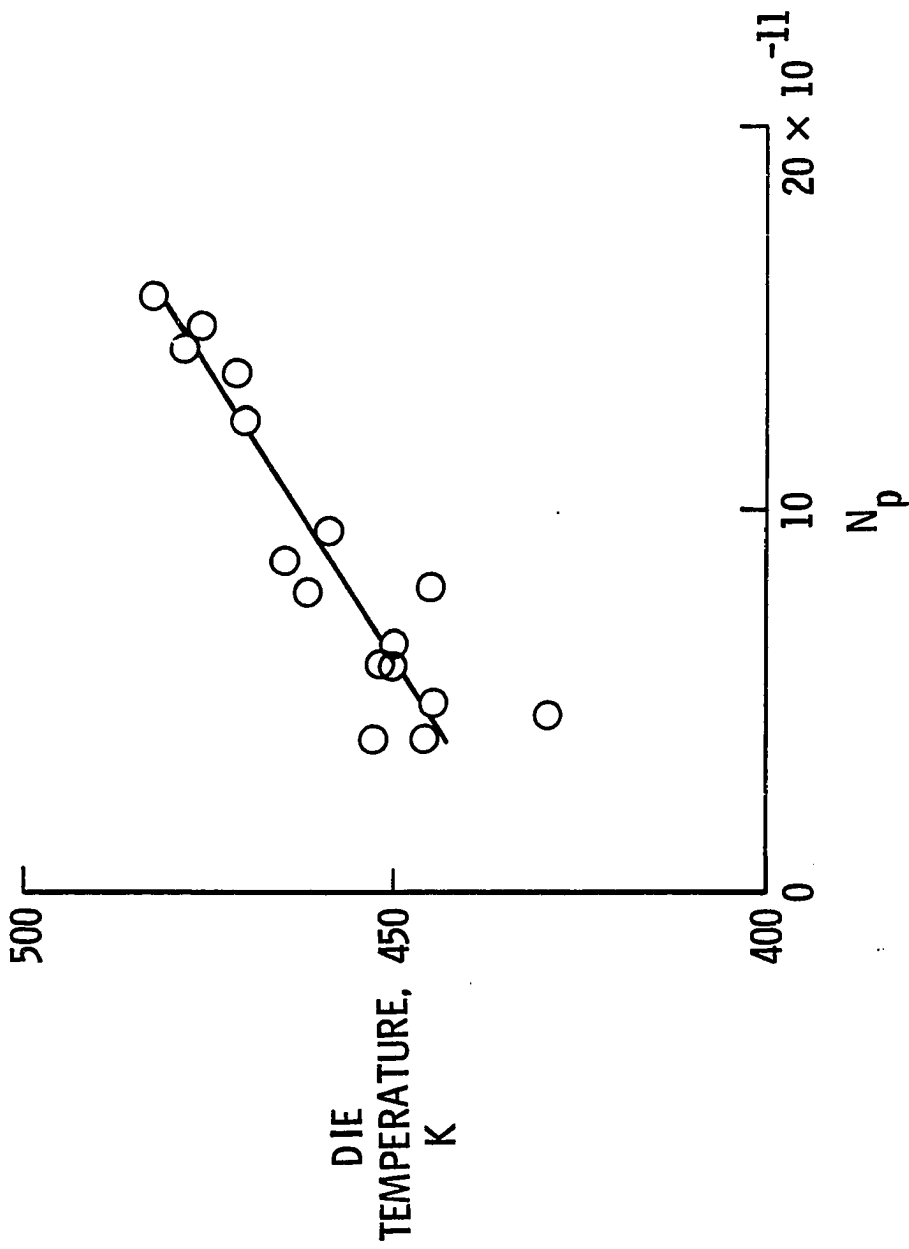


Figure 24.- Die temperature as a function of processing number.

where the width,  $w$ , is a constant set by the die, and the numerical values taken from equation 36 were determined empirically. The response variables (thickness, fiber fraction, specific gravity) become a function of the control variables (pressure, pulling speed, and temperature/microwave power). If 429 K is taken as the lowest die temperature for the highest microwave power, then, using the slope obtained in figure 23

$$T = 495 - 22\phi \quad (38)$$

Substituting equation 38 into equation 36 gives

$$\frac{\rho}{t(1-f)} = \left( \frac{3.28 \times 10^{11}}{66-22\phi} \right) \frac{wps}{\phi} \quad (39)$$

In general, the left hand side of equation 26 should be a maximum, i.e. small thickness, large fiber fraction and specific gravity. The left hand side can be made large by using low microwave power or high pressure and pulling speed. The reference point for equation 39 is the  $\phi=3$  kW,  $T=429$  K point in figure 23. However, the change in the physical properties are proportional to the pressure and speed, and inversely proportional to the square of the microwave power.

$$\frac{\rho}{t(1-f)} \sim \frac{ps}{\phi^2} \quad (40)$$

The left hand side of equation 40 provides a measure of the quality of the pultruded stock. A high value indicates a dense, large fiber fraction material in which the matrix has reacted and brought about a

reduction in the thickness. This grouping of the response variables was plotted against the control variables. The result is shown in figure 25 which includes the response variable value for the autoclaved flat section. With one exception, the value for the pultruded sections fell below that for the autoclaved sections. As the quantity  $ps/\phi^2$  increased, the properties of the pultruded sections improved and reached a peak at about  $2 \times 10^{-4} \text{ W}^{-1} \text{ m}^{-2}$ . However, five of the tests did not fit this trend, with the values for these tests falling in the upper left-hand quadrant of figure 25.

To determine how the five tests (08, 10, 13-15) differed from the others, the pressure and energy (actually  $\phi^2/s$ ) for each test was plotted. The results are shown in figure 26 which includes a demarcation line between the five tests and the other tests. All five tests fell in the high pressure-high energy quadrant. In addition the response variables made a rather abrupt change as the test coordinates moved across the demarcation line. As indicated by the t test, the response variables of the five tests differed significantly (with 95 percent confidence) from the other ten. Indeed, the average response variable number for the five tests was  $1350 \text{ m}^{-1}$  (close to the  $1380 \text{ m}^{-1}$  value for the autoclave flats) while that for the other ten tests had an average value of  $1180 \text{ m}^{-1}$ . Similar abrupt property changes such as these indicated in figure 26 are often associated with phase changes in homogeneous materials. In analogy with the p-V-T diagram for water, the break in the demarcation line might be regarded as some sort of "critical point" where phase boundaries intersect. Whatever the interpretation, the data as arranged in figure 26 indicate that within rather well-defined pressure and energy boundaries, highly compacted pultruded flat sections can be obtained.

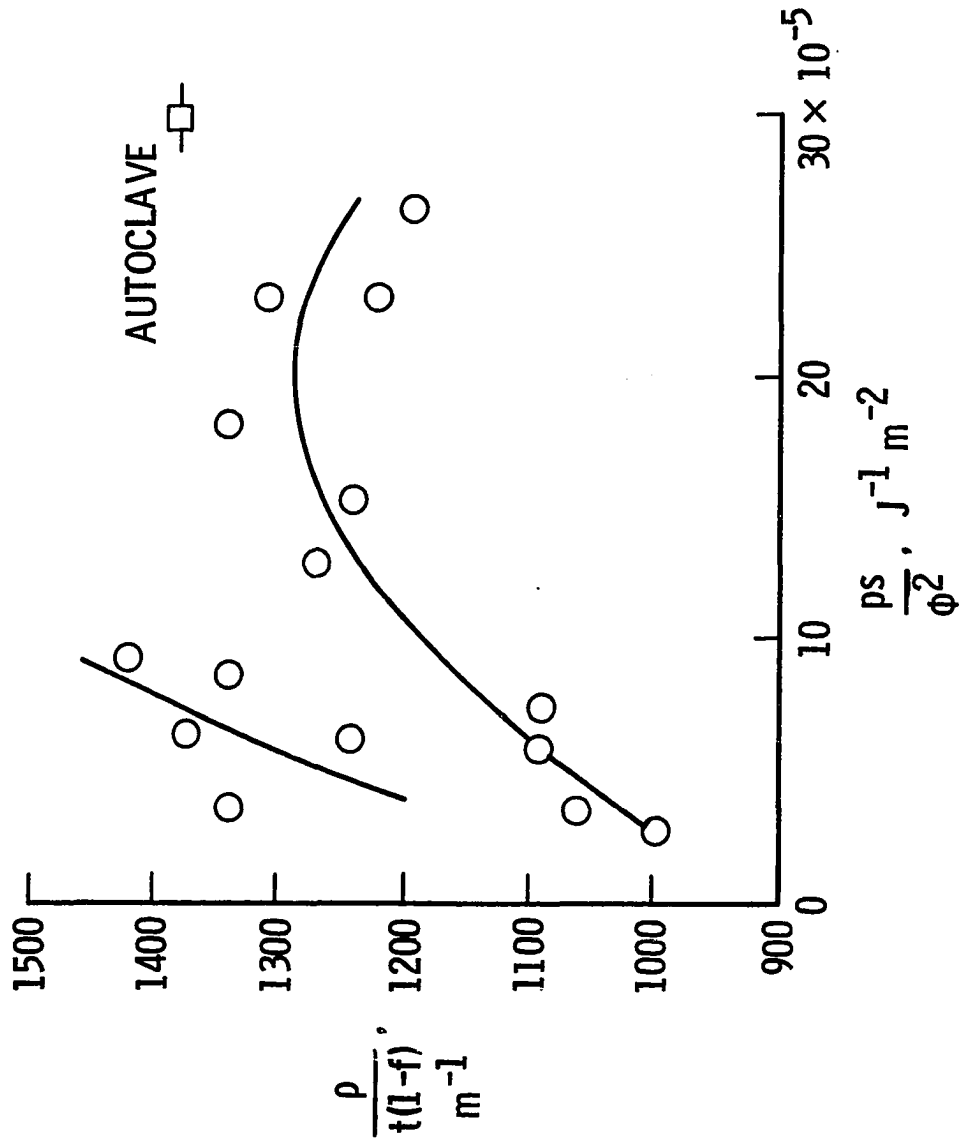


Figure 25.- Response variables as a function of control variables for isobaric process. Data from reference 39.

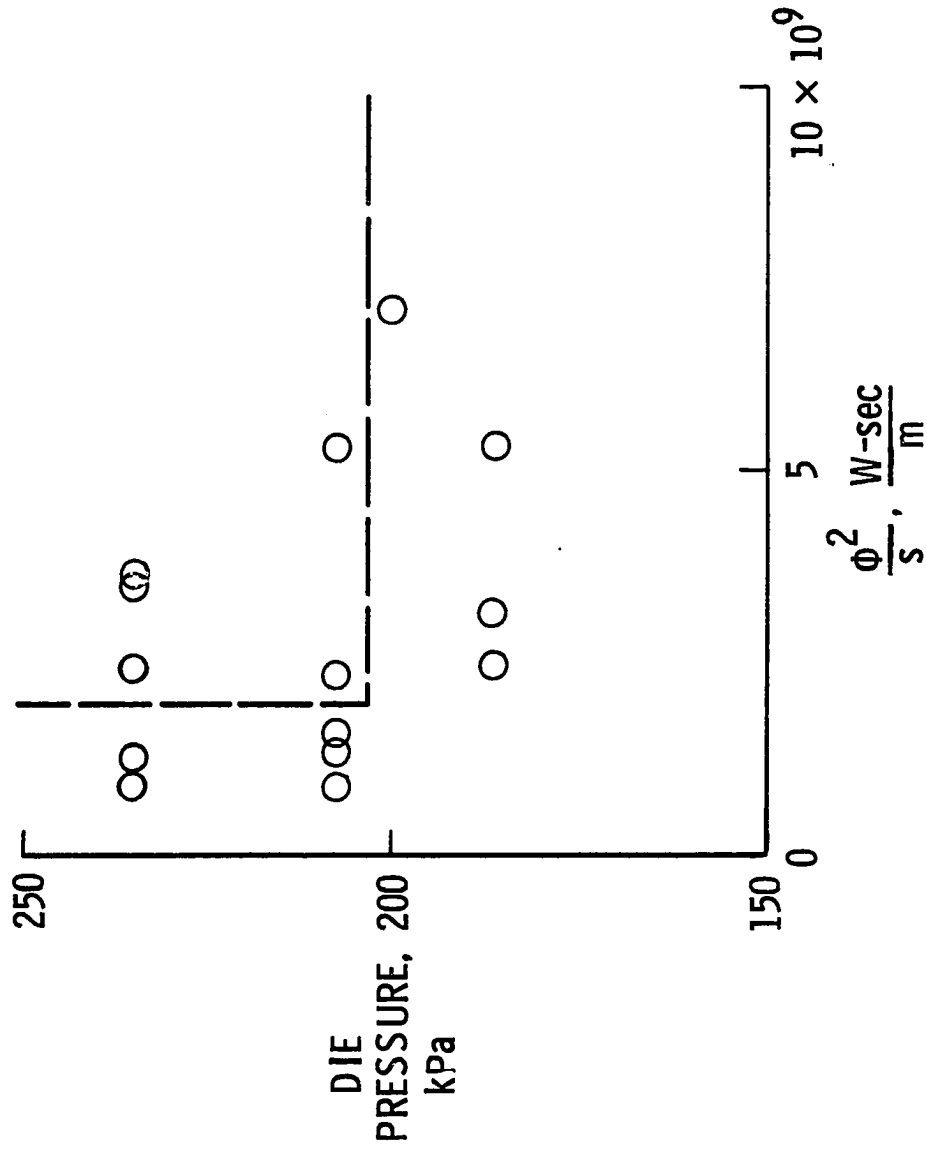


Figure 26.- Die pressure and energy impinging on resin-fiber mass in isobaric die.

In addition to the physical properties, the short beam shear strength and the flexural strength of the flat sections were measured. The results of these tests are listed in table 8 which includes the values for the autoclaved flat section.

The short beam shear data were analyzed to determine which sections had strength values which differed significantly from the overall average of 67.3 MPa. The results are shown in figure 27 which includes the autoclave value of 88.5 MPa. Four of the pultruded flat sections (tests 01-04) had shear strength significantly below average, while four (tests 06, 08, 13, 15) had strength significantly above average (with 95 percent confidence). All of the pultruded section averages were below the autoclaved section average, however. Those pultruded sections which had low strengths also had low response variables and were made at low pressures. By contrast, the higher strengths were associated with higher response variables as shown in figure 28. The data showed an upward trend with the curve reaching a limit at about 72-73 MPa. The exception to the trend was the high strength of 78 MPa obtained from test 08, the test located near the "critical point" on the pressure-energy plane in figure 26. That exception aside, the response variable grouping of thickness, specific gravity, and fiber volume fraction appears to be a useful indicator of the short beam shear strength.

The flexural strength, unlike the short beam shear strength, showed very little variation. The difference between the highest and lowest value was only about 12 percent. The overall average for both the pultruded and autoclaved flat sections was 1.08 GPa, and none of the individual section averages differed significantly from it. In addition,

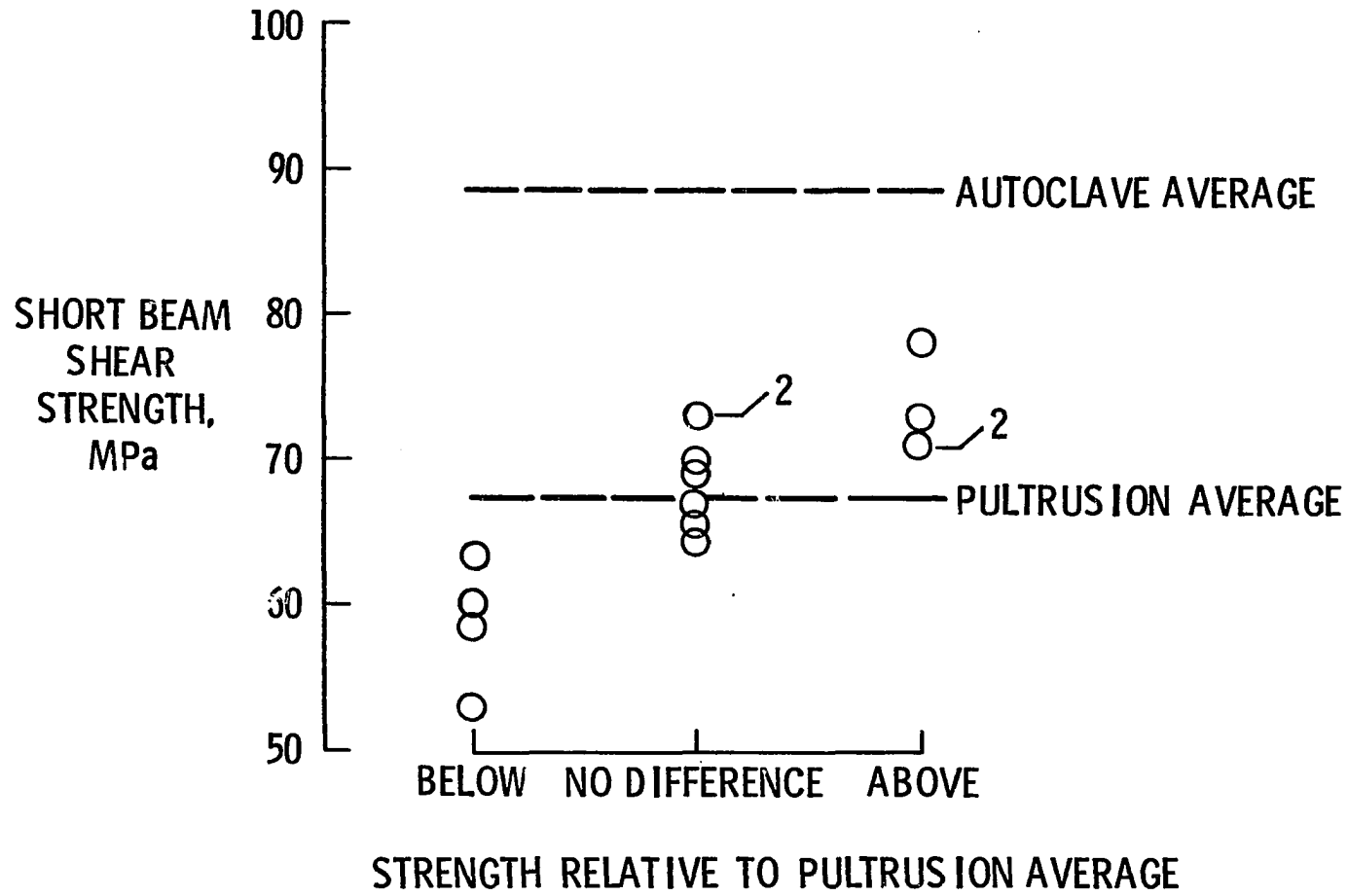


Figure 27.- Variation in short beam shear strength of pultruded flat sections.



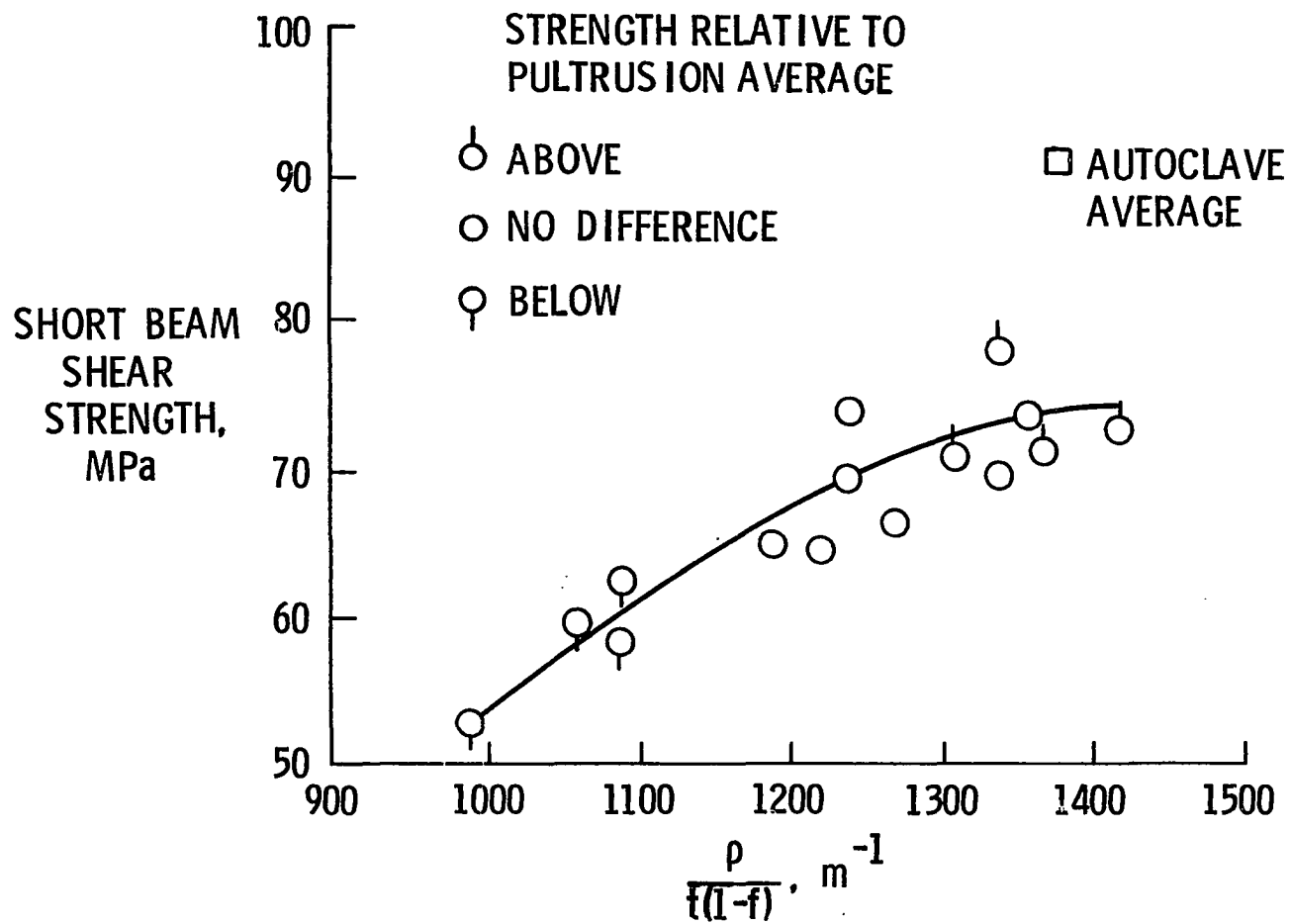


Figure 28.- Short beam shear strength as a function of response variables for pultruded flat sections. Data from reference 39.

the flexural strength showed no trend with fiber volume fraction which ranged from .575 to .642 (table 8). Whatever its value for composite applications, the flexural strength test is not a useful one for detecting changes in the pultrusion process.

In addition to the flat sections which were pultruded and tested as described in reference 39, eight more sections were made. Specimens from these eight were tested in this investigation, using the same techniques and conditions. The test results, together with the processing variables as reported in reference 39, are listed in table 9. No flexural tests were made as this test seems insensitive to processing variables as noted above. Using the demarcation line in figure 26, two of the tests (22 and 23) had processing variables which put them in the high pressure, high energy region of the figure. Judging by the analysis of the first 15 tests, tests 22 and 23 should have had properties which were superior to those of the other six tested and reported here. As listed in table 9, test 23 had properties which were generally better than any of the others. However, test 22 was very poor.

The difference can be seen in figure 29, where the response variables are plotted against the processing variables as in figure 25. The curves from figure 26 are included for comparison. The data for the present tests follow a similar but lower curve compared to figure 25. Again, not all the data fall on one curve, with test 23 showing the highest response variables. The short beam shear strength as a function of response variables is shown in figure 30 where the curve from figure 28 is included for comparison. As was the case with the other tests, the three response variables are an indication of the short beam shear strength.

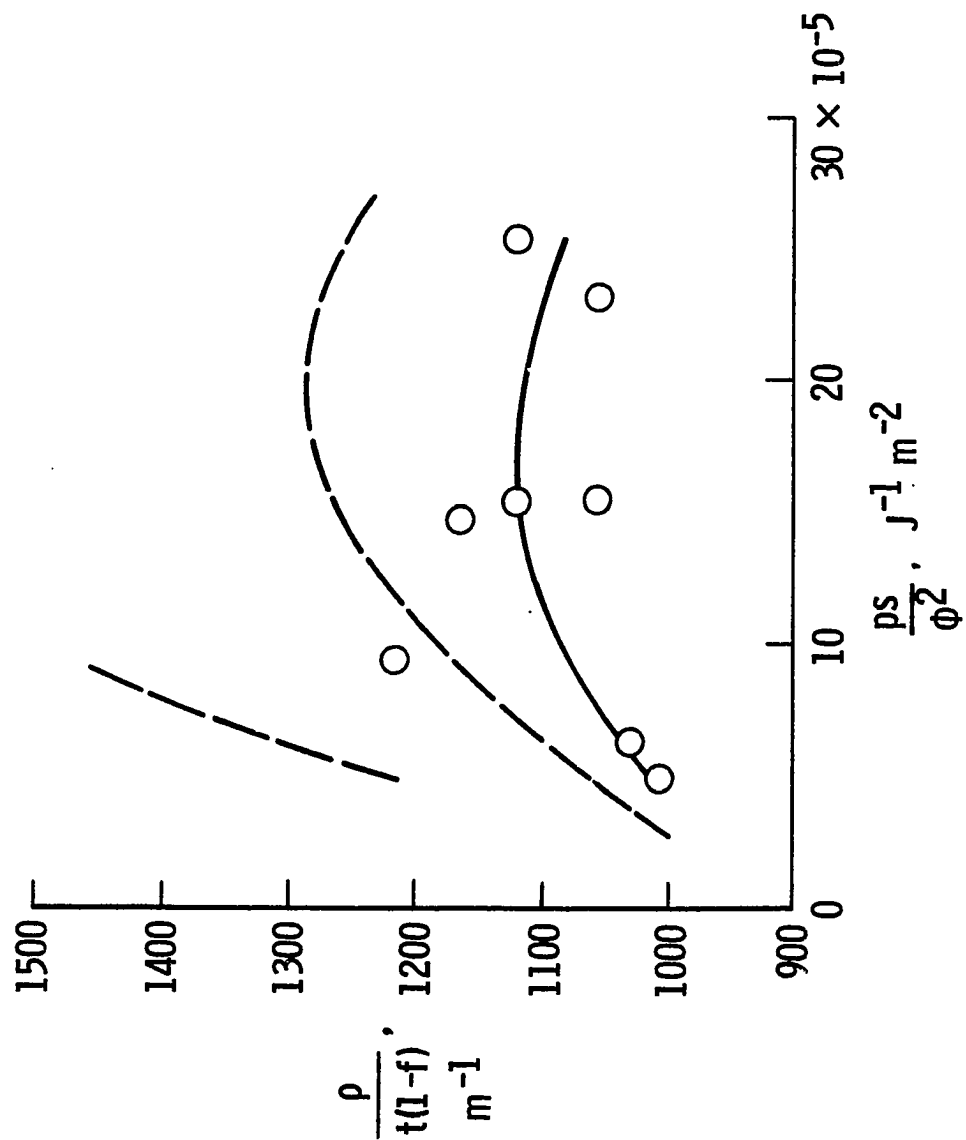


Figure 29.- Response variables as a function of control variables for isobaric process.

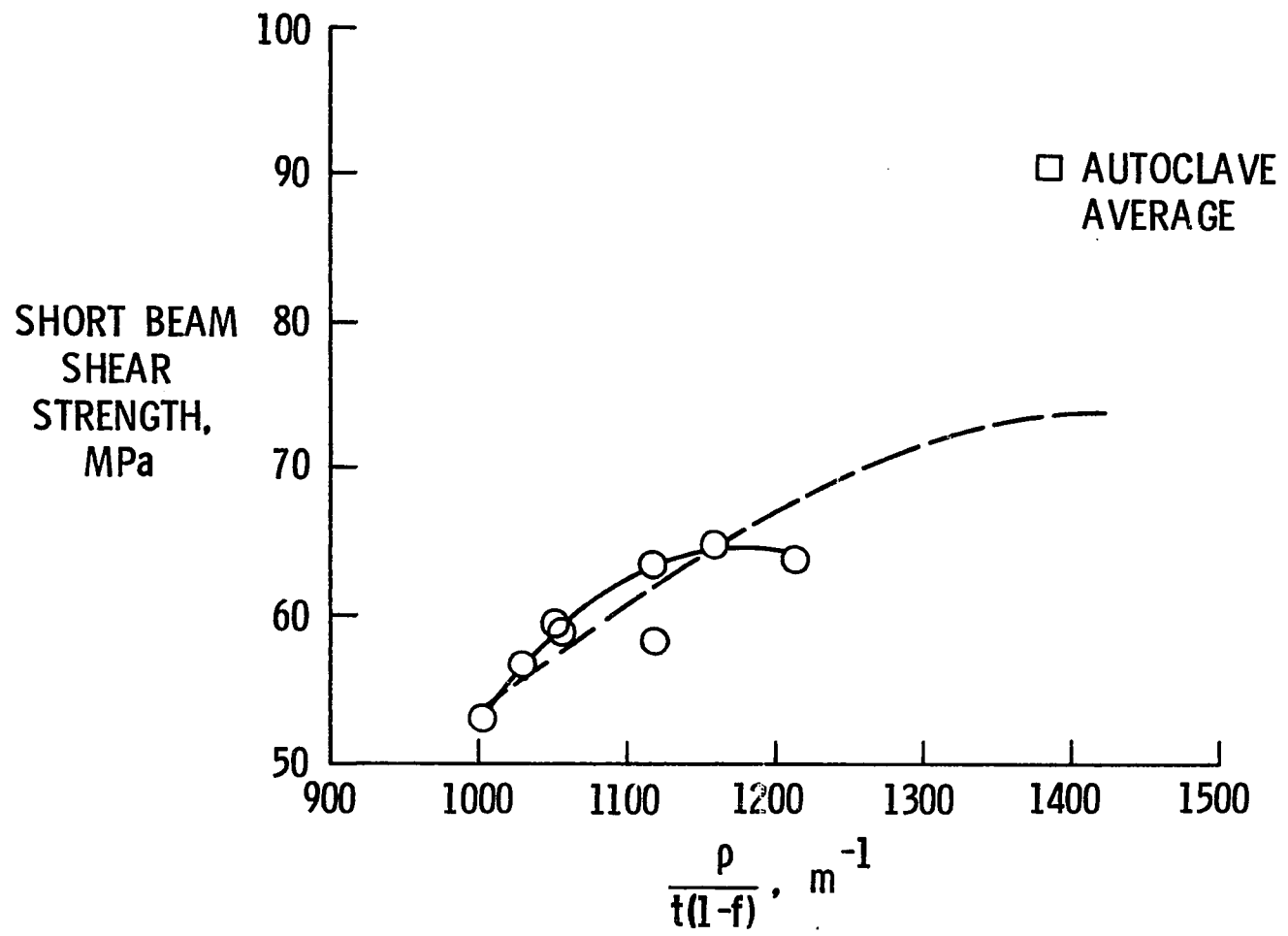


Figure 30.- Short beam shear strength as a function of response variables for pultruded flat sections.

### Isobaric Process

The isobaric process has been used to pultrude both flat and hat-shaped sections using epoxy-graphite prepreg tape. The hat section showed some resin migration similar to that for the isometric process, and property variation possibly associated with distortion of the microwave beam used to speed cure. The flat sections had properties which could be related to the processing variables. A group of three response variables -- thickness, specific gravity, and fiber fraction -- was useful as an indicator of the short beam shear strength.

## CHAPTER 9

## PULTRUSION PROCESS MODEL

"All models are fictions, some more believable than others" (ref. 73). That statement sums up the central tension inherent in any model; while the model is not physical reality, it may represent that reality reasonably well. The most important characteristics of a model (ref. 74) are organization and approximation. The purpose of information organization is to identify the important inputs (independent variables) and outputs (dependent variables). If the organizing is done properly, then irrelevant information will be set aside and not add to the burden of the investigation. The other important characteristic of a model is approximation. If no approximations are made, the model may be so complicated that it is useless. If too many approximations are made, however, the model may not represent the material or process at all.

Mathematical models of physical processes can be classified a number of ways (ref. 75), such as: linear, non-linear; lumped parameter, distributed parameter; deterministic, probabilistic. The classification which was most useful in this investigation was empirical vs. mechanistic (ref. 76). The empirical model is essentially the "black box" approach. The emphasis is on measuring the output of a system for a known input. Little understanding of the system is required, and such a model is useful in prediction

and control of unchanging systems. By contrast, the mechanistic model emphasizes relationships (mechanisms) within the system. A wide range of inputs may be considered without regard to their likelihood of existing, or the desirability of the corresponding output. Both the empirical approach, which utilizes inductive reasoning, and the mechanistic approach, which utilizes deductive reasoning, were used in developing a pultrusion process model. The model, to be described in a later section, was based on concepts gained from experience and was tested on a laboratory-scale pultruder which is described in the next section.

#### Laboratory-Scale Pultruder

The pultruder constructed for this investigation is shown in figure 31. The isometric die was mounted on the movable cross-head of a mechanical testing machine, and die temperatures to 550 K were provided by two thermocouple-controlled quartz tube radiant heaters. The die had five thermocouple wells (fig. 32) drilled so that the thermocouple heads were located along the die cavity centerline, within 0.5 mm of the cavity wall. The cavity dimensions were 20 x 2 mm and the die was 50 mm long. As the testing machine had specific crosshead speeds, the possible die residence times were 6, 12, 24, 60, 120, and 240 seconds. The testing machine load cell was capable of measuring forces to 900 N.

The test procedure was to load the required plies of prepreg tape into the room temperature die and secure the upper end of the tape in the load cell grip. The die temperature was stabilized at 300 K, and the run was started and continued at the pre-set speed. Immediately after the beginning of the run the temperature was raised

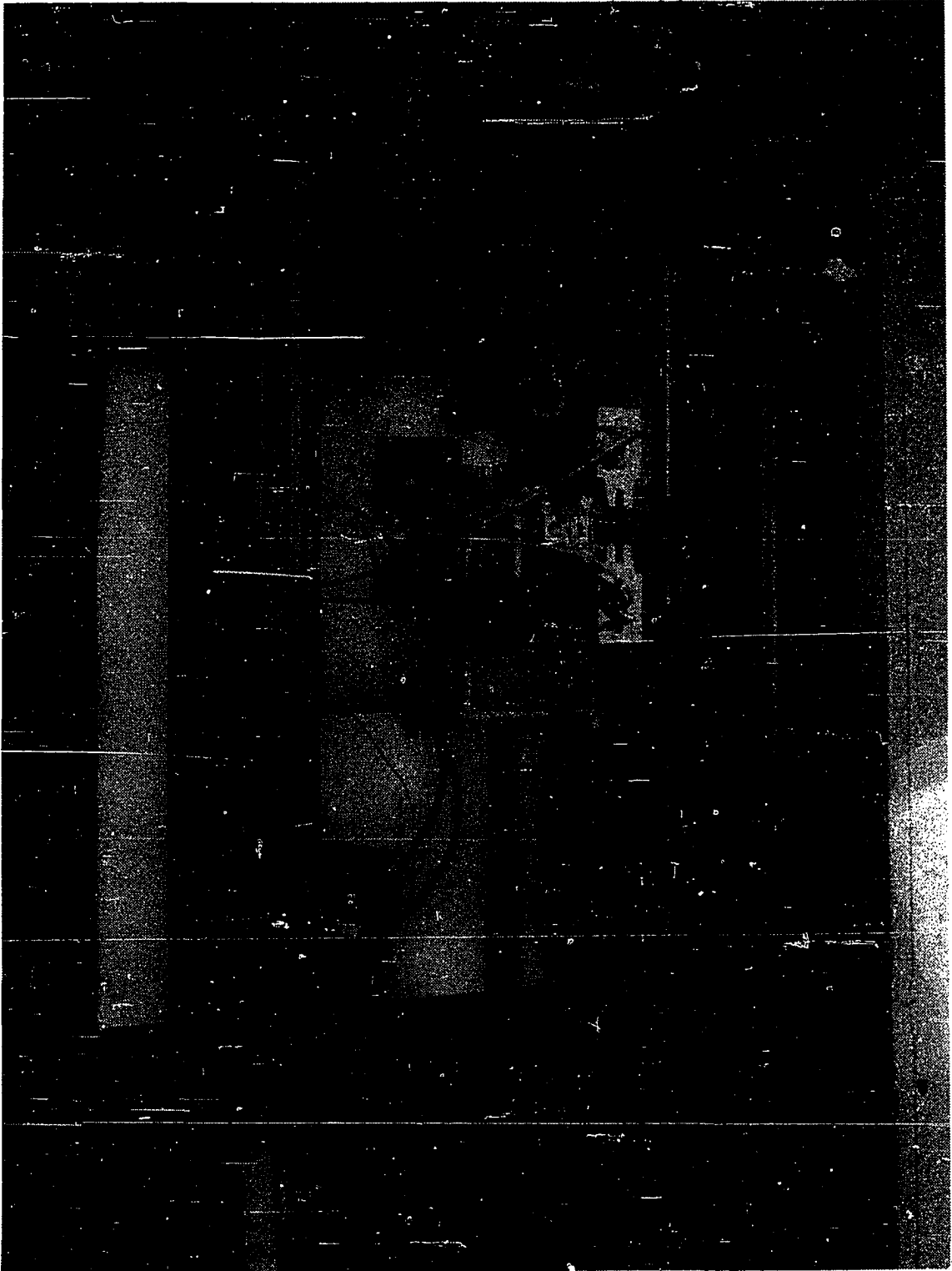


Figure 31.- Laboratory-scale pultruder incorporating mechanical testing machine.



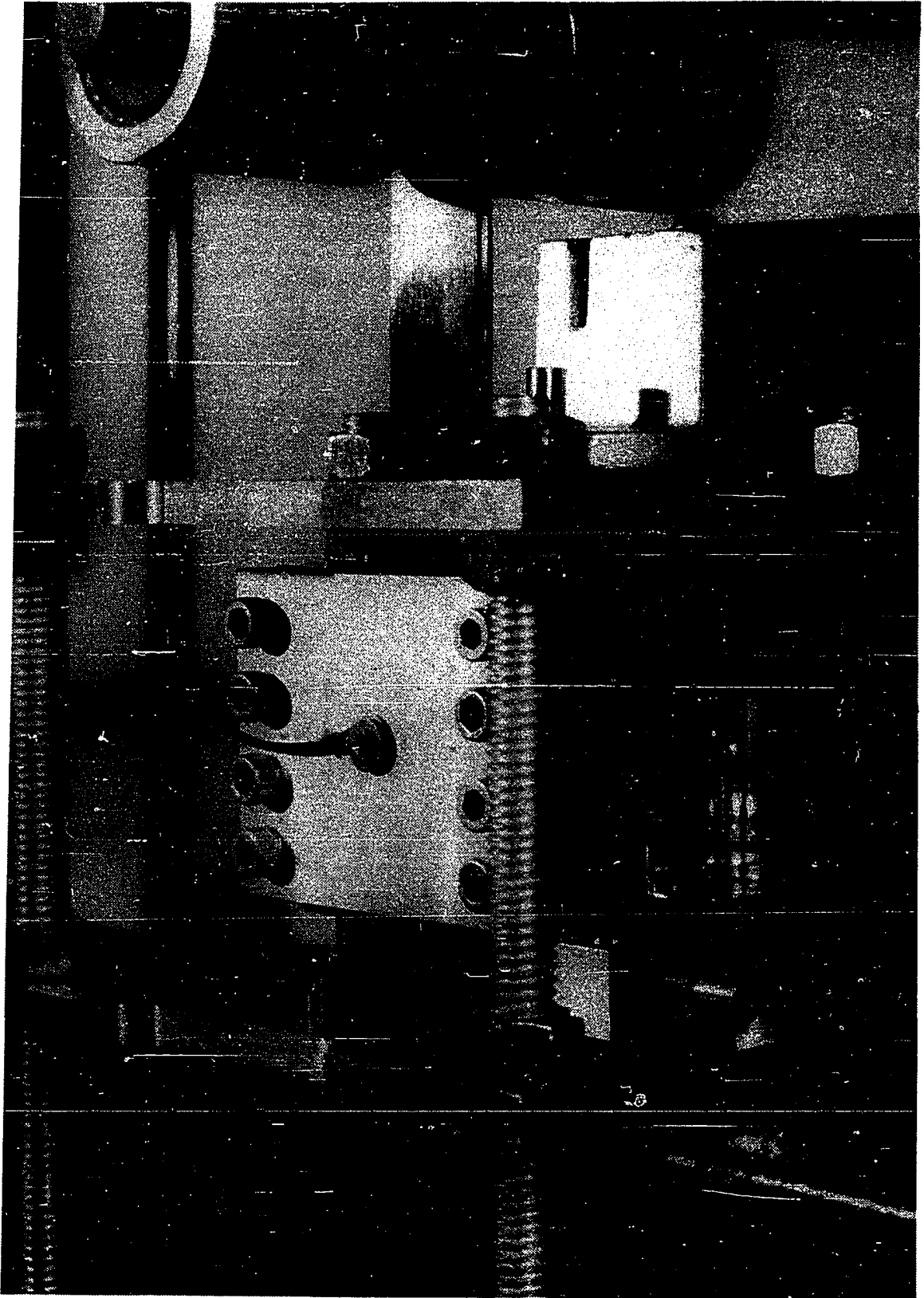


Figure 32.- Isometric die for laboratory-scale pultruder. One quartz-tube heater has been removed to show die.

at a rate of 0.3-0.5 K/sec. to a level which depended on the resin and the residence time. The run continued until the cross-head reached the lower travel limit (if trouble did not develop), producing quarter-metre-length pultruded stock. Thickness, width, and density determinations were made on selected pieces of the stock.

#### Description of the Model

The principal variables in composite material processing are temperature, pressure, and time. A similar set of variables can serve for the pultrusion process, but some changes will be advantageous.

The die temperature is an obvious variable to be considered because it is temperature which causes the curing reaction to take place. A given die temperature will not have the same effect on all resins. For example, a temperature of 400 K will cause a faster and more complete reaction in most polyester resins than will the same temperature in most epoxy resins. A more meaningful way of describing the temperature of a resin is to relate it to a characteristic temperature of that resin. Then a given die temperature can be evaluated as to how "high" it is for the particular resin. A dimensionless temperature, the Arrhenius number,  $N_A$ , has been discussed in the energy balance section. This number, which is given by the expression

$$N_A = \frac{E_k}{RT} \quad (12, \text{repeated})$$

provides a way of relating the die temperature,  $T$ , to a characteristic resin temperature,  $E_k/R$ .

A seemingly obvious pultrusion variable is the pulling speed. The speed determines how long the resin-fiber mass is exposed to the heated die, if the die length is known. An expression which combines both the pulling speed and the die length is the die residence time,  $\theta = \frac{l}{s}$ . As with the temperature, the length of time that is necessary will depend on how fast the resin will react; a resin with a large reaction rate constant will require less time than one with a small constant. A dimensionless time, which takes into account the residence time and the reaction rate, was discussed in the mass balance section. This time is the Damköhler number  $N_D$ , which is

$$N_D = C_o^{n-1} k\theta \quad (5, \text{repeated})$$

This number is a function of both material properties ( $C_o^{n-1} k$ ) and machine parameters ( $\theta$ ), and is closely coupled to temperature through the reaction rate constant,  $k$ .

The third variable is pressure, either that applied to the resin-fiber mass by an isobaric die, or that generated by attempted volume changes of a resin-fiber mass within an isometric die. The generated pressures, which influence the pulling force, are the most poorly defined variables in pultrusion. The pressures are difficult to separate and measure, and they are affected by the mass and energy changes. As discussed in the force balance section, one way of describing the pressures is by the Coulomb number,  $N_C$ ,

$$N_C = \frac{K\alpha\Delta T}{p_b} + \frac{\eta s}{p_v l} + \frac{\tau_x}{p_s} \quad (22, \text{repeated})$$

This number is, like the other two dimensionless numbers discussed above, a function of both material properties and machine parameters. As material properties are involved, the Coulomb number is also coupled to the mass and energy changes. However, it serves more as a way of defining the processing limits; the process must be carried out in such a way that the Coulomb number does not exceed unity. By contrast, both  $N_A$  and  $N_D$  can have any positive value, but probably will not have a value as high as 50.

The three dimensionless numbers - temperature,  $N_A$ ; time,  $N_D$ ; pressure,  $N_C$ -provide a model which brings together material properties and machine parameters. The three numbers were used as the control variables for a laboratory-scale pultruder (fig. 31), which was designed and built as a combined reactor-rheometer. The pultruder was used with epoxy-graphite prepreg tape to test and modify the model.

#### Test of Model

The Coulomb number defines a limit on the process. As the pultruder had a maximum pulling force of 900 N, the maximum stress on a 2 x 20 mm cross section was 22.5 MPa. This stress was far below the estimated 800 MPa or more required to fracture the pultruded stock, so  $N_C$  was always much less than unity by reason of machine limitations.

However, other aspects of the pressure, volume, and pulling force relationship were investigated. As additional plies of prepreg tape are introduced into an isometric die, the pulling force would be expected to increase. This force increase was measured by stacking the prepreg tape so that an additional ply was introduced in the center of the stack at one-and-one-half-die-length intervals. The thinnest end of the tape was fed into the die first. The die temperature was set at

375 K, a temperature high enough to melt the resin, but low enough so the resin would not cure during the residence time (240 seconds) in the die. The results are shown in figure 33 which includes a representative force-time curve as an inset. As an additional ply entered the die, the pulling force increased until the leading edge of that ply had passed through the die. While back flow undoubtedly provided some relief, that relief was not adequate to keep the pulling force down. The force maintained a constant value until the next ply entered the die. The constant value was measured for the prepreg tapes, using 12-15 plies for R 5209, 13-16 plies for Hy-E, and 15-18 plies for E 702. (The usual number of plies was 13 for R 5209, 14 for Hy-E, and 16 for E 702 tape.) Each tape had a different thickness per ply (see Table 2). So, the results were normalized by dividing the thickness of all the plies in the die by the nominal cavity height (2 mm).

With the thickness so normalized, and the pulling force plotted on a logarithmic scale (fig. 33), the data for all three tapes fell very close together. For a linear increase in prepreg thickness, the pulling force increased logarithmically. Indeed, the pulling force for the Hy-E tape at the highest relative thickness value reached the limit of the pultruder. As the ordinate is a force and the abscissa a distance, figure 33 may be regarded as something of a bulk stress-strain curve. The slope of the curve can be regarded as a measure of bulk modulus. If the same tests had been made at a higher temperature, the forces would not have been as high, and the slope of the curve would have been lower.

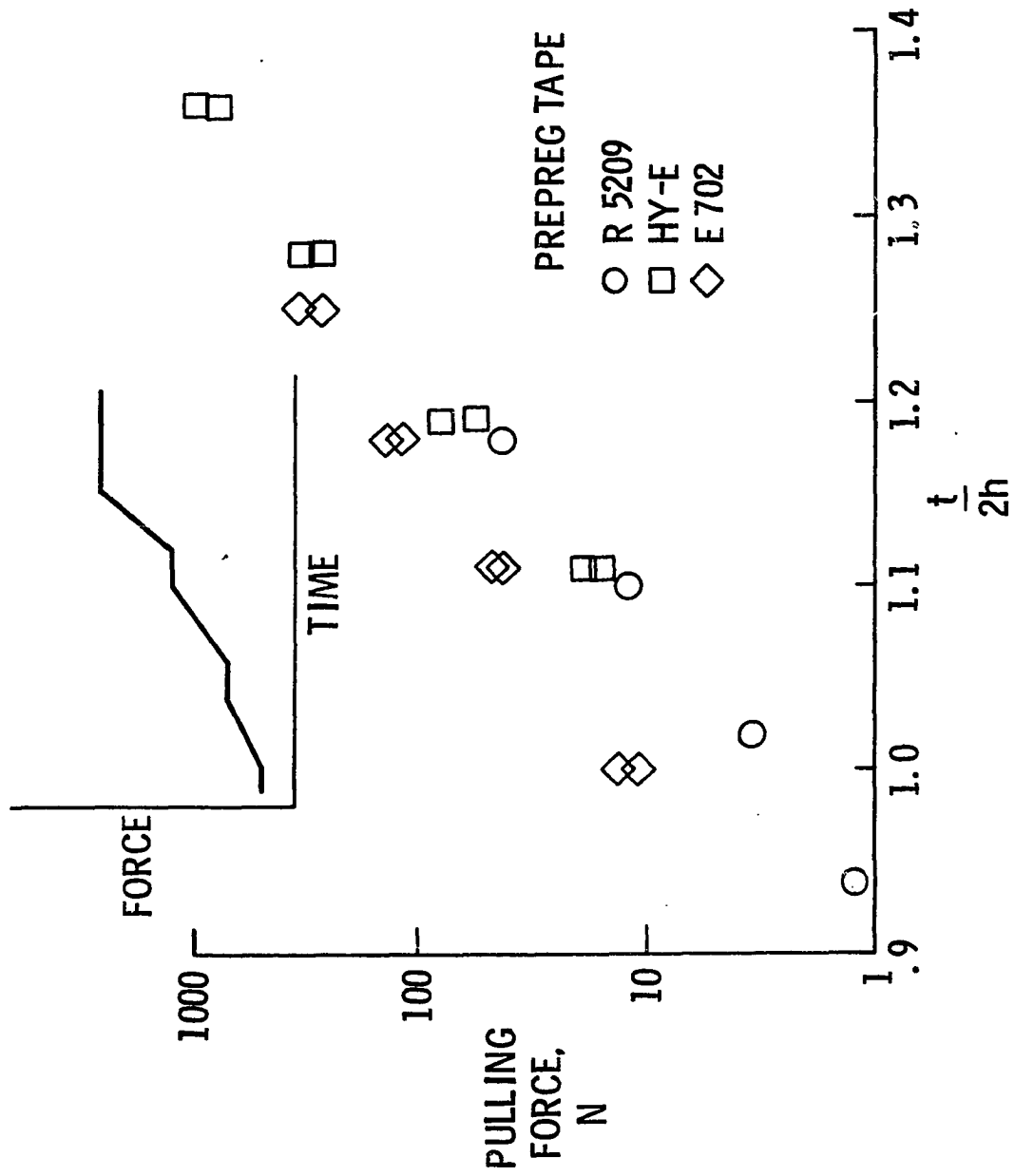


Figure 33.- Pulling force as a function of normalized thickness for epoxy resin-graphite fiber prepreg tape.

As the die temperature went to higher values, the pulling force got smaller for a given prepreg tape and residence time. The variation in the force as a function of temperature from 400 to 500 K is shown in figure 34 for the Hy-E and E 702 tapes. When the temperature reached the 440-450 K range, the curing reaction began and the pulling force increased sharply. For the longest residence time, or lowest pulling speed for the single-length die, the increase was much larger than that of the other two times. In fact, for the shortest residence time, the force reached a peak value and then began to decrease again. But at the lowest pulling speed, the force was high, and in one case (at a temperature of 480-490 K) exceeded the limit of the pultruder. The test was stopped, the resin-fiber mass was bonded to the die, and the die had to be burned out at 650 K so the sections could be separated. A long residence time is helpful in obtaining a complete cure of the resin, but a short residence time can be beneficial in keeping the pulling force down.

A part of the pulling force increase which accompanies the cure reaction is due to an increase in the resin viscosity. The Coulomb number contains a viscous drag component which is

$$\mu_v = \frac{\eta s}{p_v l} \quad (16, \text{repeated})$$

As the ratio  $s/l$  is constant for a given test, this component will increase only if viscosity,  $\eta$ , increases faster than pressure,  $p_v$ , generated by the attempted resin expansion as cure begins. The relationship between viscosity and pressure was investigated using a rotary rheometer in the cone and plate mode. In these tests, samples

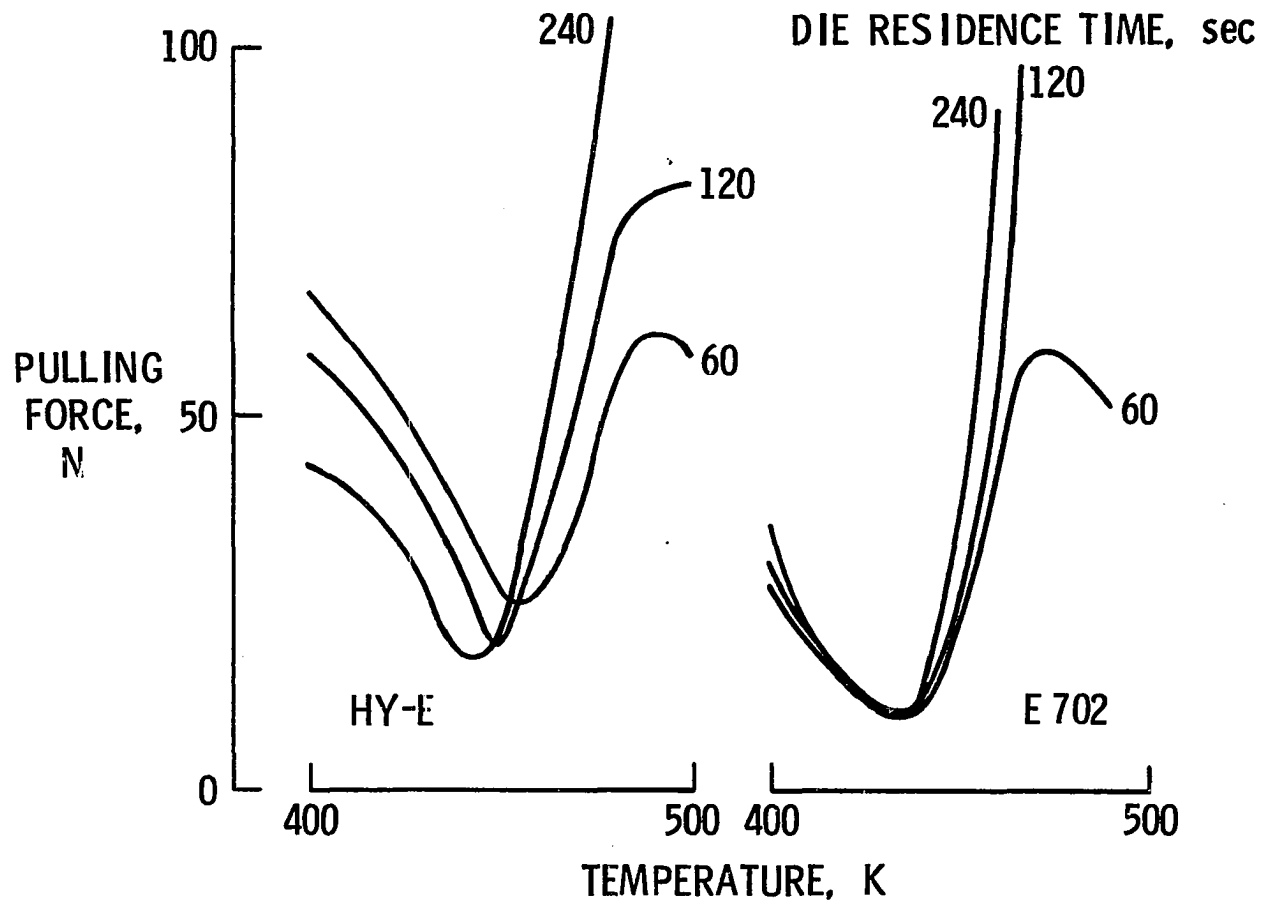


Figure 34.- Pulling force as a function of die temperature at three residence times for epoxy resin-graphite fiber prepreg tapes.



of the F 979 and E 702 resins were sheared at a rate of  $1 \text{ sec}^{-1}$  and a temperature of 375 K. The low temperature insured that the samples would reach thermal equilibrium long before the cure reaction began, and that the reaction would take place slowly enough so that a reasonable amount of data could be obtained. Measurements of both the torque and the normal force were made simultaneously, and the resulting change of viscosity and pressure with time is shown in figure 35. After an induction time ( $\sim 1700$  seconds for F 979,  $\sim 2000$  seconds for E 702) the resins started the cure reaction and both viscosity and pressure increased. The values for E 702 resin increased faster than those for F 979, but the viscosity increased more rapidly than did the pressure for both resins. The ratio of viscosity to pressure is plotted in figure 35. The ratio began with a value near 0.5 and increased with test time. Measurements were made to the limits of the rheometer. The maximum pressures recorded were  $\sim 80$  kPa ( $\sim 12$  psi) which, though small, were large enough to extrude resin fibers out from the cone and plate. Still, the tests showed that the viscosity increased faster than the pressure, and so the viscous drag component would increase as the cure reaction takes place.

The cure reaction which so strongly influences the pultrusion forces is itself influenced by both time and temperature. The effect of the two variables, expressed as dimensionless time and temperature, was investigated using Hy-E and E 702 prepreg tape and the laboratory-scale pultruder. The procedure was to make a run with a fixed residence time but with a constantly rising temperature. The strip chart record of pulling force and die temperature was run at the same speed as the testing machine crosshead. Hence, it was a simple

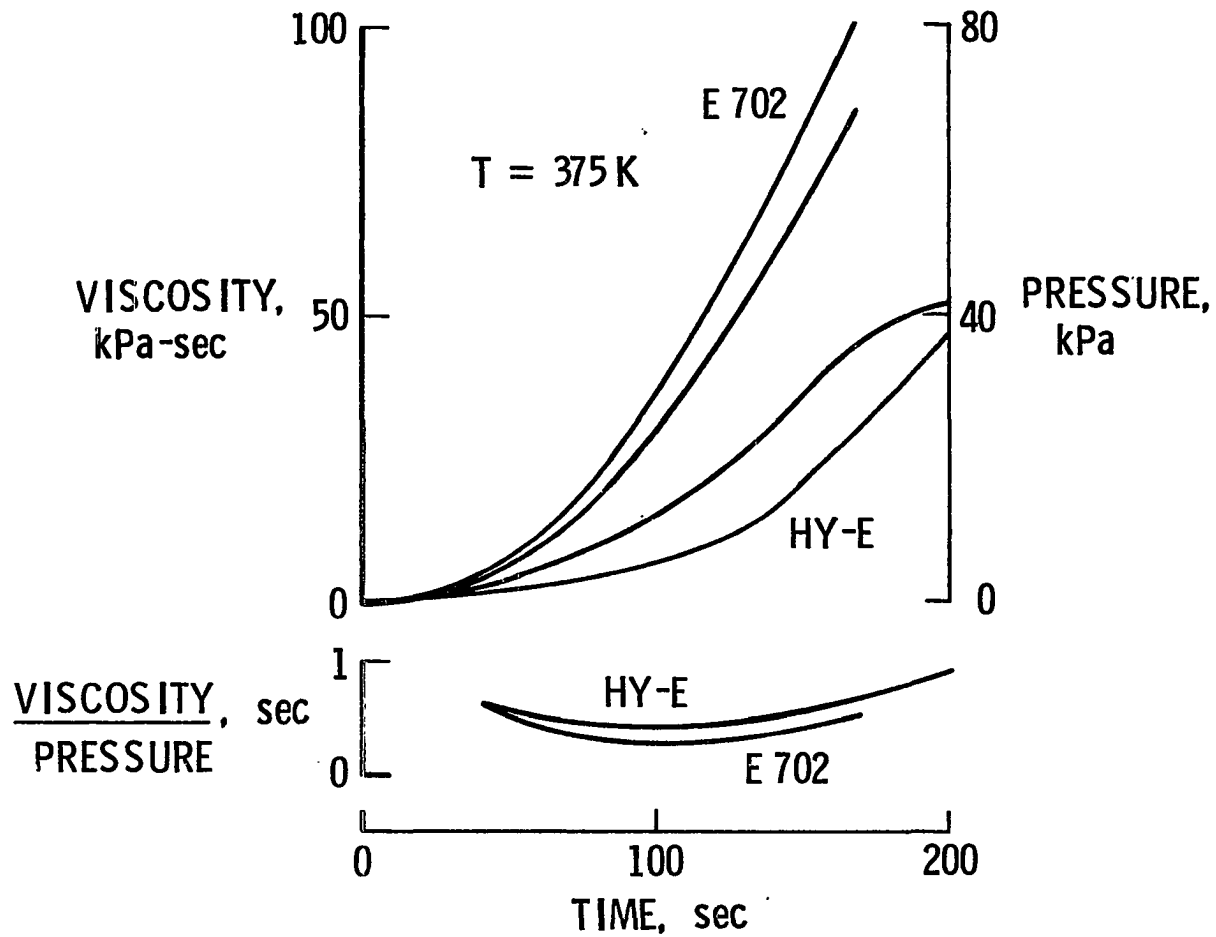


Figure 35.- Shear viscosity and normal pressure as a function of time after cure reaction begins for epoxy resins.

matter to determine the die temperature for any point along the length of pultruded stock. Sections of the stock, equal to one-half (25 mm) of the die length, were cut from the pultruded stock. The average die temperature was determined for each section, and width, thickness, and specific gravity measurements were made for each one. In this way, a single run could yield several points of information as the temperature generally was rising throughout most of the run. As the heat-up time of the epoxy-graphite tape was so short (see energy balance section), the residence time in the die was taken as the time available for the reaction to take place. The temperature was expressed as the dimensionless Arrhenius number,  $N_A$ , and the time as the dimensionless Damköhler number,  $N_D$ .

The test results, obtained as described above, are listed in tables 10 and 11, and plotted in figures 36 and 37. Three residence times, 60, 120, and 240 seconds, were used for the test runs. The specific gravity was divided by the cross section area to give an indication of how well the tape had been compacted and reacted. The results for the Hy-E tape are shown in figure 36 where a logarithmic scale is used for the Damköhler number. The die temperature,  $T$ , appeared in the denominator of the Arrhenius number. Hence, a high die temperature gives a low  $N_A$ . Considering the  $\rho/A$  value for each of the data points in figure 36, contours of constant ratio were drawn. These contours indicated a region in the  $N_A$ - $N_D$  plane in which dense, well-compacted pultruded stock could be obtained. This region is indicated by the dashed contour between the two 3.7 contours. The smallest  $N_A$  along the contour was  $\sim 14$ , which indicated a die temperature of  $\sim 470$  K. Below that temperature, the resin apparently did not react

Table 10. - PULTRUDER SETTINGS AND PULTRUDED STOCK PROPERTIES  
FOR HY-E 1079 EPOXY-GRAPHITE PREPREG TAPE

Residence Time, sec	Die Temperature K	N <sub>D</sub>	N <sub>A</sub>	Cross Section Area, mm <sup>2</sup>	Specific Gravity	ρ/A
60	435	0.67	15.12	46.1	1.383	3.00x10 <sup>-2</sup>
	450	1.12	14.62	41.7	1.497	3.59
	470	2.08	14.00	40.6	1.510	3.72
	480	2.78	13.71	40.6	1.484	3.66
	495	4.22	13.29	40.6	1.441	3.55
	505	5.48	13.03	40.7	1.421	3.49
120 a	410	0.54	16.05	42.9	1.474	3.44x10 <sup>-2</sup>
	440	1.61	14.95	41.3	1.507	3.65
	465	3.57	14.15	40.3	1.508	3.74
	a 480	5.57	13.71	41.0	1.452	3.54
	495	8.44	13.29	40.5	1.445	3.57
	a 506	11.28	13.00	40.5	1.459	3.60
240	395	0.58	16.66	44.2	1.442	3.26x10 <sup>-2</sup>
	445	3.79	14.78	40.9	1.530	3.74
	480	11.13	13.71	40.9	1.528	3.74
	a 490	14.72	13.43	41.4	1.521	3.67

<sup>a</sup>Two-test mean

TABLE 11. - PULTRUDER SETTINGS AND PULTRUDED STOCK PROPERTIES FOR  
E 702 EPOXY-GRAPHITE PREPREG TAPE

Residence Time, sec	Die Temperature K	N <sub>D</sub>	N <sub>A</sub>	Cross Section Area, mm <sup>2</sup>	Specific Gravity	ρ/A
60	415	0.29	14.26	47.1	1.257	2.67x10 <sup>-2</sup>
	430	0.48	13.76	47.1	1.410	2.99
	445	0.77	13.30	41.0	1.530	3.73
	460	1.19	12.86	41.0	1.503	3.67
	475	1.78	12.46	41.1	1.459	3.55
	485	2.30	12.20	41.0	1.446	3.53
	490	2.61	12.08	40.6	1.444	3.56
	500	3.32	11.84	39.9	1.440	3.61
120	405	0.41	14.61	41.8	1.552	3.71x10 <sup>-2</sup>
	440	1.32	13.45	40.9	1.552	3.79
	465	2.72	12.73	40.8	1.528	3.75
	490	5.22	12.08	40.6	1.498	3.69
	505	7.47	11.72	39.5	1.509	3.82
	515	9.37	11.49	38.5	1.528	3.97
	a	518	10.02	11.42	37.6	1.556
240	430	1.08	13.76	40.8	1.542	3.78x10 <sup>-2</sup>
	450	3.57	13.15	41.0	1.508	3.68
	b	455	4.12	13.01	39.9	1.529

<sup>a</sup>Four-test mean.

<sup>b</sup>Three-test mean.

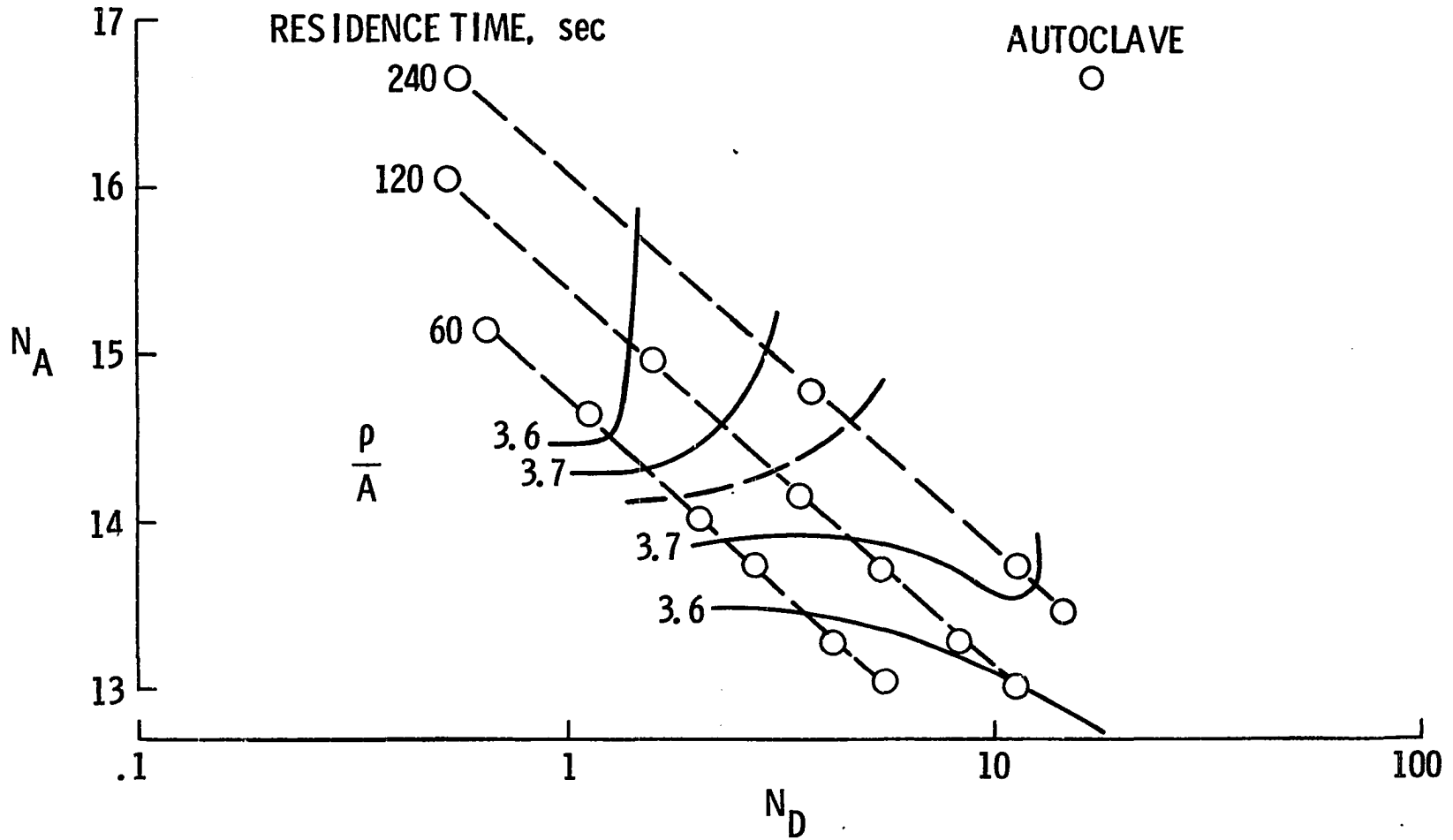


Figure 36.- Density-cross section area ratio on  $N_A - N_D$  plane for Hy-E prepreg tape. Coordinates for typical autoclave cure are shown for comparison.

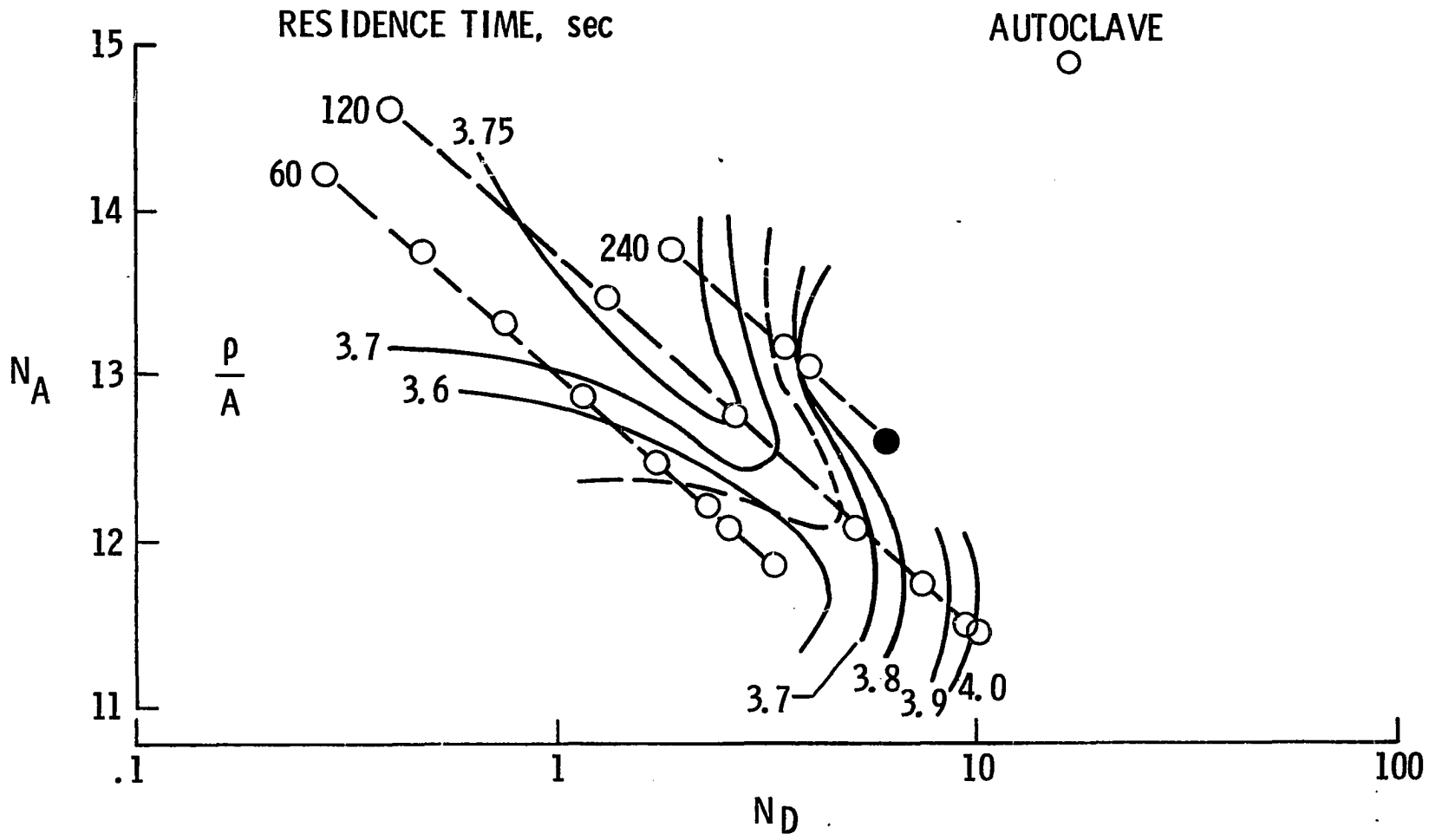


Figure 37.- Density-cross section area ratio on  $N_A - N_D$  plane for E 702 prepreg tape. Coordinates for typical autoclave cure are shown for comparison.

to a high enough fraction during the die residence time. Above that temperature, the reaction proceeded so rapidly that the stock could not be compacted by the pressures in the die. The dashed contour, indicating the maximum  $\rho/A$ , provides an estimate of adjustments in residence time which would be needed for a given adjustment in temperature.

The test results for E 702 prepreg tape are listed in Table 11 and shown in figure 37. The range of Damköhler numbers was about the same as that for the Hy-E tape, but the Arrhenius numbers were lower. The overall results were different, also. Unlike the Hy-E tape which had a maximum in the  $\rho/A$  value (figure 36), the E 702 had a minimum as indicated by the dashed contour in figure 37. The  $\rho/A$  values rose rapidly for control variables ( $N_A$  and  $N_D$ ) to the right of the minimum contour. For settings of  $N_A = 11.4$  and  $N_D = 10.0$ , dense, well compacted pultruded stock was obtained. The rapid rise, however, indicated that accurate process control would be needed with the E 702 in some control variable regions. For example, the closed data point in figure 37 indicates the settings for which the pulling force reached the pultruder limit and the die, resin, and fiber were all bonded together. No attempt was made to find the force limit for the other residence times, but such limits undoubtedly exist for sufficiently high temperatures (low  $N_A$ ) and long die residence time (high  $N_D$ ). Indeed, some minimum pulling speed may have to be used in all cases.

The minimum contour may be a reflection of the presumed mixture of curing agents in the E 702 resin. The DSC curves for both the resin and the tape (figures 9 and 13) had a scarcely noticeable minimum in the reaction plateau at  $\sim 485$  K. This temperature, for this resin,



gives  $N_A = 12.2$ . This value is close to that of the horizontal portion of the minimum contour (fig. 37). No information was available as to what curing agents were used in the E 702 resin. However, a mixture of initiators is sometimes used with polyesters, one for curing in a low temperature range, another for a higher temperature range. The same idea may have been used for this epoxy resin.

#### Pultrusion Model

A pultrusion process model has been developed and tested. The most widely used pultrusion process variables are die temperature and pulling speed which are both pultrusion machine parameters. The model developed here described three principal processing variables of temperature, time, and pressure as dimensionless numbers. These numbers were Arrhenius number,  $N_A$  (temperature), Damköhler number,  $N_D$  (time), and Coulomb number,  $N_C$  (pressure), all expressed in terms of machine parameters as well as material properties. The model was tested on a laboratory-scale pultruder using epoxy resin-graphite fiber prepreg tape. The tests showed that additional volume of material introduced into an isometric die resulted in a pulling force increase. This increase was logarithmic with increasing volume. The increasing resin viscosity during cure caused a pulling force increase, large enough in one case to exceed the pultruder limits. The force increase was larger at lower pulling speeds, so a minimum pulling speed, independent of the die length, may be necessary. As the die temperature generally was increasing during a run on the pultruder, a single piece of pultruded stock provided information for several points on the  $N_A$ - $N_D$  plane. When the stock was evaluated, the results showed the range of  $N_A$ - $N_D$  settings which were needed to produce dense, well compacted stock. The evaluation

contours over the  $N_A-N_D$  plane tended to reflect some aspects of the DSC curves obtained on the prepreg tape. Most elements of the model differ considerably from what is usually considered important in the pultrusion process. The model emphasis was on material properties as well as machine parameters, and the interaction between them. This emphasis stemmed from considering the pultruder die as both a reactor and a rheometer.

## CHAPTER 10

## CONCLUSIONS

Pultrusion, like any other physicochemical process, must satisfy the laws of conservation of mass, energy, and momentum. As a means of applying these laws, the pultrusion die was treated as both a reactor and rheometer: a chemical reactor in which low molecular weight, liquid resin undergoes a chemical reaction to become a higher molecular weight, crosslinked composite material matrix; a slit rheometer in which a volume of material entering the die undergoes changes which generate pressures and resisting forces. This investigation has been conducted by applying the conservation laws to the resin and fiber in the die, by analyzing two pultrusion systems, and by developing and testing a pultrusion process model on a laboratory-scale pultruder.

The mass balance refers to changes which take place in the reactive (thermosetting) resin; the reinforcing fibers have a moderating effect on that reaction. Useful kinetic and thermal parameters can be obtained from DSC tests. While tests of the resin-fiber combination are preferable, tests of the resin itself can provide reasonable estimates the results to be expected from such a combination. Once the kinetic parameters are determined, the Damköhler number,  $N_D$ , provides a useful means of estimating reaction times, or die residence times, and the effect that die temperature would have on those times.

An energy balance was determined by estimating the spatial and temporal temperature distribution in the resin-fiber mass within the die. A finite difference program was used to make the estimates. Under isothermal conditions, neither a polyester-glass nor an epoxy-graphite combination would have a large exothermic temperature rises (for part thickness to 10 mm). Under adiabatic conditions, the exothermic reaction can be controlled through two parameters, the Arrhenius number,  $N_A$ , and the adiabatic temperature rise  $\Delta T'_{ad}$ . Both parameters are functions of the resin and fiber and can be adjusted to some extent. The Arrhenius number can be thought of as a dimensionless temperature which is a function of the actual temperature and activation energy of the material. As such, it may be of more value than the temperature alone.

The force balance in a pultrusion die can be thought of in terms of a coefficient of friction, a ratio of shearing forces to normal forces. The components of friction arise from resin back flow at the die entrance, viscous drag as the resin begins to cure, and sliding friction of the curing stock. If these three resisting forces do not exceed the fracture force of the resin-fiber mass, then the Coulomb number,  $N_C$ , will be less than unity, and the pultrusion processes will not be limited by an unfavorable force balance.

An analysis of an isometric (constant volume) and an isobaric (constant pressure) process was made. Estimates of required die residence times for circular rods, made with the isometric process, were within the range of times which were used by the manufacturer. For the isobaric process, pultruded flat sections had properties which

could be related to processing variables. A group of three response variables—thickness, specific gravity, and fiber fraction—was useful as an indicator of the short beam shear strength.

A pultrusion process model was developed which expressed the three principal processing variables of temperature, time, and pressure as dimensionless numbers. These numbers were Arrhenius number,  $N_A$  (temperature), Damköhler number,  $N_D$  (time), and Coulomb number,  $N_C$  (pressure), all expressed in terms of machine parameters as well as material properties. The model was tested on a laboratory-scale pultruder using epoxy resin-graphite fiber prepreg tape. The results showed the range of  $N_A$ - $N_D$  settings which were needed to produce dense, well compacted stock. Most elements of the model differed considerably from what is usually considered important in the pultrusion process. The model emphasis was on material properties as well as machine parameters, and the interaction between them. This emphasis stemmed from considering the pultruder die as both a reactor and a rheometer.

## REFERENCES

1. Dietz, Albert G. H.: Composite Materials. 1965 Edgar Marburg Lecture, Am. Soc. Test. Mat., 1965, p. 2.
2. Loewenstein, K. L.: Glass Systems; in Holiday, Leslie, ed.: Composite Materials. Elsevier Pub. Co., 1966, p. 129.
3. Meyer, Leonard S.: Pultrusion, Modern Plastics Encyclopedia 1970-71, vol. 47, no. 10A, Oct. 1970, p. 592.
4. Meyer, Leonard S.: Pultrusion. Soc. Plas. Ind. 25th Ann. Tech. Conf. Proc., 1970, Paper 6-A.
5. Kannebly, G.: Extrusion of Thermosetting Materials. Plas. Polym., Feb. 1972, pp. 13-18.
6. Zinsser, William: Recap of 1977: Who Was Pultruded Anyway? Smithsonian, vol. 8, no. 11, Feb. 1978, p. 136.
7. Howald, Arthur M.; and Meyer, Leonard S.: Shaft for Fishing Rods. U. S. Patent 2,571,717, 16 Oct. 1951.
8. Goldsworthy, William Brandt; and Landgraf, Fred: Apparatus for Producing Elongated Articles From Fiber-Reinforced Plastic Material. U. S. Patent 2,871,911, 3 Feb. 1959.
9. Goldsworthy, W. Brandt: Pultrusion. Soc. Plas. Ind. 23rd Ann. Tech. Conf. Proc., 1968, Paper 18-A.
10. Segawa, Joichiro; and Nakagowa, Bungo: Continuous Molding Method of Fiber Glass Reinforced Plastics of Various Profiles. Soc. Plas. Ind. 23rd Ann. Conf. Proc., 1968, Paper 18-B.
11. Goldsworthy, William Brandt: Pultrusion Machine and Method. U. S. Patent 3,556,888, 19 Jan. 1971.
12. Garnett, G.; Hancox, N. L.; and Spencer, R.A.P.: A Comparison of the Mechanical Properties of Pultruded and Wet Lay-up Carbon Fibre Composites. Plas. Ins. Conf. on Reinforced Plas. Research Proj. III, London, 10 Nov. 1971, Paper 10.
13. Comey, John: Designing Thermoset Shapes for Pultrusion. Machine Design, vol. 43, 23 Dec. 1971, pp. 45-49.
14. Hardesty, E. E.: Recent Advances in Automated Manufacture of Composite Structures, e.g., Tape Laying and Pultrusion. Soc. Aero. Mat. Proc. Engr. 4th Nat. Tech. Conf. Proc., vol. 4, Oct. 1972, pp. 345-360.

15. Hill, James E.; Goan, John C.; and Prescott, Roger: Properties of Pultruded Composites Containing High Modulus Graphite Fibers. SAMPE Quarterly, vol. 4, no. 2, Jan. 1973, pp. 21-27.
16. Tickle, John D.: Current Capabilities of Reinforced Plastic Pultrusion. Soc. Auto. Engr. Int. Auto. Engr. Cong, Detroit MI, Jan. 1973, Paper 730172.
17. Hardesty, E. E.: Advanced Composites, the On-Going Transition From Handmade Prototypes to Machine-Fabricated Composites. Soc. Plas. Ind. 28th Ann. Tech. Conf. Proc., 1973, Paper 15-D.
18. Morrison, Robert S.: Structural Plastic Rods and Beams are Light and Corrosion Resistant. Mat. Engr., vol. 77, no. 4, April 1973, pp. 36-39.
19. Jones, Brian H.: Pultruding Filamentary Composites--An Experimental and Analytical Determination of Process Parameters. Soc. Plas. Ind. 29th Tech. Conf. Proc., 1974, Paper 15-C.
20. Spencer, R. A. P.: Advances in Pultrusion of Carbon Fibre Composites. Plas. Polym. Conf. Suppl., vol. 6, 1974, pp. 140-147.
21. Anon: Making It a Lot Easier With Modular RP Pultrusions. Modern Plastics, vol. 52, no. 7, July 1975, p. 30.
22. Jones, Brian H.: Design and Manufacturing Technology for Pultruded Composite Structural Elements. Soc. Plas. Ind. 31st Ann. Tech. Conf., 1976, Paper 17-D.
23. Halsey, N.; Marlow, D. E.; Mitchell, R. A.; and Mordfin, L.: Pultruded Rods for Antennas Guys; Catenaries, and Communications Structures. AFML-TR-76-42, May 1976.
24. Comey, John: Take a Look At Pultrusion for High Performance, Complex Shapes. Plas. Design & Proc. vol. 16, no. 5, May 1976, pp. 8-9.
25. Thompson, Vere; and Bradley, Robert J.: Pultrusion of Advanced Composites. Soc. Manf. Engr. Conf. on Adv. Composites, Los Angeles, CA, June 1976, Paper EM76-415.
26. Pepper, Roger T.; Gigerenger, Horst; and Zack, Thomas A.: Development of Graphite Fiber Reinforced Aluminum Tubes. Soc. Adv. Mat. Proc. Engr. 8th Nat. Tech. Conf. vol. 8, Seattle, WA, Oct. 1976, ppl 338-342.
27. Jones, Brian H.; and Jakway, William: MM&T-Pultruded Composite Structural Elements. USAAMRDL-TR-76-5, Dec. 1976.
28. Fesko, Donald G.: Flexural Fatigue of Unidirectional Fiberglass-Reinforced Polyester. Polym. Engr. & Sci., vol. 17, no. 4., April 1977, pp. 242-245.

29. Tickle, John D.: Pultrusions Step Up the Challenge to Structural Steels. *Machine Design*, vol. 49, no. 24, 20 Oct. 1977, pp. 163-167.
30. Chung, Harvey H.: Study of Low-Cost Fabrication Methods for Aerospace Composite Materials. NASA CR-145330, Jan. 1978.
31. Werner, Robert I.: Fiberglass Ladders and Pultrusion: A Challenge to a Young Industry. Soc. Plas. Ind. 33rd Ann. Tech. Conf. Proc., 1978, Paper 8-A.
32. Haarsma, John C.: Characteristics of Pultruded Resin Bonded Glass Fiber Rod. Soc. Plas. Ind. 33rd Ann. Tech. Conf. Proc., 1978, Paper 8-B.
33. Loveless, H. S.: Mechanical Properties of Pultruded Rod Stock. Soc. Plas. Ind. 33rd Ann. Tech. Conf. Proc., 1978, Paper 8-C.
34. Sumerak, Joseph E.; and Colangelo, Frank V.: Pultruded FRP Structural Members Are Key in Hypobaric Container Program. Soc. Plas. Ind. 33rd Ann. Tech. Conf. Proc., 1978, Paper 8-D.
35. McQuarrie, Terry S.: New Generation Resins for Pultrusion. Soc. Plas. Ind. 33rd Ann. Tech. Conf. Proc., 1978, Paper 8-E.
36. Tickle, John D.; Halliday, George A.; Lazaron, Joe; and Riseborough, Brian: Designing Structures With Pultruded Fiber Glass Reinforced Plastic Structural Profiles as Compared to Standard Steel Profiles. Soc. Plas. Ind. 33rd Ann. Tech. Conf. Proc., 1978, Paper 8-F.
37. Rolston, J. Albert: Process and Economic Factors for Pultrusion Soc. Plas. Ind. 33rd Ann. Tech. Conf. Proc., 1978, Paper 8-G.
38. Martin, Jeff: Pultrusion-An Overview of Applications and Opportunities. Soc. Plas. Ind. 33rd Ann. Tech. Conf. Proc., 1978, Paper 8-H.
39. Bradley, R.: Pultrusion of Graphite/Epoxy Prepreg for Flat and Hot Section Specimens. NASA CR 158899, March 1978.
40. Klein, Theodore H.: Process for Producing Pultruded Clad Composites. U.S. Patent 4,012,267, 15 Mar. 1977.
41. Anon.: Pultrusion Comes on as a New Process for Cost-Saving Mass Production. *Modern Plastics*, vol. 55, no. 5, May 1978, pp. 50-52.
42. Carberry, James J.: Chemical and Catalytic Reaction Engineering: McGraw-Hill Book Co., 1976.



43. Aris, Rutherford: Elementary Chemical Reactor Analysis, Prentice-Hall, Inc., 1969.
44. Hill, Charles G., Jr.: An Introduction to Chemical Engineering Kinetics & Reactor Design. John Wiley & Sons, 1977.
45. Han, Chang Dae: Measurement of the Rheological Properties of Polymer Melts with Slit Rheometer. I. Homopolymer Systems. *J. App. Polym. Sci.*, vol. 15, 1971, pp. 2567-2577.
46. Han, Chang Dae: Rheology in Polymer Processing. Academic Press, 1976, Chapter 5.
47. Ellerstein, Stuart M.: The Use of Dynamic Differential Calorimetry For Ascertaining the Thermal Stability of Polymers. In Porter, Roger S.; and Johnson, Julian F., ed.: Analytical Calorimetry, Plenum Press, 1968, pp. 279-287.
48. Abolafia, Oscar R.: Application of Differential Scanning Calorimetry to Epoxy Curing Studies. *Soc. Plas. Engr. 27th Ann. Tech. Conf. Proc.*, Tech. Papers Vol. XV, 1969, pp. 610-616.
49. Willard, P. E.; Alvarez, M.; and Cha, L. C.: Mathematics of Linear-Temperature Programmed, First Order Kinetics in Peroxide Catalyzed Polymerizations. *Polym. Engr. Sci.*, Vol. 11, No. 2, Mar. 1971, pp. 160-164.
50. Drislane, N. J.; DeNicola, J. P.; Wareham, W. M.; and Tanner, R. I.: A New Versatile Rheological Instrument: Design, Testing and Data Analysis. *Rheol. Acta*, vol. 13, 1974, pp. 512-519.
51. Haarsma, John C.: Evaluation of Resin-Glass Fiber Interface Under Environmental Stress. *Soc. Plas. Ind. 33rd Ann. Tech. Conf. Proc.* Feb. 1978, Paper 22-E.
52. Loveless, H. S.; and Ellis, J. H.: A Comparison of Methods for Determining the Shear Properties of Glass/Resin Unidirectional Composites. *J. Test. Eval.*, Vol. 5, No. 5, Sept. 1977, pp. 369-374.
53. Pittman, Claud M.; and Brinkley, Kay L.: One-Dimensional Numerical Analysis of the Transient Thermal Response of Multilayer Insulative Systems. NASA TM X-3370, April 1976.
54. Willard, P. E.: Determination of Cure of Diallyl Phthalate Using Differential Scanning Calorimetry. *Polym. Engr. Sci.*, Vol. 12, No. 2, Mar. 1972, pp. 120-124.
55. Willard, P. E.: Evaluation of Initiators and Fillers in Diallyl Phthalate Resins by Differential Scanning Calorimetry. *J. Macromol. Sci.-Chem.*, Vol. 8A, 1974, pp. 33-41.

56. Riga, Alan T.: Inhibitor Selection for Vinyl Monomers by Differential Scanning Calorimetry. *Polym. Engr. Sci.*, Vol. 16, No. 12, 1976, pp. 836-840.
57. Sourour, S.; and Kamal, M. R.: Differential Scanning Calorimetry of Epoxy Cure: Isothermal Cure Kinetics. *Thermochimica Acta*, Vol. 14, 1976, pp. 41-59.
58. Prime, R. Bruce: Dynamic Cure Analysis of Thermosetting Resins. In Porter, Roger S.; and Johnson, Julian F., eds.: Analytical Calorimetry - Vol. 2. Plenum Press, 1970, pp. 201-210.
59. Barrett, K. E. J.: Determination of Rates of Thermal Decomposition of Polymerization Initiators With a Differential Scanning Calorimeter. *J. App. Polym. Sci.*, Vol. 11, 1967, pp. 1626-1647.
60. Plueddenmann, Edwin P.: Catalytic Effects in Bonding Thermosetting Resins to Silane-Treated Fillers. In Deanin, Rudolph D.; and Schott, Nick R., eds: Fillers and Reinforcements for Plastics. Am. Chem. Soc. Adv. in Chem. Ser. 134, 1974, pp. 86-94.
61. Broyer, Ephriam; and Macosko, Christopher W.: Heat Transfer and Curing in Polymer Reaction Molding. *AIChE J.*, Vol. 22, No. 2, Mar. 1976, pp. 268-276.
62. Broyer, Ephriam; et al: Curing and Heat Transfer in Polyurethane Reaction Molding. *Polym. Engr. Sci.*, Vol. 18, No. 5, April 1978, pp. 382-387.
63. Whiting, L. F.; and Carr, P. W.: Effect of Thermal Lag and Measurement Precision in Differential Scanning Calorimetry. *Anal. Chem.*, Vol. 50, No. 14, Dec. 1978, pp. 1997-2006.
64. Rummler, Donald R.; and Clark, Ronald K.; Mechanical and Thermo-physical Properties of Graphite-Polyimide Composites. *Proc. CASTS Proj. Tech. Symp. on Graphite-Polyimide, 1979*. To be published as a NASA Conf. Pub. (CP).
65. Bisson, Edmond E.; and Anderson, William J.: Advanced Bearing Technology. NASA SP-38, 1964.
66. McGlone, W. R.; and Keller, L. B.: Volume and Pressure Effects in Compression Molding - Part I. *Modern Plastics*, Mar. 1957, pp. 173 ff.
67. McGlone, W. R.; and Keller, L. B.: Volume and Pressure Effects in Compression Molding-Part II. *Modern Plastics*, Apr. 1957, pp. 137 ff.
68. Stonecypher, Thomas E.; et al: Special Problems in Curing Highly Exothermic Propellants. *Chem. Engr. Prog. Symp. Ser. 62*, No. 61, 1966, pp. 7-13.

69. Nisizawa, Mizuho: A Modified Capillary Dilatometer for Polymerization. *J. App. Polym. Sci.*, Vol. 11, 1967, pp. 1627-1629.
70. Marker, L.; and Ford, B.: Rheology and Molding Characteristics of Glass Fiber Reinforced Sheet Molding Compounds. *Soc. Plas. Ind. 32nd Ann. Tech. Conf. Proc.*, Feb. 1977, Paper 16-E.
71. Price, H. L.; and Murray, K. H.: Finite Element Analysis of the Diametral Test of Polymer Moldings. *J. Engr. Mat. Tech.*, Vol. 95, Series H, No. 3, July 1973, pp. 186-191.
72. Bassett, Charles E.; and Welty, James R.: Non-Newtonian Heat Transfer in the Thermal Entrance Region of Uniformly Heated, Horizontal Pipes. *AICHE J.*, Vol. 21, No. 4, July 1975, pp. 699-706.
73. Roberts, Sanford M.: Dynamic Programming in Chemical Engineering and Process Control. Academic Press, 1964, p. 416.
74. Petrie, Christopher J. S.: Mathematical Modelling and the Systems Approach in Plastics Processing: The Blown Film Process. *Polym. Engr. Sci.*, Vol. 15, No. 10, Oct. 1975, pp. 708-724.
75. Himmelblau, David M.; and Bischoff, Kenneth B.: Process Analysis and Simulation. John Wiley & Sons, 1968, pp. 42-44.
76. Box, G. E. P.; and Hunter, William G.: The Experimental Study of Physical Mechanisms. *Technometrics*, Vol. 7, No. 1, Feb. 1965, pp. 23-42.

APPENDIX  
INSTRUMENT CALIBRATION

This appendix describes the procedures which were followed in the calibration of the differential scanning calorimeter (DSC), rotary rheometer, and laboratory-scale pultruder.

Differential Scanning Calorimeter

The temperature scale was calibrated by noting the apparent melting temperature of indium (429K) and of tin (505K) as indicated by the DSC. Determinations were made at temperature rates of 10, 20, 40, and 80 K/min. The apparent melting points increased by as much as 9 K over that range of temperature rates, with the largest increase ( $\sim 5$ K) taking place between 40 and 80 K/min. The trim potentiometers were adjusted to give a correct temperature scale for a 40 K/min rate. Hence, the temperatures for the 10 and 20 K/min tests could be as much as 5 K below, and those for the 80 K/min tests as much as 5 K above, the true test temperature. As the reactions were taking place in the 400-500 K range, these differences represented  $\sim 1$  percent deviation from the true temperature.

The enthalpy rate was calibrated over the 350-500 K range in 10 K increments using synthetic sapphire as the test material. A determination at a given temperature was made by scanning from 310 K to the temperature, and then maintaining the test specimen at that temperature. The change in enthalpy rate which occurred with the change from increasing temperature to constant temperature was taken as an indication

of the specific heat of sapphire. The specific heat at that temperature was calculated from the test data and compared to the values given in reference 77. Differences between the calculated and the reference values were less than 0.1 percent, so the enthalpy rate was considered to be sufficiently accurate.

#### Rotary Rheometer

All tests with the rotary rheometer were made at a strain rate of  $1 \text{ sec}^{-1}$ . With a 20-mm-radius, 0.018 radian cone, the required rotational speed was 0.172 RPM. The rheometer speed was set to a nominal 1 RPM, and the trim potentiometer on the drive speed command circuit board was adjusted so that ten revolutions were completed in  $600 \pm 3$  seconds. The output of the tachometer on the driven platen was adjusted to 10 vDC for this 1 RPM speed. Then the drive speed command potentiometer was adjusted downward until the output was 1.72 vDC. The tachometer voltage was monitored during the tests, with adjustments being made to the drive speed command potentiometer if the voltage varied by more than 0.05 vDC. Hence, the rotational speed, and strain rate, could vary by as much as  $\pm 3$  percent.

#### Laboratory-Scale Pultruder

The laboratory-scale pultruder incorporated a mechanical testing machine. The machine load cell was calibrated with dead weights to an accuracy of 0.5 percent or better. The pultruder die temperature was checked using iron-constantan thermocouples in the first, third, and fifth thermocouple wells (see figure 32). Another thermocouple was placed in the die cavity, and was pressed against the wall by a piece of epoxy-graphite pultruded stock. The quartz tube heaters were set to 450 K, and the thermocouples were monitored as the temperature rose.

During the temperature rise, the temperature at the ends of the die lagged behind the center temperature by 2-3 K. Once at temperature, however, the ends were no more than  $\sim 1$  K lower than the center. As the temperature gradients were small, only the center temperature was measured during an actual pultrusion run. Once the temperature had settled out at the set point, it varied by less than 1 K above or below that point.

## VITA

HOWARD L. PRICE, JR., born 1932 in Virginia; attended public schools and graduated from public universities; B.S., June 1957, Virginia Polytechnic Institute; M. Engr., June 1970, Old Dominion University; U.S. Army Ordnance Corps, 1953-55; Professional Engineer registered in Virginia; materials engineer with NASA - Langley Research Center since 1957; author or co-author of some 30 publications on materials processing and properties; representative publications include:

Molecular Orientation and Mechanical Anisotropy in Polymer Films. SPE J., Vol. 24, Feb. 1968, pp. 54-59.

Internal Structure and Load Response of Plastics. Am. Soc. Civil Engr. Misc. Pub. Structural Plastics: Properties and Possibilities, 1969.

Finite Element Analysis of the Diametral Test of Polymer Moldings (with K. H. Murray). J. Engr. Mat. Tech., Vol. 95, Series H, No. 3, 1973, pp. 186-191.

Friction and Friction-Generated Temperature at a Polymer-Metal Interface (with Harold D. Burks). Polym. Engr. Sci., Vol. 14, No. 4, April 1974, pp. 288-291.

Properties and Applications of a Pitch Carbon Microsphere Composite (with James B. Nelson). Polym. Engr. Sci., Vol. 17, No. 5, May 1977, pp. 341-348.

Rapid Viscosity Measurements of Powdered Thermosetting Resins (with Harold D. Burks and S. K. Dalal). Soc. Plas. Ind. 33rd Ann. Tech. Conf. Proc. 1978, Paper 16-A.